NAS CR-152250
LSI ER-258-7

TECHNOLOGY ADVANCEMENT OF THE ELECTROCHEMICAL CO_2 CONCENTRATING PROCESS

(NASA-C.'-152250) TECENOLOGY ADVANCEMENT OF THE ELECTROCHEMICAL CO2 CONCENTRATING PROCESS Final Report, Feb. 1975 - Mar. 1979 (Life Systems, Inc., Cleveland, Ohio.) 125 p HC A06/MF A01 CSCL 07D G3/25
N79-26135
Unclas
27352

FINAL REPORT

by

F. H. Schubert, D. B. Heppner,
T. M. Hallick and R. R. Woods

May, 1979

Prepared Under Contract NAS2-8666

by

Life Systems, Inc.
Cleveland, OH 44122

for

AMES RESEARCH CENTER
National Aeronautics and Space Administration

Life Systems, Inc.

ER-258-7

TECHNOLOGY ADVANCEMENT OF THE ELECTROCHEMICAL CO_2 CONCENTRATING PROCESS

FINAL REPORT

by

F. H. Schubert, D. B. Heppner,
T. M. Hallick and R. R. Woods

May, 1979

Prepared Under Contract NAS2-8666

by

Life Systems, Inc.
Cleveland, OH 44122

for

Ames Research Center
National Aeronautics and Space Administration

FOREWORD

The development work described herein was conducted by Life Systems, Inc. at Cleveland, OH, under Contract NAS2-8666, during the period of February, 1975 through March, 1979. The Program Manager was Franz H. Schubert. The personnel contributing to the program and their responsibilities are outlined below:

Personnel	Area of Responsibility
Steve Czernec	Mechanical Component/System Assembly and Checkout
Ron J. Davenport, Ph.D.	Electrode Kinetics Study
Robert W. Ellacott	Electrochemical Cell Assembly
Tim M. Hallick	Program Testing, Data Reduction, Modu'- 'Cell Configurations
Dennis B. Heppner, Ph.D.	Component Design, Laboratory Breadboard Testing, System Integration and Testing
Don W. Johnson	Electronic Assembly and Checkout
Richard D. Marshall	System Integration, Electrochemical Design, Optimum Current Density Study
J. David Powell	Control and Monitor Instrumentation and Sensor Designs
Joe W. Schmidt	Electronic Assembly and Wiring
Franz H. Schubert	Program Manager, System Analysis and Design
Daniel C. Walter	Mechanical Component Design and System Packaging
Richard R. Woods, Jr.	Supporting Technology Studies, Electrochemical and Chemical Performance Analysis
Rick A. Wynveen, Ph.D.	Program Administration, Electrochemical Support, Concept Evaluations
Pat Y. Yang, Ph.D.	Control and Monitor Instrumentation Software

The contract's Technical Monitor was P. D. Quattrone, Chief, Advanced Life Support Office, NASA Ames Research Center, Moffett Field, CA.

TABLE OF CONTENTS

LIST OF FIGURES

List of Figures - continued

LIST OF TABLES

LIST OF ACRONYMS

ARS	Air Revitalization System
ARX-1	One-Person, Experimental, Air Revitalization System
B-CRS	Bosch Carbon Reduction Subsystem
CHCS	Cabin Humidity Control Subsystem
C/M I	Control/Monitor Instrumentation
CPU	Central Processing Unit
CRS	CO_2 Reduction Subsystem
CS-3	Preprototype Electrochemical CO_2 Concentrator Subsystem
CX-1	One-Person, Self-Contained CO_2 Concentrating Subsystem
DAS	Data Acquisition System
EC/LSS	Environmental Control/Life Support System
EDC	Electrochemical Depolarized CO_2 Concentrator
EDCM	EDC Module
FSU	Fluid Supply Unit
NGM	Nitrogen Generation Module
NSS	Nitrogen Supply Subsystem
OGS	Oxygen Generation Subsystem
ORS	Oxygen Recovery System
TACU	Test Accessories Control Unit
TSA	Test Support Accessories
WHS	Water Handling Subsystem

SUMMARY

Regenerative carbon dioxide removal concepts are needed to sustain man in space for extended periods of time. A program to develop an Electrochemical Carbon Dioxide Concentration technique has been underway at the National Aeronautics and Space Administration and Life Systems, Inc. for the past several years. The work reported herein is a portion of the overall program.

During the contractual period, activities in seven major areas were successfully completed:

1. Further development of the liquid-cooled advanced Electrochemical Depolarized Carbon Dioxide Concentrator including the fabrication of two one-person capacity liquid-cooled modules.

2. Testing of the advanced liquid-cooled Electrochemical Depolarized Carbon Dioxide Concentrator integrated with a Sabatier Carbon Dioxide Reduction Subsystem in a laboratory breadboard Oxygen Recovery System.

3. Development, testing and delivery of a three-person Preprototype Electrochemical Depolarized CO_2 Concentrator.

4. Testing of an air-cooled, four-person capacity Electrochemical Depolarized Carbon Dioxide Concentrator integrated with a Bosch Carbon Dioxide Reduction Subsystem and an Oxygen Generation Subsystem to form a laboratory breadboard Oxygen Recovery System.

5. Development and testing of subsystem hardware integrated into a one-person, experimental Air Revitalization System based on the advanced, liquid-cooled Electrochemical Depolarized Carbon Dioxide Concentrator.

6. Development of Test Support Accessories to support single cell, subsystem and system level testing of Electrochemical Depolarized Carbon Dioxide Concentrators.

7. Technology advancement studies of the basic electrochemical carbon dioxide concentration process to improve carbon dioxide removal and electrical efficiencies over broad operating ranges and to provide a basis for the design of the next generation cell, module and subsystem hardware.

Two multicell, liquid-cooled, advanced Electrochemical Depolarized Carbon Dioxide Concentrator modules were fabricated. The cells utilized advanced, lightweight, plated-anode current collectors, internal liquid cooling and lightweight cell frames. Both were designed to meet the carbon dioxide removal requirements of one-person, i.e., 1.0 kg/d (2.2 lb/d).

A five-cell module was successfully tested as part of an integrated Oxygen Recovery System which also included a Sabatier-based Carbon Dioxide Reduction Subsystem and an Oxygen Generation Subsystem. A 30-day test of this Oxygen Recovery System was performed. The test demonstrated the long-term, multicell, liquid-cooled, advanced Electrochemical Depolarized Carbon Dioxide Concentrator Module operation and verified satisfactory operation with the hydrogen generated by the Oxygen Generation Subsystem. At an operating current density of 30.1 mA/cm^2 (28 ASF) the average cell voltages obtained were 0.40 V for the Electrochemical Depolarized Carbon Dioxide Concentrator and the module exhibited an average carbon dioxide transfer efficiency of 76% for the duration of the test. The Sabatier reactor also demonstrated efficient operation with the Electrochemical Depolarized Carbon Dioxide Concentrator exhaust gas. The hydrogen conversion efficiency of the Sabatier reactor throughout the testing averaged 97%.

The second liquid-cooled module, consisting of six cells, was fabricated and integrated with other air revitalization functions to form a self-contained, one-person Air Revitalization System. Cabin humidity control subsystem hardware supplying preconditioned air to the Electrochemical Depolarized Carbon Dioxide Concentrator as well as controlling cabin humidity was designed and fabricated to be an integral part of the Electrochemical Depolarized Carbon Dioxide Concentrator Subsystem.

The combined carbon dioxide and water removal hardware was functionally integrated with other major Air Revitalization System components such as a Contractor-developed Sabatier Reactor, water handling and distribution hardware and liquid coolant loop components. Also, a centralized Control and Monitor Instrumentation, including one-button startup and shutdown of the total integrated system, was designed and fabricated. An Oxygen Generation Subsystem and a Nitrogen Supply Subsystem being developed under other NASA Ames Research Center contracts were integrated with the hardware developed under this program to complete the Air Revitalization System.

During a 30-day integrated test, excellent Electrochemical Depolarized Carbon Dioxide Concentrator performance was demonstrated. At a current density of 23 mA/cm^2 (21 ASF), the average cell voltage obtained was 0.46 V and the module exhibited an average transfer efficiency of 87%. A substantial reduction in the total number of components, interconnections and subsystem interfaces was demonstrated by treating the required Air Revitalization System processes at the functionally integrated system level rather than as a series of individual subsystems that must be integrated. Also, generation of "real world" data (by testing in the projected final application configuration) as well as demonstration of savings in testing costs and Test Support Accessories hardware were demonstrated.

A three-person preprototype Electrochemical Depolarized Carbon Dioxide Concentration Subsystem was designed, fabricated, tested and delivered to the National Aeronautics and Space Administration to be integrated and tested in the Regenerative Life Support Evaluation experiment. The 15 cell, air-cooled subsystem exhibited a cell voltage performance of 0.40 V at 30.1 mA/cm^2 (28 ASF) and an average transfer efficiency of 80%.

Support of other integrated subsystem test programs in the area of carbon dioxide removal was provided as part of the program. A four-person capacity laboratory breadboard Oxygen Recovery System consisting of an air-cooled Electrochemical Depolarized Carbon Dioxide Concentrator, a Bosch-based Carbon Dioxide Reduction Subsystem and an Oxygen Generation Subsystem was successfully tested. A total of 3,000 hours of testing including checkout, shakedown, design verification and endurance testing was accomplished.

New single cell, subsystem and system level Test Support Accessories were designed and constructed. The single cell facilities were modifications and refurbishments of previously developed test stands. A new Air Supply Unit with automatic controls was constructed for subsystem testing. This closed-loop Air Supply Unit simulates spacecraft environments and provides the capability for controlling and monitoring the air temperature, dew point temperature, carbon dioxide partial pressure, oxygen partial pressure and air flow rate. This facility provides a long-term test capability for Electrochemical Depolarized Carbon Dioxide Concentrator Subsystems ranging from a one- to six-person capacity. Additionally, Test Support Accessories for the one-person Air Revitalization System were developed.

The technology advancement studies included investigations into nine specific areas relating to the Electrochemical Depolarized Carbon Dioxide Concentrator process. These areas were:

1. The influence of the Teflon catalyst binder loading in the electrodes on performance of the Electrochemical Depolarized Carbon Dioxide Concentrator.

2. The development of a higher performance, lower cost alternate anode current collector design.

3. The scale-up and fabrication of a cell matrix fabricator.

4. An application study of using the cell hardware to perform a moisture removal function.

5. The identification of the causes of occasionally observed performance deviations associated with maldistributions of carbon dioxide removal rate, water evolution rate and dry bulb temperature variations over the cell electrode surface.

6. A study to determine the optimum current density of an Electrochemical Depolarized Carbon Dioxide Concentrator when used as an electrical power source as well as a carbon dioxide remover.

7. The development of cell hardware configurations and concepts that enable the attainment of higher level performance goals, i.e., cell voltage of 0.50 V and a carbon dioxide removal efficiency of 82% at a current density of 21.5 mA/cm^2 (20 ASF).

8. Studies of electrolyte mixtures to enhance concentrator performance levels.

9. Studies of the use of hydrated salts to improve cell voltage and moisture tolerance performance.

Based on the results of the technology advancement studies and subsystem developments, a new set of performance goals has been adopted. These goals have been defined as performance standards at the subsystem level for future Electrochemical Depolarized Carbon Dioxide Concentrator developments. Specifically, a cell voltage of 0.53 V and a carbon dioxide removal efficiency of 82% at a current density of 21.5 mA/cm^2 (20 ASF) have been adopted.

It is concluded from the results reported herein that an Electrochemical Depolarized Carbon Dioxide Concentrator is a viable solution for the removal of metabolically-generated carbon dioxide aboard manned spacecraft. Continued development of related technology is recommended to further improve performance, decrease equivalent weight and increase hardware reliability. Successful completion of this development will produce timely technology necessary to plan future advanced environmental control and life support system programs and experiments.

PROGRAM ACCOMPLISHMENTS

Key program accomplishments were:

- Developed and delivered a three-person Preprototype Electrochemical Carbon Dioxide (CO_2) Concentrator Subsystem (CS-3) with a computer-based, advanced Control/Monitor Instrumentation (C/M I).

- Developed and tested a self-contained, one-person Air Revitalization System (ARS) based on a liquid-cooled Electrochemical Depolarized CO_2 Concentrator (EDC). Over 500 hours of integrated testing was accumulated.

- Completed the development and testing of several components required for an EDC-based ARS. Some of these components were successfully tested for over 10,000 hours of operation.

- Developed an advanced, high performance, liquid-cooled EDC module (EDCM) utilizing advanced lightweight, plated-anode current collectors and internal liquid cooling.

- Performed the integration and testing of a four-person capacity Bosch Oxygen Recovery System (ORS) consisting of an air cooled EDC, a Bosch Carbon Reduction Subsystem (B-CRS) and an Oxygen Generation Subsystem (OGS). Over 900 hours of integration testing was accumulated.

- Successfully completed several studies expanding the technology base for the EDC.

- Established and demonstrated new EDC performance standards for future EDC development. These standards include a 0.50 V cell voltage and a CO_2 removal efficiency of 82% at 21.5 mA/cm^2 (20 ASF).

INTRODUCTION

Regenerative processes for the revitalization of spacecraft atmospheres are essential in making long-term manned missions in space a reality.[1,2] An important step in this overall revitalization process is the collection and concentration of the metabolically-produced CO_2 for oxygen (O_2) recovery.

The subject program continued the development and advancement of an electrochemical CO_2 concentrating process, a technique that allows for the continuous and efficient removal of CO_2 from a spacecraft's cabin atmosphere and delivery of the CO_2 premixed with hydrogen (H_2) to a CO_2 Reduction Subsystem (CRS) for subsequent O_2 recovery.

Background

The Skylab program marked the beginning of the use of regenerative techniques for CO_2 collection using cyclic absorption/desorption beds containing commercial zeolites. The emerging requirement for maintaining the CO_2 content of a spacecraft's atmosphere at a CO_2 partial pressure (pCO_2) below 400 Pa (3 mm Hg) made the zeolite systems unattractive due to their resulting high weight and volume penalties.[3]

The electrochemical technique of concentrating CO_2 from an air environment has evolved over the past 13 years.[4-12] During this time the concept has progressed from single cell operation through the fabrication, testing and integration of multiperson, self-contained subsystems for spacecraft application.

The electrochemical removal technique works as follows: CO_2 is continuously removed from a flowing cabin air stream. The removal takes place in a module consisting of a series of electrochemical cells. Each cell consists of two electrodes separated by a matrix containing an aqueous carbonate electrolyte solution. Plates adjacent to the electrodes provide passageways for distribution of gases and electrical current. Figure 1 shows a functional schematic of the EDC cell while Figure 2 details the specific electrochemical and chemical reactions. As shown in Figure 2, the overall reaction is:

$$O_2 + 2CO_2 + 2H_2 = 2CO_2 + 2H_2O + \text{electrical energy} + \text{heat} \qquad (1)$$

Two moles of CO_2 are theoretically transferred for one mole of O_2 consumed. The observed ratio of CO_2 transferred to O_2 consumed represents the process removal efficiency with a defined efficiency of 100% occurring when 2.75 kg (6.05 lb) of CO_2 is removed for each kg (2.2 lb) of O_2 consumed.

(1,2) References cited at the end of this report.

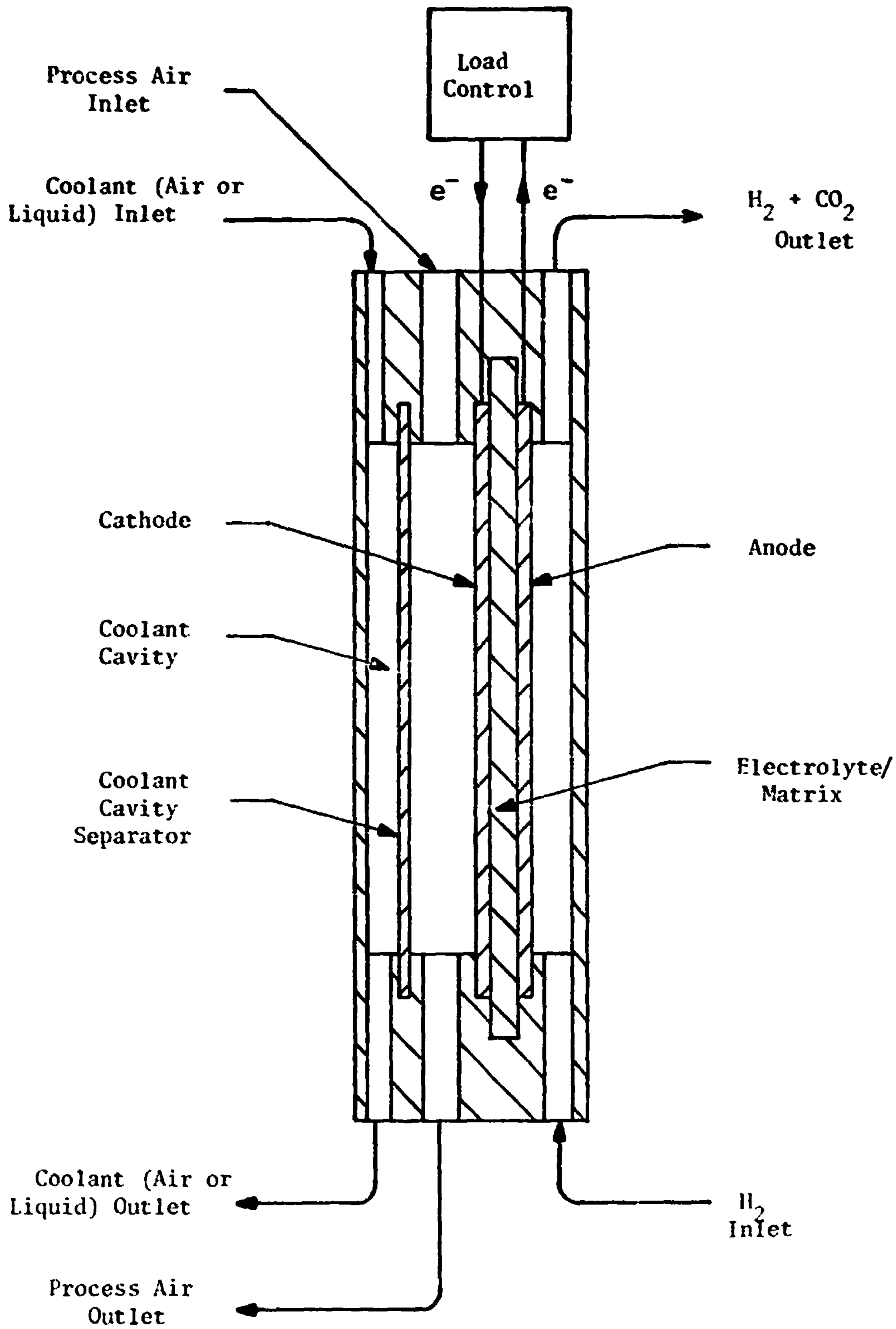

FIGURE 1 EDC CELL FUNCTIONAL SCHEMATIC

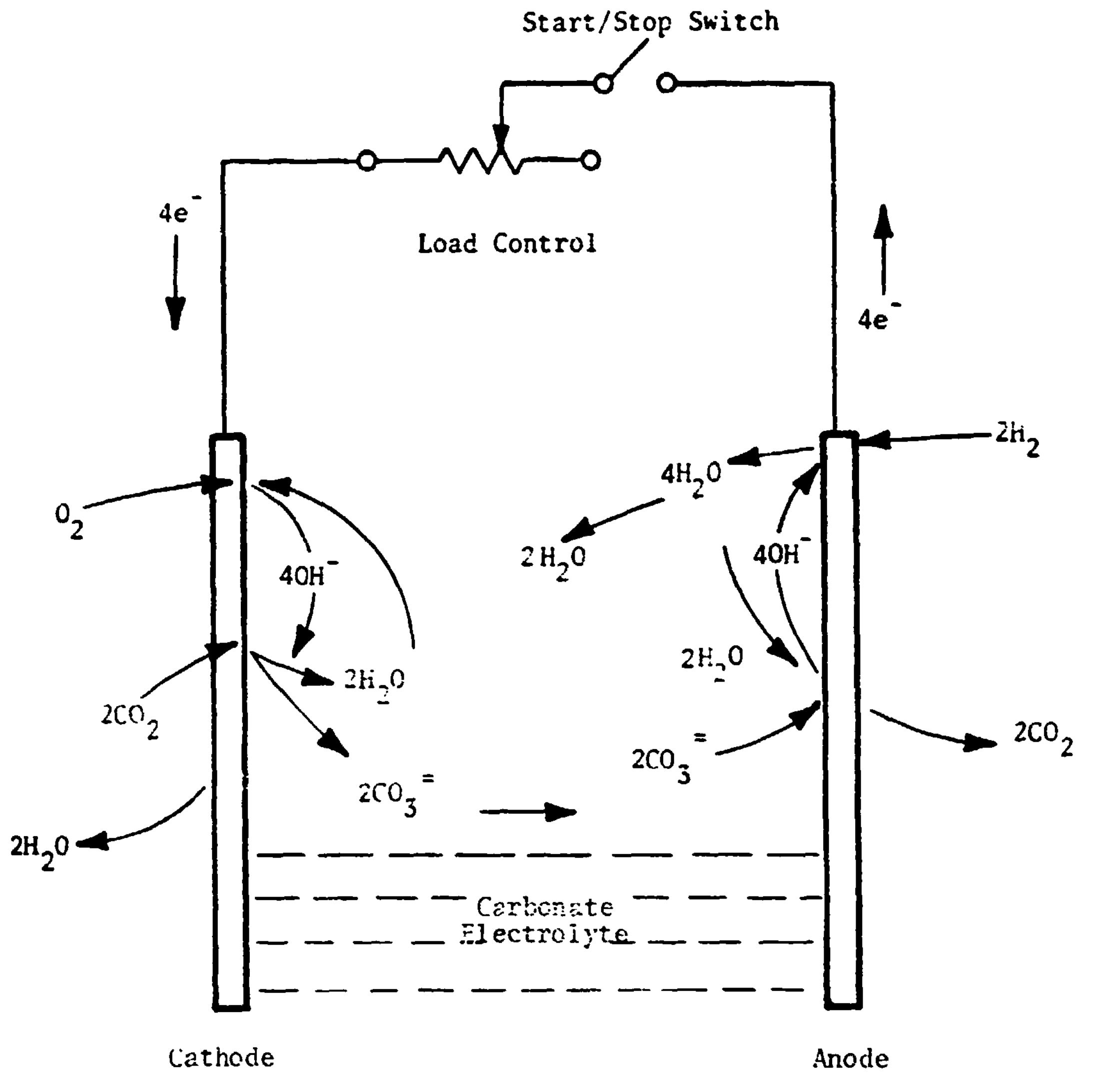

Cathode Reactions:

$$O_2 + 2H_2O + 4e^- = 4OH^-$$
$$4OH^- + 2CO_2 = 2H_2O + 2CO_3^=$$

Anode Reactions:

$$2H_2 + 4OH^- = 4H_2O + 4e^-$$
$$2CO_3^= + 2H_2O = 4OH^- + 2CO_2$$

Overall Reaction:

$O_2 + 2CO_2 + 2H_2 = 2CO_2 + 2H_2O$ + Electrical Energy + Heat

FIGURE 2 EDC ELECTROCHEMICAL AND CHEMICAL REACTIONS

Program Objectives

The overall objectives of the subject program were to:

1. improve the performance of the electrochemical CO_2 removal technique by increasing CO_2 removal efficiencies at pCO_2 levels below 400 Pa (3 mm Hg), increasing cell power output and broadening the tolerance of electrochemical cells for operation over wide ranges of cabin relative humidity (RH);
2. design, fabricate and assemble development hardware to continue the evolution of the electrochemical concentrating technique from the existing level to an advanced level able to efficiently meet the CO_2 removal needs of a spacecraft ARS;
3. develop and incorporate into the EDC the components and concepts that allow for the efficient integration of the electrochemical technique with other subsystems to form a spacecraft ARS;
4. combine ARS functions to enable the elimination of subsystem components and interfaces and
5. demonstrate the integration concepts through actual operation of a functionally-integrated ARS.

Program Organization

To meet the above objectives the program was divided into five tasks plus documentation and program management functions. The five tasks were:

1.0 Design, fabricate and assemble development hardware to evolve the EDC's technology from the existing level to an advanced level capable of efficiently removing CO_2 from a spacecraft's atmosphere and integrating with other Environmental Control/Life Support System (EC/LSS) subsystems to form a spacecraft ARS.

2.0 Design, develop, fabricate, assemble, functionally check out and calibrate Test Support Accessories (TSA) to be compatible with the test objectives of the subsystem hardware and the supporting research and technology test program.

3.0 Establish, implement and maintain a mini-Product Assurance program through all phases of contractual performance including design, fabrication, purchasing, assembly, testing, packaging and shipment consistent with a program in the early stages of development.

4.0 Perform a variety of subsystem and integrated system/subsystem testing required to demonstrate readiness of the EDC concept.

5.0 Complete essential and desirable supporting research and development efforts to further expand the technology base associated with the spacecraft EDC with special emphasis on the development of the electrochemical cell: the electrodes, the electrolyte retaining matrix and the electrolyte.

Report Organization

This Final Report covers the work performed during the period February, 1975 through March, 1979. Portions of the work documented in this report are covered in greater detail in two Annual Reports.[11,12] The following five sections of this report present the technical results grouped according to (1) Subsystem Developments, (2) System Integration Developments, (3) TSA Developments, (4) Mini-Product Assurance Program and (5) Technology Advancement Studies. These sections are followed by Conclusions and Recommendations based on the work performed.

SUBSYSTEM DEVELOPMENTS

The subsystem development activities performed as part of this program included (1) continuing advancement of liquid-cooled EDCs and (2) developing a three-person preprototype EDC subsystem.

Liquid-Cooled EDC

Activities completed under previous EDC development programs had shown that liquid-cooled EDC cells exhibited substantially higher CO_2 removal efficiencies than air-cooled cells, especially at low pCO_2 levels.[10] The result of such testing is demonstrated in Figure 3. The CO_2 removal efficiency is plotted versus process air inlet pCO_2 for a liquid-cooled single cell and compared to a least squares fit of previous air-cooled EDC performance data.

The initial liquid-cooled cell testing had been performed with a modified old style 2.3 dm^2 (0.25 ft^2) cell. Subsequent development activities resulted in the design and fabrication of a 4.6 dm^2 (0.5 ft^2) active cell area, lightweight, advanced EDC cell frame capable of being injection molded with provisions for either internal air cooling or internal liquid cooling.[11] As part of this program, a one-person capacity, liquid-cooled module was fabricated using the advanced liquid-cooled cells and tested as part of a one-person laboratory breadboard Sabatier-based O_2 Recovery System (LBS-S/ORS-1(L)). To test the module, the hardware developed for a one-person, self-contained CO_2 concentrating subsystem (CX-1)[5] was refurbished and modified. Similarly, the TSA previously used with the CX-1 was modified to support the projected liquid-cooled module testing.

Past liquid-cooled performance data had indicated that a five-cell module with an 4.6 dm^2 (0.5 ft^2) active cell area and operating at 30 mA/cm^2 (28 ASF) could remove the 1 kg/d (2.2 lb/d) CO_2 metabolically generated by one person. Five advanced liquid-cooled cell frames were fabricated. The frames used the advanced lightweight, plated-anode current collector concept.[10] Figure 4 shows a functional schematic of internally liquid-cooled advanced cell frames. Figure 5 shows the liquid-cooled cell frame and parts that make up an advanced liquid-cooled cell. The five cells were assembled using plexiglass end plates. Following assembly the module was charged with 61.5% cesium carbonate (Cs_2CO_3) electrolyte. The module was then integrated with the CX-1 and its TSA for testing. This activity is further described under the System Integration Developments section.

A second module consisting of six advanced, liquid-cooled cells of the construction discussed above was fabricated. Stainless steel end plates were used.

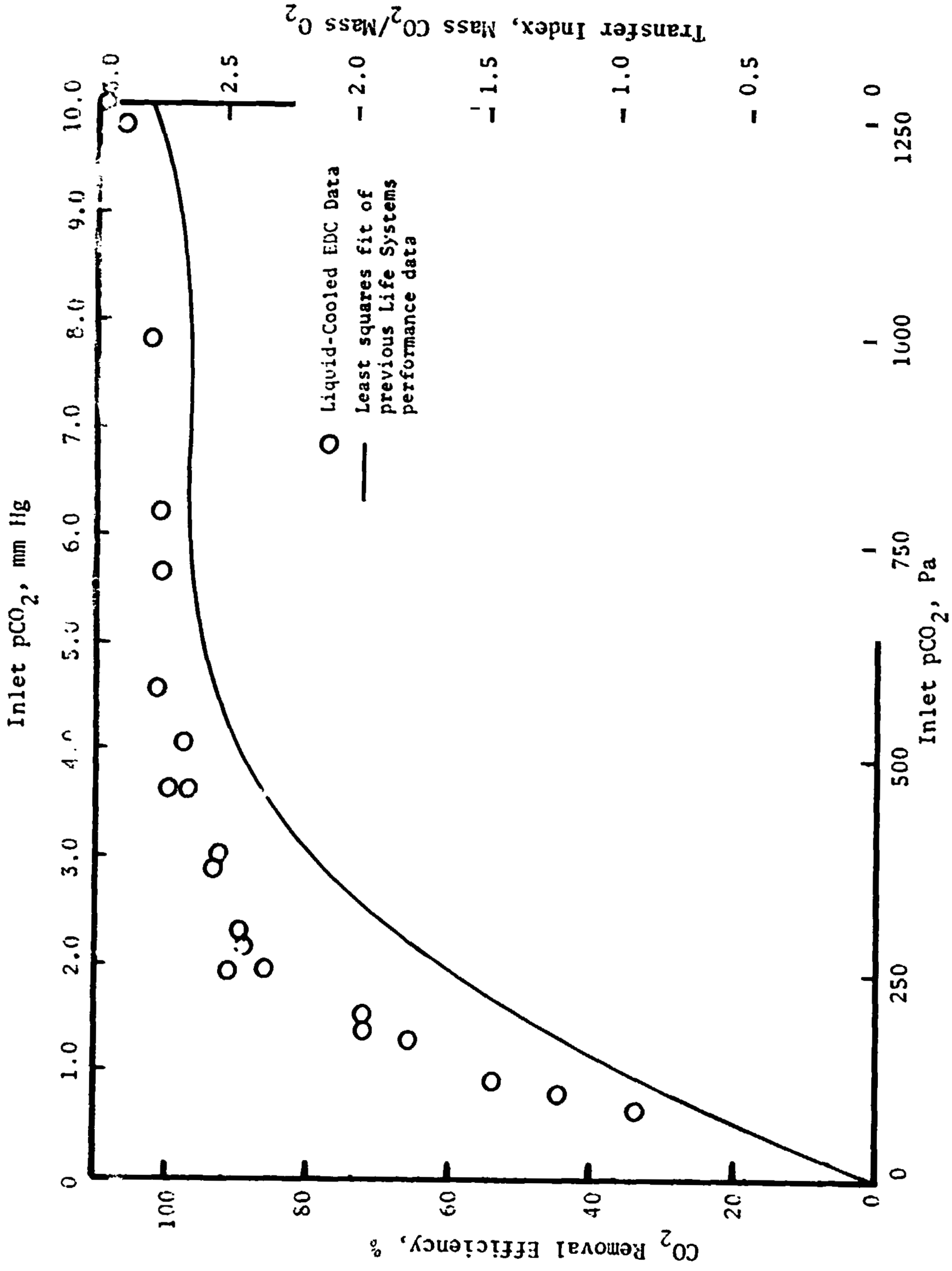

FIGURE 3 LIQUID-COOLED EDC PERFORMANCE AS A FUNCTION OF AIR INLET pCO_2

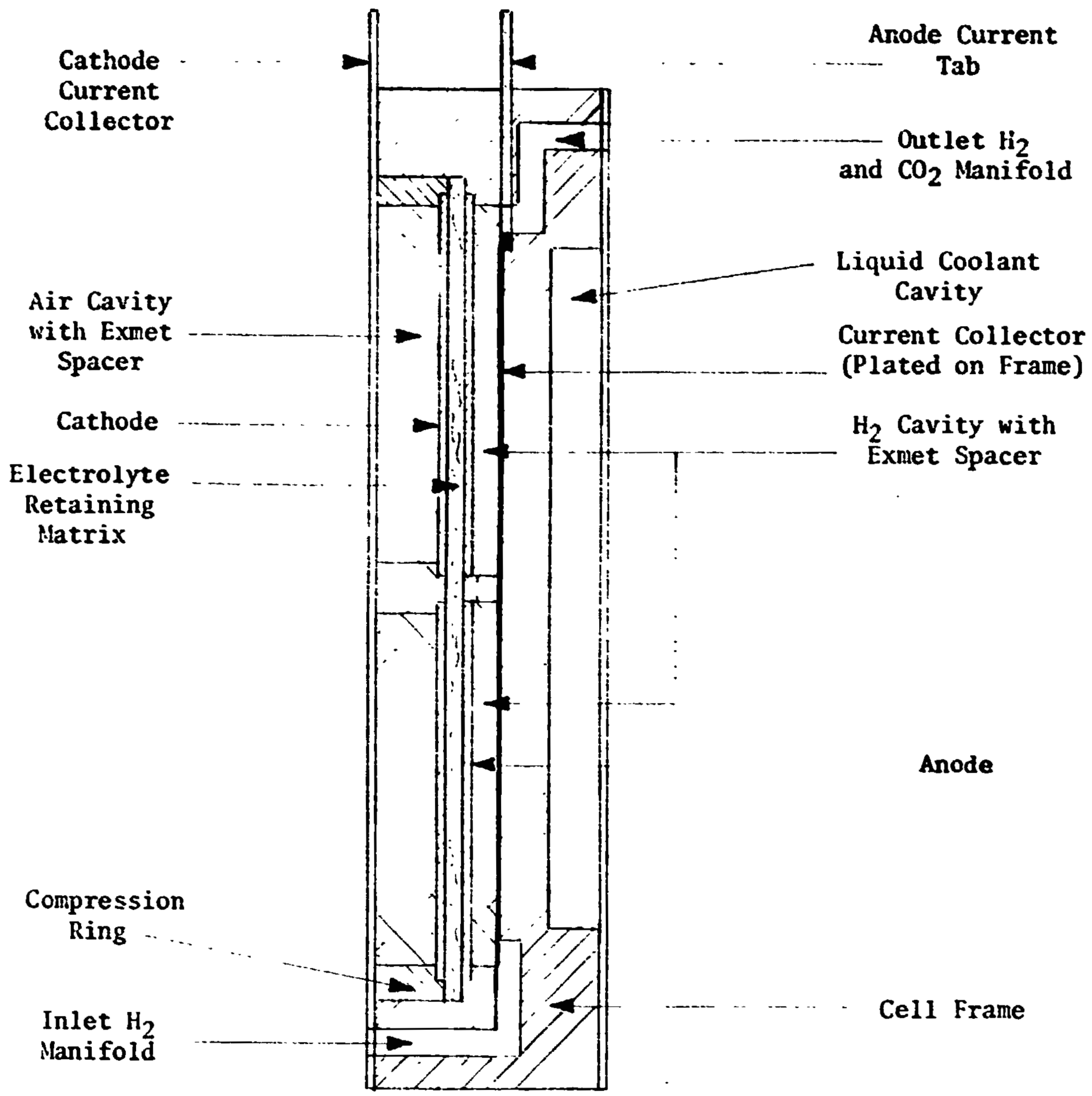

FIGURE 4 ADVANCED LIQUID-COOLED EDC CELL FUNCTIONAL SCHEMATIC

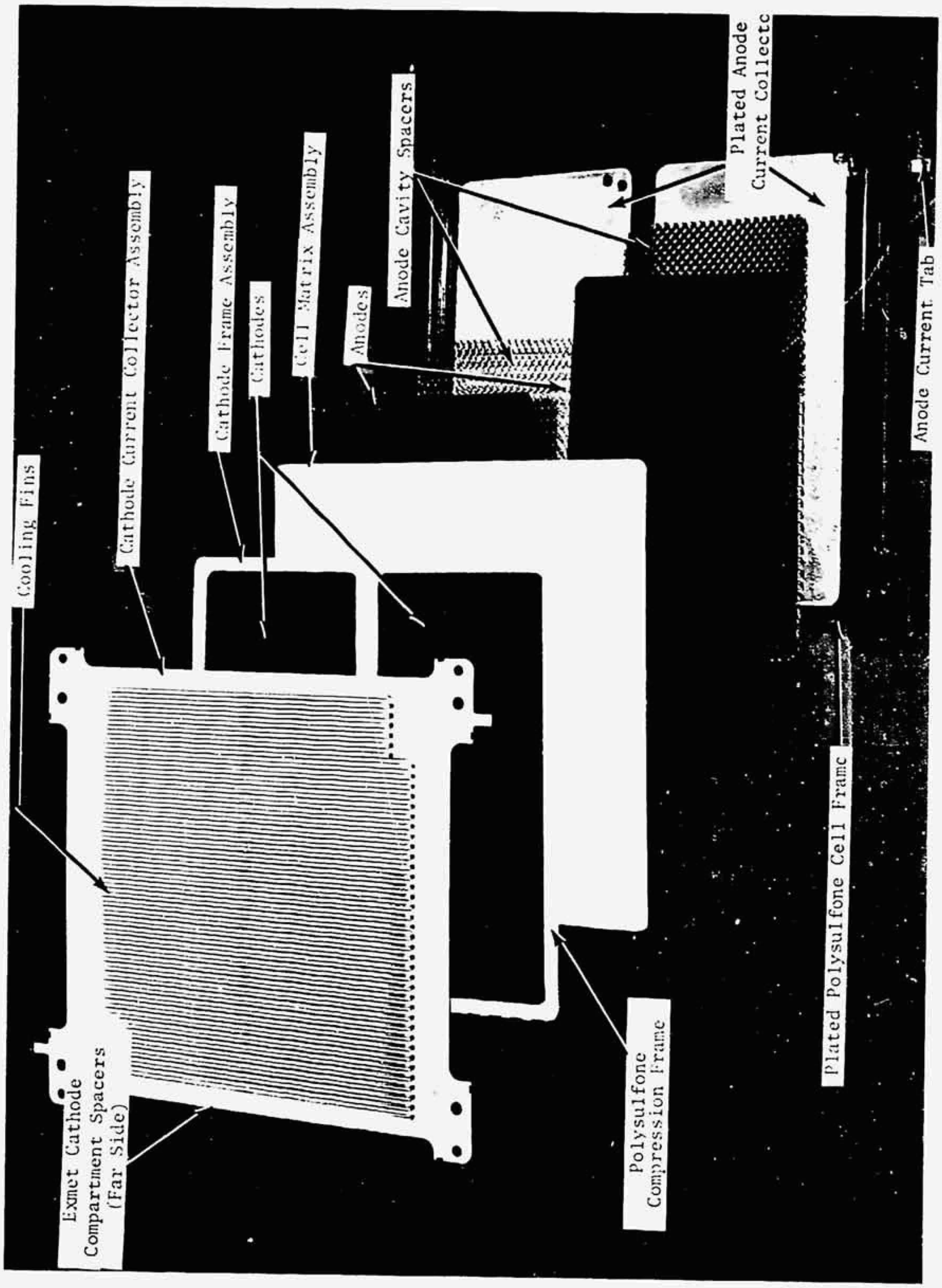

FIGURE 5 ADVANCED EDC LIQUID-COOLED CELL PARTS

Figure 6 is a photograph of the assembled six-cell module. This EDCM was used to support the one-person ARS development and testing which is also discussed below.

Three-Person Preprototype Subsystem

A major hardware development performed under this program was the design, fabrication, testing and delivery of a three-person preprototype EDC Subsystem. A math model of the subsystem was also developed. Termed the CS-3, this subsystem was designed to operate in the NASA's Regenerative Life Support Evaluation (RLSE) experiment in conjunction with other air revitalization subsystems. The objective of the RLSE experiment was to demonstrate, possibly by a Spacelab flight, the operational readiness of regenerable life support hardware.

The CS-3 design requirements are given in Table 1 and reflect the Spacelab cabin conditions. The CS-3 is designed to remove the CO_2 generated by three persons in a Spacelab cabin environment. As such, it is designed to remove the CO_2 at a rate corresponding to 0.125 kg/h (0.275 lb/h).

CS-3 Schematic and Operation

The schematic of the preprototype CS-3 is shown in Figure 7. Process air is drawn from an actual or simulated cabin air source through an isolation valve (V2), a filter (AF1) and the EDCM (EM1) by a single process air fan (B1). The process air is returned to the source through an outlet isolation valve (V1). The isolation valve prevents the module from drying out during nonoperational, low RH periods. Internally, the process air is manifolded to flow in parallel through the process air cavities of the 15-cell, air-cooled module.

A dew point sensor (D1) and a triple redundant temperature sensor (T1) monitor the inlet process air to protect the subsystem from out-of-tolerance conditions of temperature and RH. The temperature of the module is monitored using a triple redundant temperature sensor (T2) located in the process air stream exiting from the electrochemical cell cavities. A cooling air fan (B2) draws air through the cooling air cavities of the 15 cells of the module to control module temperature. Cooling air is drawn from the cooling air supply, enters the subsystem at the bottom and is returned to the cooling air stream at the top. The cooling air temperature is measured upstream and downstream of the module using temperature sensors T3 and T4, respectively.

Hydrogen supplied by the OGS of the RLSE passes through a flow sensor (F1) prior to entering the module. The H_2/CO_2 exhaust stream from the module then passes through a second flow sensor (F2), pressure sensors (P2 and P3) and exhausts the subsystem either through a backpressure regulator (PR1) and a valve (V5) or to the CRS through V6. Pressure in the H_2 line, as sensed by P1, is maintained at greater than or equal to 108 kPa (15.7 psia) during operation to ensure that any possible H_2 leakage would be from internal-to-external.

Nitrogen (N_2) purge gas is provided through valve V3. The N_2 flow is controlled by an orifice (RX1) and is pressure monitored by P1. The purge gas stream is exhausted through V5 to vacuum vent.

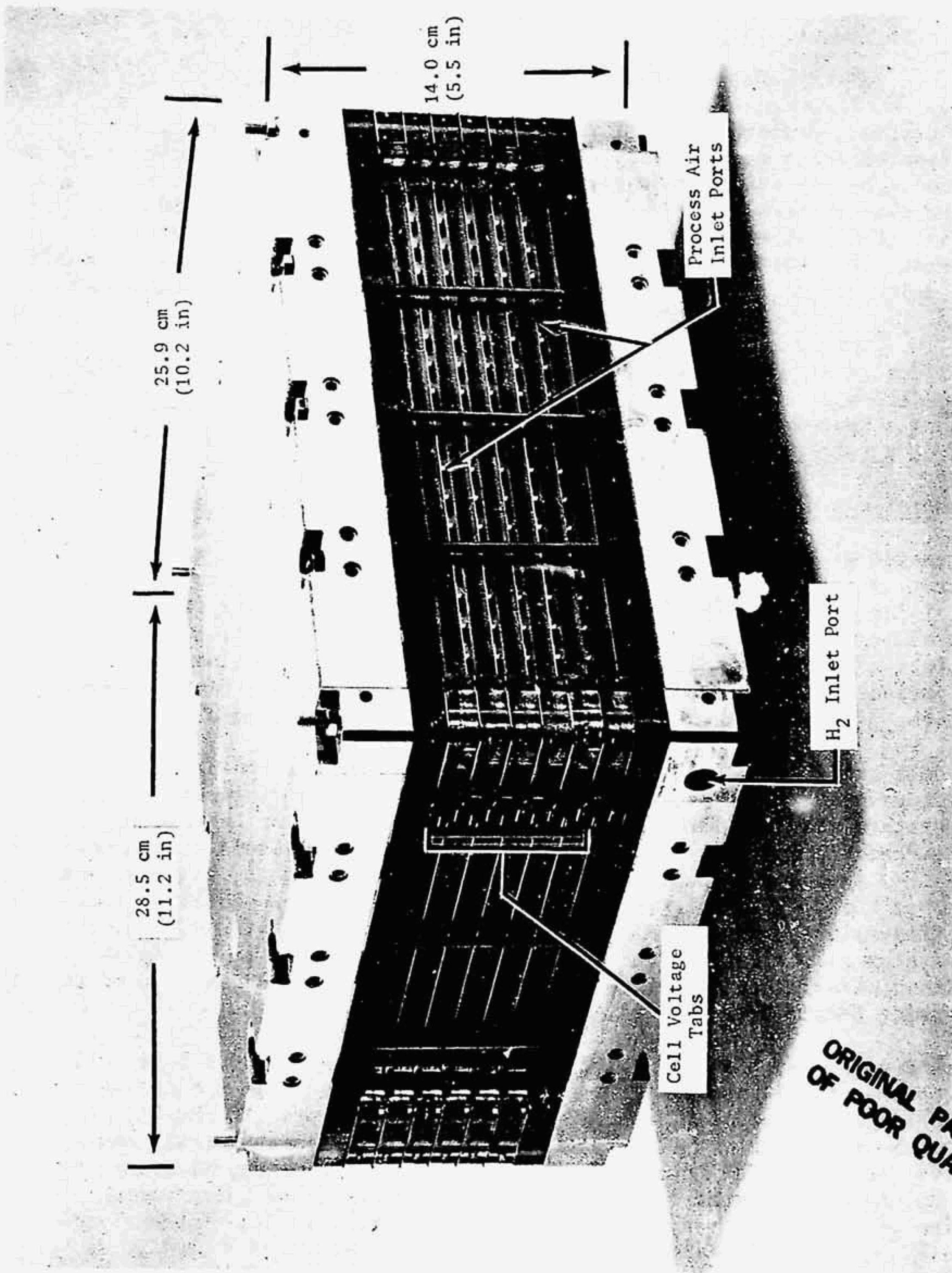

FIGURE 6 SIX-CELL LIQUID-COOLED EDCM

TABLE 1 CS-3 DESIGN SPECIFICATIONS

Crew Size	3
CO_2 Removal Rate, kg/h (lb/h)	0.125 (0.275)
Cabin pCO_2, Pa (mm Hg)	400 (3.0)
Cabin pO_2, kPA (psia)	22.1 (3.2)
Cabin Temperature, K (F)	291 to 300 (65 to 80)
Cabin Pressure, kPa (psia)	101 (14.7)
Process Air	
Relative Humidity, %	80 ±5
Dry Bulb, K (F)	284 to 287 (52 to 58)
Cooling Air Temperature, K (F)	284 to 287 (52 to 58)
H_2 Supply Flow Rate, kg/h (lb/h)	0.022 (0.048)
H_2 Relative Humidity, %	95 Max
Purge Gas	N_2
Purge Gas Pressure, kPa (psia)	311.0 (45)
Electrical Power, VAC	115/200, 400 Hz, 3Ø
Gravity	0 to 1

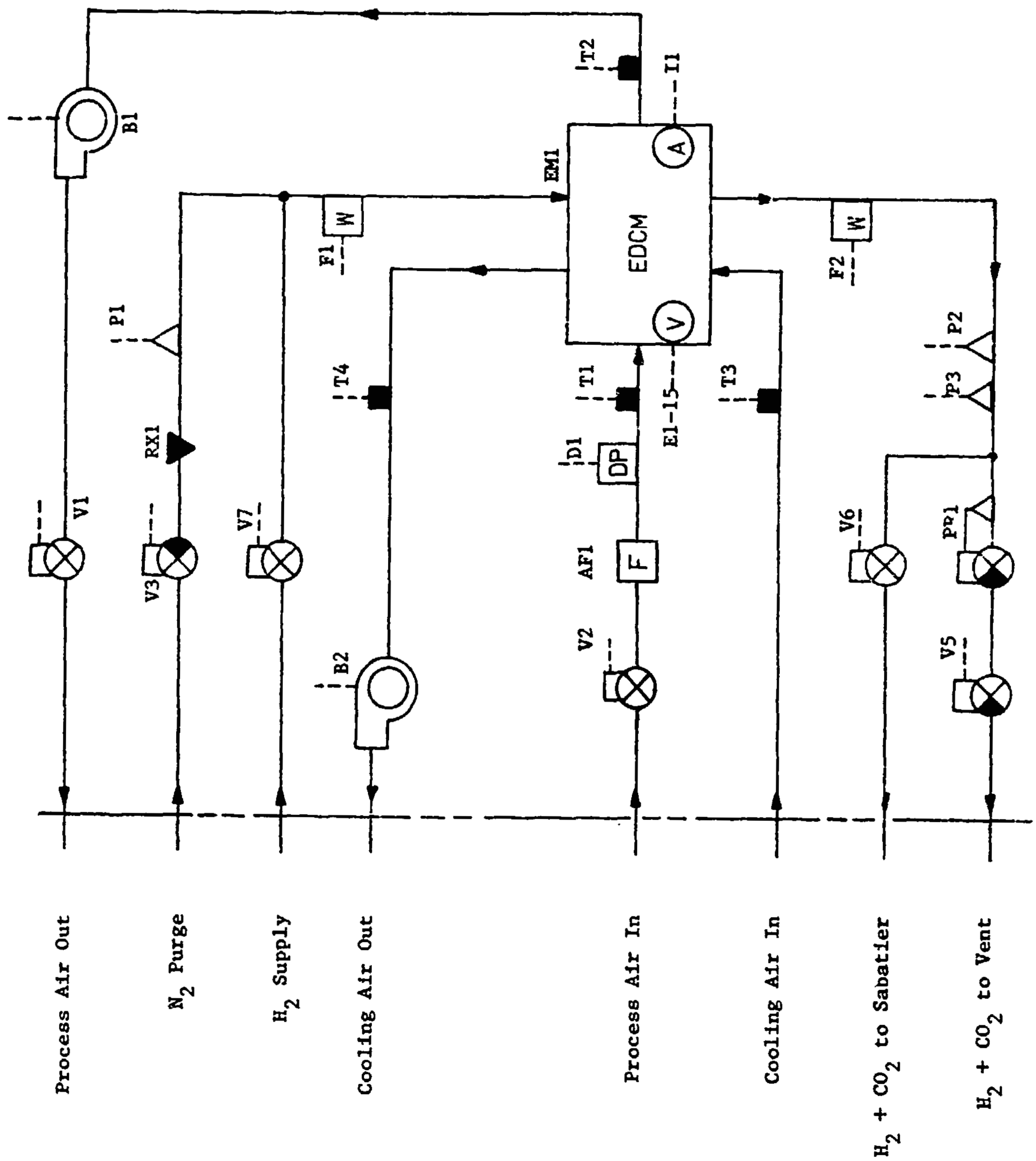

FIGURE 7 CS-3 SCHEMATIC

Hardware Description

The hardware to accomplish the CS-3 function is contained in two separate packages. The mechanical hardware contains the 15-cell EDCM, actuators, sensors, ducting and frame. The second package contains the C/M I. They are interconnected by electrical cabling.

Mechanical Hardware. A front view of the CS-3 mechanical hardware is shown in Figure 8. It is 43 x 46 x 66 cm (17 x 18 x 26 in) and weighs 46 kg (102 lb). One feature of the mechanical design is that all ancillary components are line replaceable units (LRU) and are located near the front of the subsystem. All are maintainable from the front. The EDCM is not an LRU but employs an in situ cell maintenance concept. This means that an individual cell can be electrically jumpered out of operation without physically dismantling the module.

A rear view of the CS-3 is shown in Figure 9 and illustrates the mechanical and electrical interfaces. Four fluid lines supply H_2, N_2 and exhaust the H_2/CO_2 to either vent or the CRS. The process air inlet and outlet ducting connect to a 3.8 cm (1.5 in) diameter flange which mates to the isolation valves. A 12.7 cm (5 in) duct is attached to the cooling air inlet duct flange located beneath the CS-3. The outlet cooling air can be vented directly to the ambient or a return duct can be connected to the fan outlet.

Control/Monitor Instrumentation. The CS-3 C/M I provides automatic mode and mode transition control, automatic shutdown provisions for self-protection, provisions for monitoring typical subsystem parameters and provisions for interfacing with ground test instrumentation, including a Data Acquisition System (DAS). In its normal operating mode the CS-3 is continuously removing CO_2 from the process air passing through it. In addition to this mode, there are four other modes that the subsystem can be in. These are illustrated in Figure 10 which also shows the allowable mode transitions which can occur. The Derated Mode permits operation at the one-person level by reducing module current and operating with seven cells. The other modes are self-descriptive. The sequences which occur when the subsystem is changing from one mode to another are governed by the C/M I.

The preprototype C/M I hardware, excluding interface cabling, is contained in a 53 x 56 x 73 cm (21 x 22 x 28.6 in) enclosure. Included within the enclosure are signal conditioning, power supplies and computer analog/digital interface circuitry.

The CS-3 C/M I is a minicomputer-based automatic instrumentation. The minicomputer of the C/M I consists of a 16-bit Central Processing Unit (CPU), 16K core memory, a Real-Time Clock, Power-Fail control circuits, a communication link to an external DAS and a communication line to a line printer. The CPU executes the control/monitor programs stored in the 16K core memory. The Real-Time Clock allows the programs to be executed on a real-time basis. The Power-Fail control circuits allow the computer to detect and differentiate between a short-term power interruption and a long-term power failure. The communication link to the DAS allows the sensor data to be recorded on the

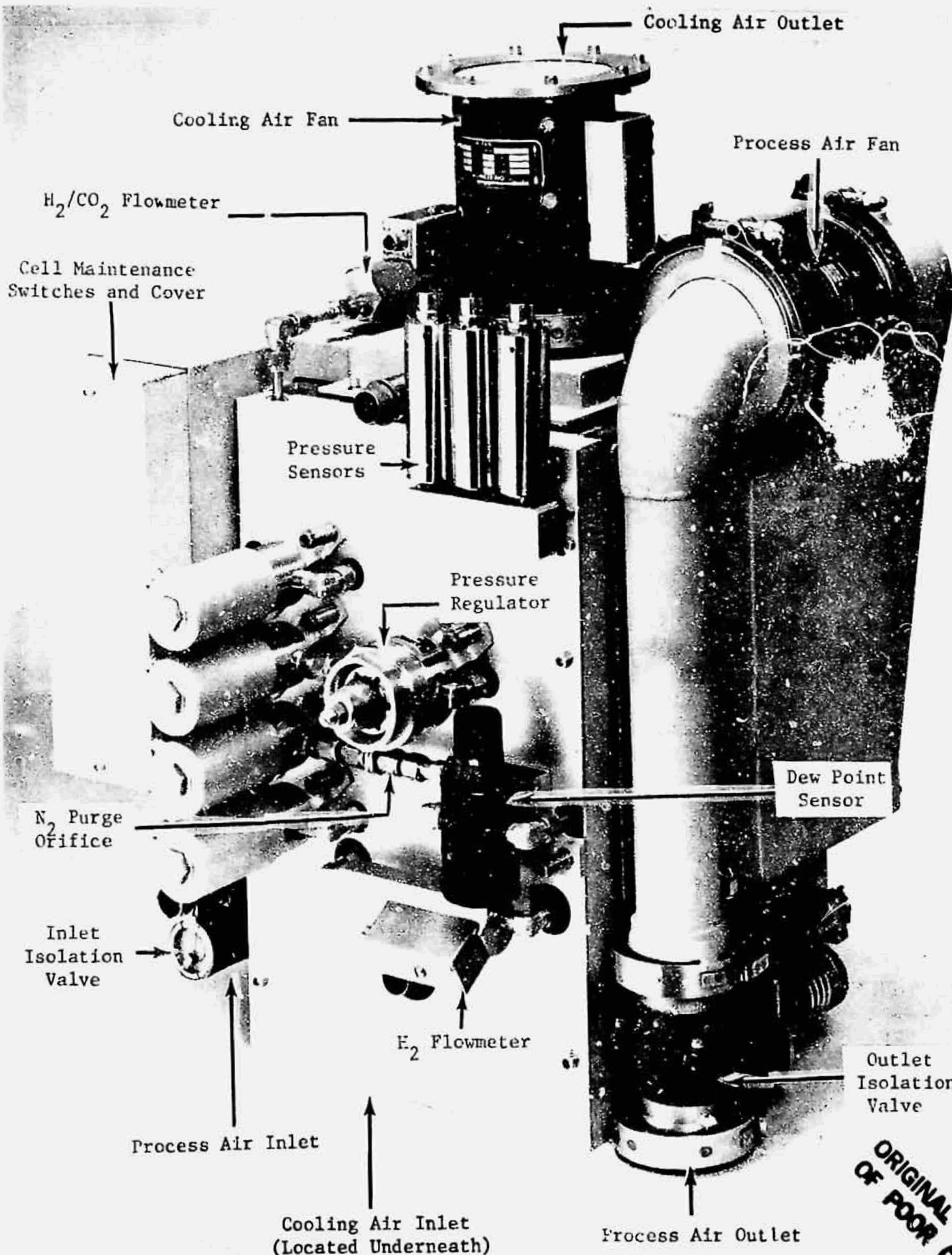

FIGURE 8 CS-3 MECHANICAL HARDWARE (FRONT VIEW)

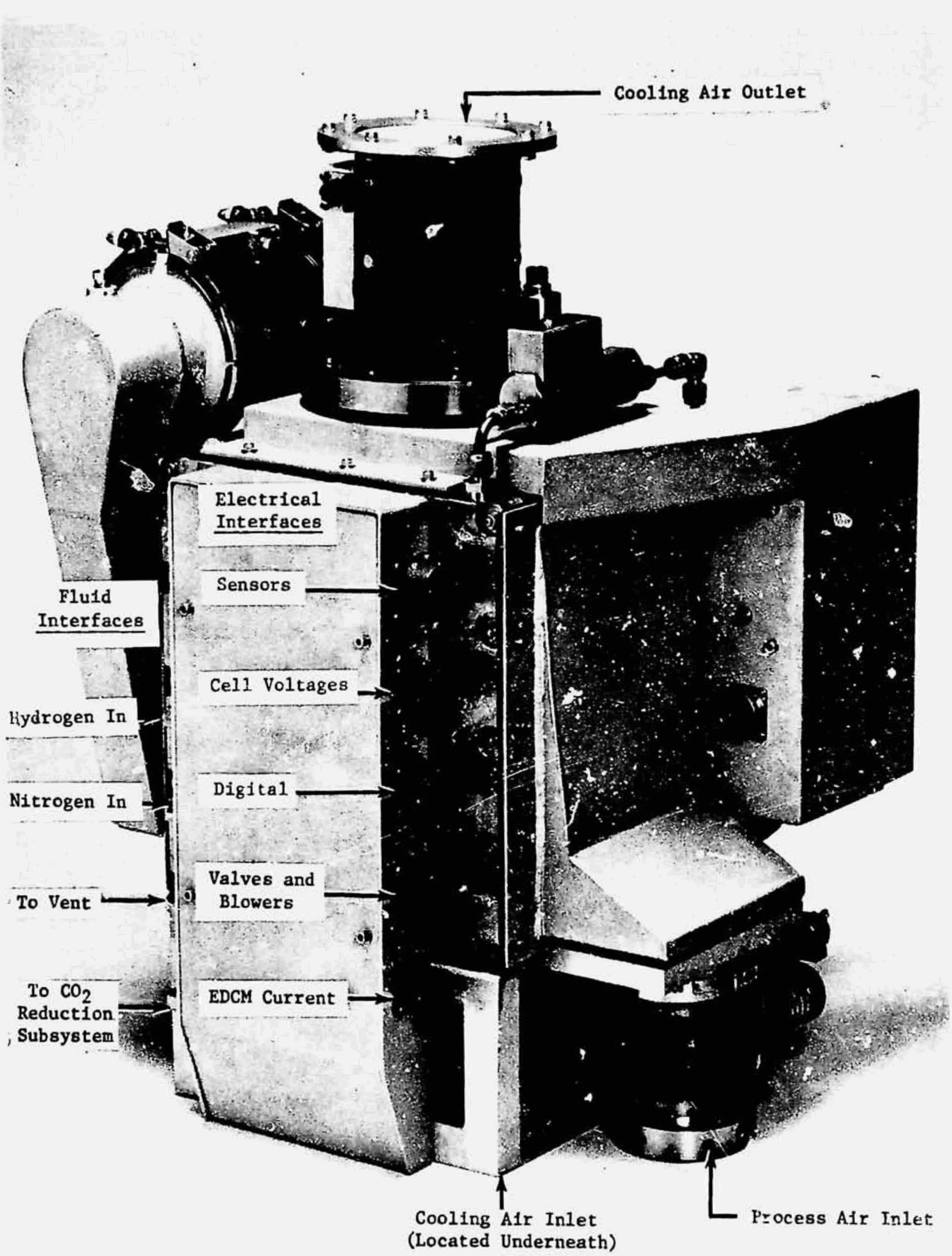

FIGURE 9 CS-3 MECHANICAL HARDWARE (REAR VIEW)

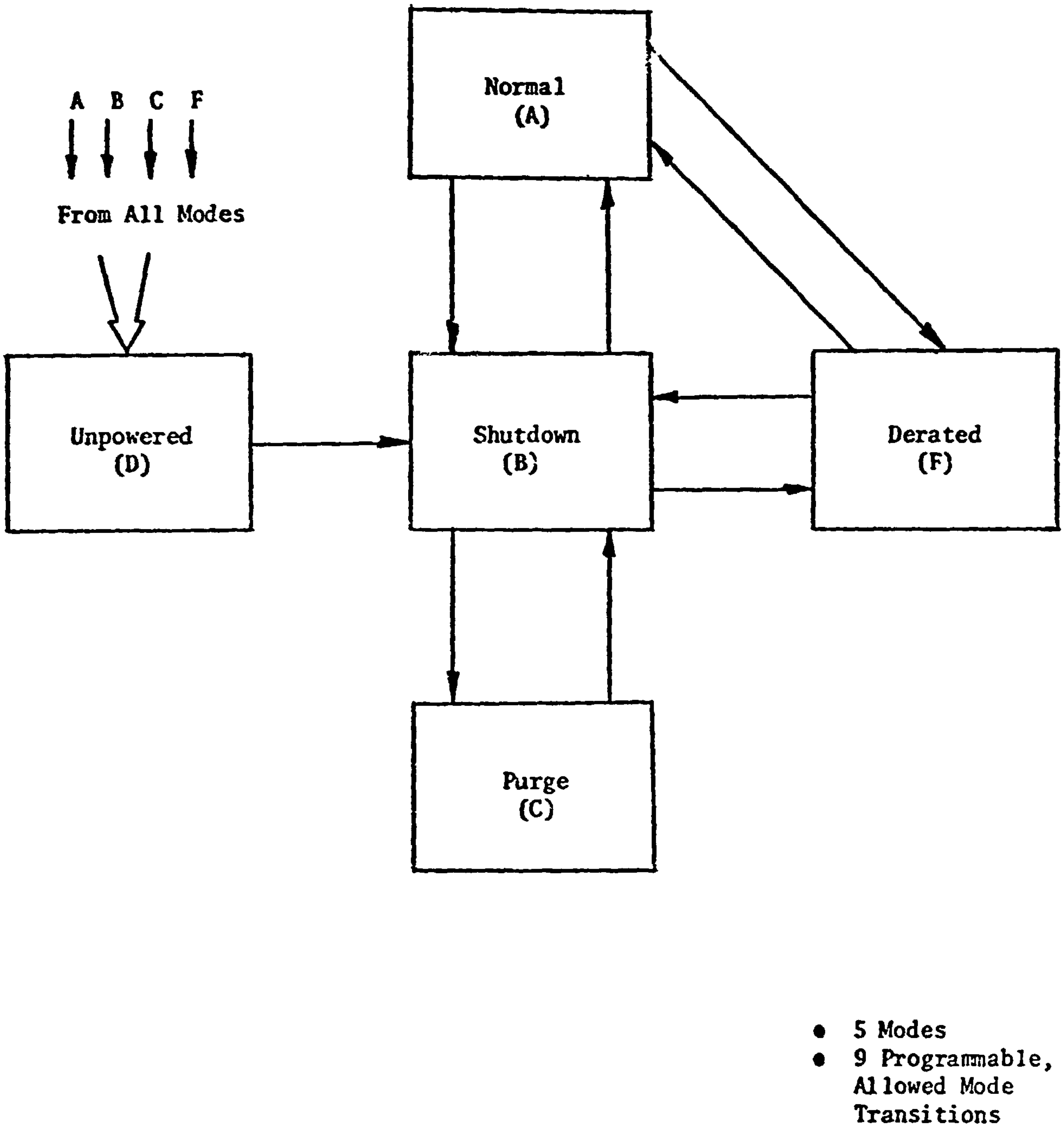

FIGURE 10 CS-3 OPERATING MODES AND ALLOWABLE MODE TRANSITIONS

DAS. The line printer communication link allows the operator/subsystem messages displayed on the CRT to be printed on the line printer.

The C/M I hardware and software are organized to permit real-time communication between the operator and the mechanical subsystem. On the process side, an analog and digital interface board is used for communication of the minicomputer with the sensors and the actuators on the mechanical portion of the subsystem. On the operator/subsystem interface side, the C/M I provides the operator with a front panel and keyboard designed to accept operator commands and display subsystem messages.

Figure 11 shows the operator/subsystem front panel of the CS-3 C/M I. All commands, control and status information of the CS-3 are communicated through this panel. Detailed description of its operation is contained in a separate report.[13]

CS-3 Testing

Parametric and endurance testing was conducted following fabrication, checkout and sensor calibration. The nominal test conditions are shown in Table 2. Two sets of process air dry bulb temperature and RH conditions were explored. Initial data was accumulated at the design specification range of 75 to 85% RH. Later testing indicated a 12% improvement in CO_2 removal efficiency could be achieved by operating at 60% RH. The 60% RH level was adopted as a new baseline.

As part of characterizing CS-3 performance in both RH ranges, a process air pCO_2 span was performed. The results are shown in Figure 12 where CO_2 removal efficiency and cell voltage are plotted against process air inlet pCO_2. The data shows that the performance was at or above the design points. Similarly, a current density span was obtained recording CO_2 removal efficiency and cell voltage as a function of current density. The results are shown in Figure 13. Again the performance was as predicted.

A total of 72 hours of operation with the CS-3 were accumulated in the Derated Mode (one-person capacity). In this mode all cells had gas flows but eight cells were electrically switched out and did not carry current. The remaining seven cells operated at 20.5 mA/cm^2 (19 ASF). The performance is shown in Figure 14 and was as expected, i.e., sufficient CO_2 was removed to satisfy the metabolic needs of one person. Control of module temperature and exit RH to single value levels while satisfying cells with and without current was found to be extremely difficult. In general, it required operation so that the outlet RH was in the wet region (88% RH compared to 68% RH for Normal Mode) to prevent dry out of the noncurrent-carrying cells. As a result, electrolyte was lost from the operating cells, as observed following completion of the 72 hours of testing. It was recommended that this mode of operation be modified by operating all cells but at a reduced current density. The reduced current density should however be sufficiently high to minimize cell subcooling to prevent electrolyte loss.

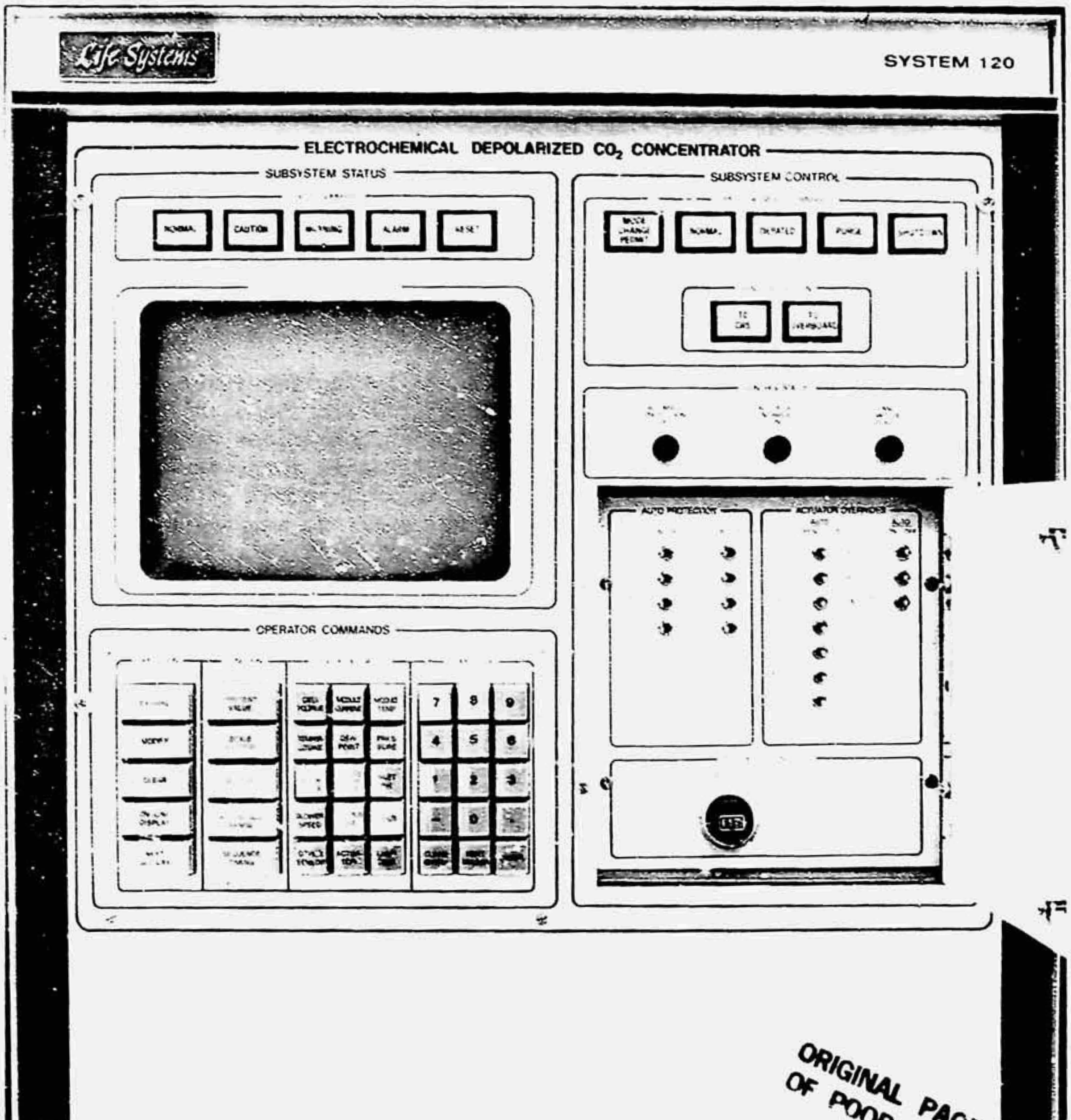

FIGURE 11 C/M I OPERATOR/SUBSYSTEM FRONT PANEL

TABLE 2 NOMINAL CS-3 TEST CONDITIONS

Number of Cells	15
Process Air Flow Rate/Cell, dm^3/min (scfm)	45 (1.6)
pCO_2, Pa (mm Hg)	400 (3)
Inlet Relative Humidity, %	64
Inlet Process Air Temperature, K (F)	290 (63)
Cooling Air Flow Rate/Cell (Max.), dm^3/min (scfm)	283 (10.0)
Cooling Air Temperature, K (F)	290 (63)
Current, A	13.9
Current Density, mA/cm^2 (ASF)	30.1 (28.0)
H_2 Supply Flow Rate, kg/h (lb/h)	0.022 (0.048)

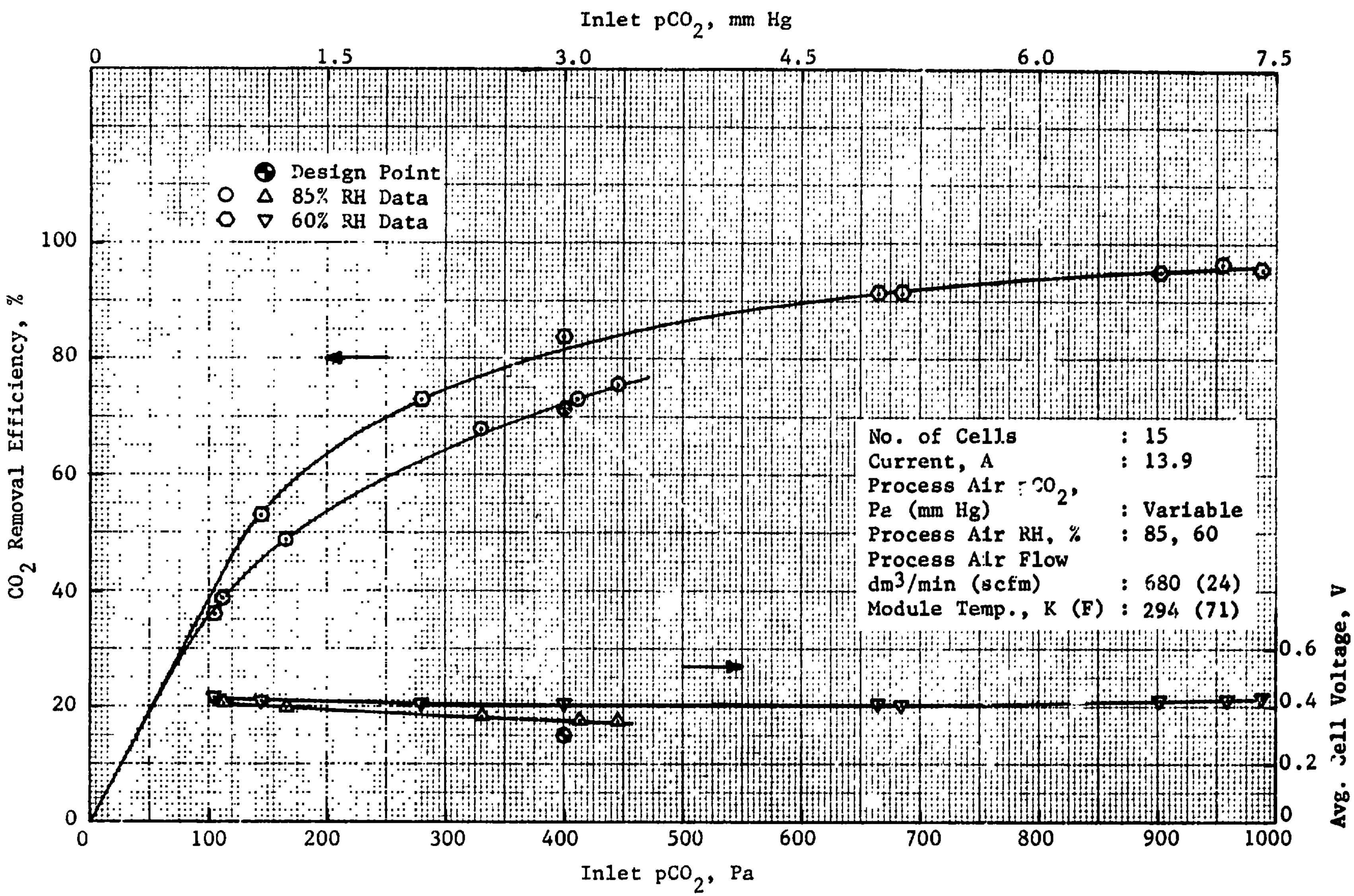

FIGURE 12 CS-3 PERFORMANCE AS A FUNCTION OF PROCESS AIR pCO_2

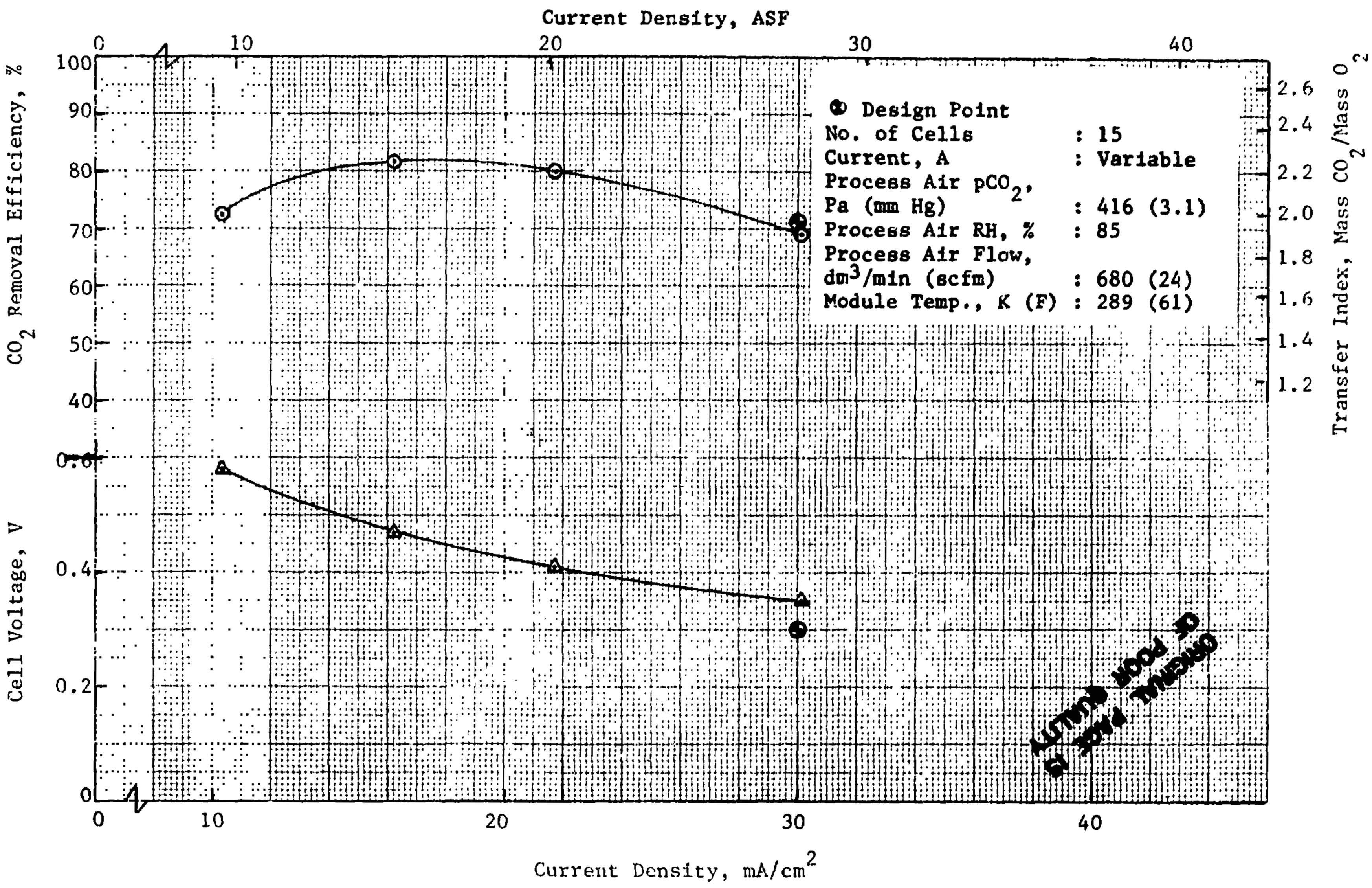

FIGURE 13 CS-3 PERFORMANCE AS A FUNCTION OF CURRENT DENSITY (85% RH)

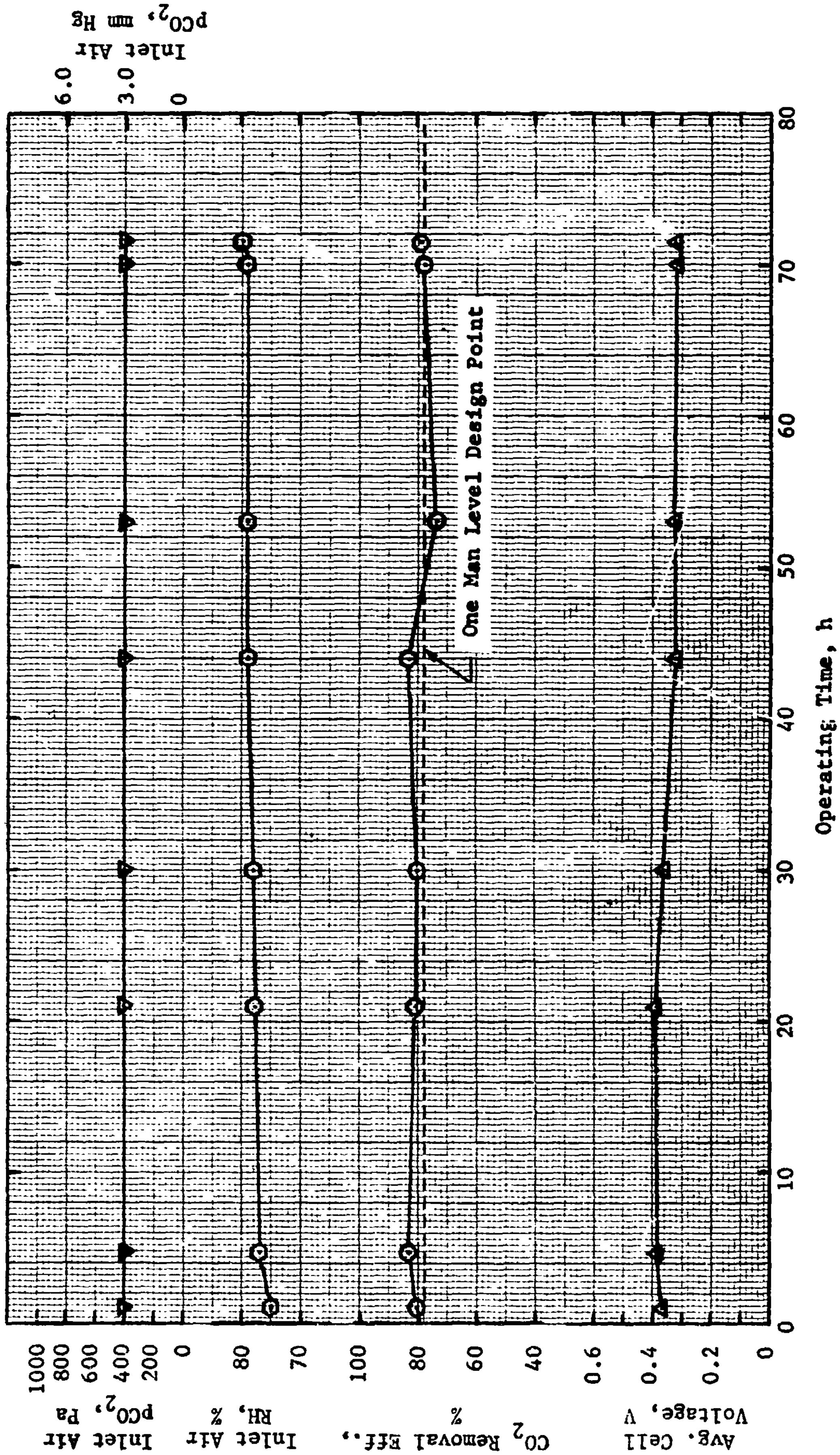

FIGURE 14 CS-3 CUMULATIVE OPERATION IN DERATED MODE

Figure 15 summarizes the CS-3 performance over the entire testing period. Module performance (average cell voltage and CO_2 removal efficiency) as well as inlet process RH and pCO_2 are plotted against cumulative operating time. The derated mode and pCO_2 testing gaps shown were discussed above. Operation of the CS-3 in the Normal Mode reached a cumulative total of 840 h (35 d). Cumulative subsystem operating time in all of its modes prior to delivery was 2,232 h (93 d). It was demonstrated that at the design pCO_2 level of 400 Pa (3.0 mm Hg) and the modified RH range, the CS-3 could surpass its goal of removing 3 kg/d (6.6 lb/d) of CO_2. An average CO_2 removal level equivalent to that generated by 3.4 persons was achieved.

CS-3 Math Model

As part of the CS-3 program, a steady-state computer simulation, or math model, was developed to describe the subsystem performance. The model combined mathematical expressions describing the performance of the EDC cells with expressions that characterize the major mechanical components of the subsystem. Expressions for overall mass and energy balances were included. The model was capable of predicting performance over wide operating ranges and the computer simulation results agreed with experimental data over the prediction range.

The computer program calculated the steady-state performance characteristics of the subsystem and its components subject to a given set of input conditions. The calculations included module parameters, intercomponent and subsystem fluid interface parameters (flows, temperatures and pressure), component and subsystem power and heat generation and subsystem equivalent weight.

Several experiments were conducted with the hardware components to support the computer module. These (1) established the performance characteristics of the hardware and (2) verified the predictions of the model. The experiments characterized the EDCM, the process and cooling air blowers, the N_2 flow orifice and the H_2 solenoid valve.

The math model computer program was organized to read a set of input conditions, perform the calculations and print the results. The program can be used as a subroutine in a larger program which would simulate the integrated operation of the CS-3 subsystem as will occur with the RLSE hardware. Details of the math model and results can be found in a separate report.[14]

SYSTEM INTEGRATION DEVELOPMENTS

The system integration development activities performed as part of this program focused on the EDC as part of laboratory breadboard integration of ORSs or ARSs. These activities included (1) the five-cell, liquid-cooled EDCM integrated with an OGS and a Sabatier-based CO_2 Reduction Subsystem (S-CRS) to form the LBS-S/ORS-1(L), (2) an air-cooled EDC integrated with an OGS and a B-CRS to form a four-person Bosch-based ORS (LBS-B/ORS-4(A)) and (3) the six-cell, liquid-cooled EDC combined with other components to form a self-contained, one-person, experimental ARS. The following sections discuss the design, fabrication and testing of these integrated systems.

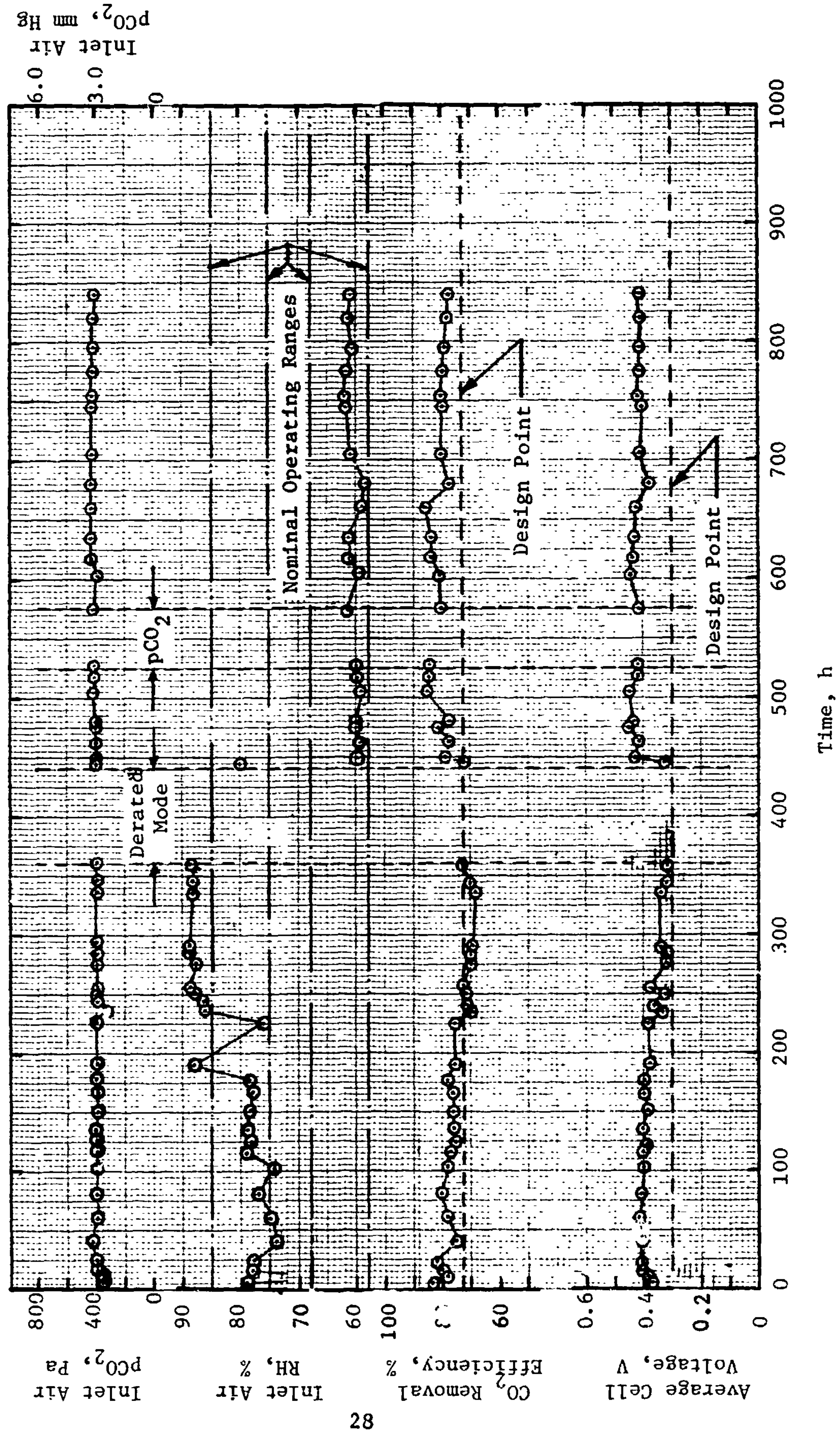

FIGURE 15 CS-3 CUMULATIVE OPERATION IN NORMAL MODE (30 mA/cm^2 (28 ASF))

One-Person Laboratory Breadboard System

The five-cell, one-person capacity, liquid-cooled EDC installed in the CX-1 was integrated with an OGS and an S-CRS to form a LBS-S/ORS-1(L) and was tested for a 30-day period. The overall objectives of the test were to:

- Demonstrate long-term, multicell, liquid-cooled EDC operation using advanced cell hardware
- Test the EDC with OGS-generated H_2
- Test the Contractor-developed Sabatier reactor with EDC exhaust gas, i.e., H_2, CO_2 and water vapor
- Expand integration technology by operating three subsystems as one ORS

The integrated testing followed refurbishment and modification to the CX-1 and its TSA. The major modifications included upgrading the system's capability to allow operation of the larger (4.6 dm^2 (0.5 ft^2) versus 2.3 dm^2 (0.25 ft^2)) advanced cells at elevated current densities. Also, provisions for liquid cooling, including feedback controlled temperatures, were added to the subsystem and TSA.

Figure 16 is a block diagram of the one-person ORS. As Figure 16 shows, the integrated system had a capability to vary the amount of H_2 entering the EDC or the Sabatier reactor by supplying an external H_2 source. This could simulate eventual integration with the Nitrogen (N_2) Supply Subsystem (NSS) based on hydrazine (N_2H_4) technology.

Figures 17, 18 and 19 are photographs of the EDC (CX-1), OGS and Sabatier reactor used as part of the one-person ORS. The Sabatier reactor was developed and fabricated as part of a Contractor-funded activity but was tested as part of the present program. Figure 20 shows the integrated one-person ORS test facilities, including TSA. Following individual subsystem shakedown testing, a 30-day integrated endurance test was performed. Prior to test initiation, baseline operating conditions for the integrated system were established. These conditions are listed in Table 3. The endurance test was performed by maintaining the baseline conditions at constant values.

The performance of the one-person, liquid-cooled EDC and the S-CRS for the 30 days of testing is shown in Figure 21. Of special interest is the high cell voltage of 0.4 V per cell for the EDC and the high average transfer efficiency of 76% for the duration of the test, since the advanced module was operated at a current density of 30.1 mA/cm^2 (28 ASF). As shown, the H_2 conversion efficiency of the Sabatier reactor averaged approximately 97% throughout the total test time.

In addition to the performance characteristics obtained from the testing, significant contributions to the operation of integrated systems were established in the areas of startup sequence, shutdown sequence, common system purge and subsystem performance monitoring.

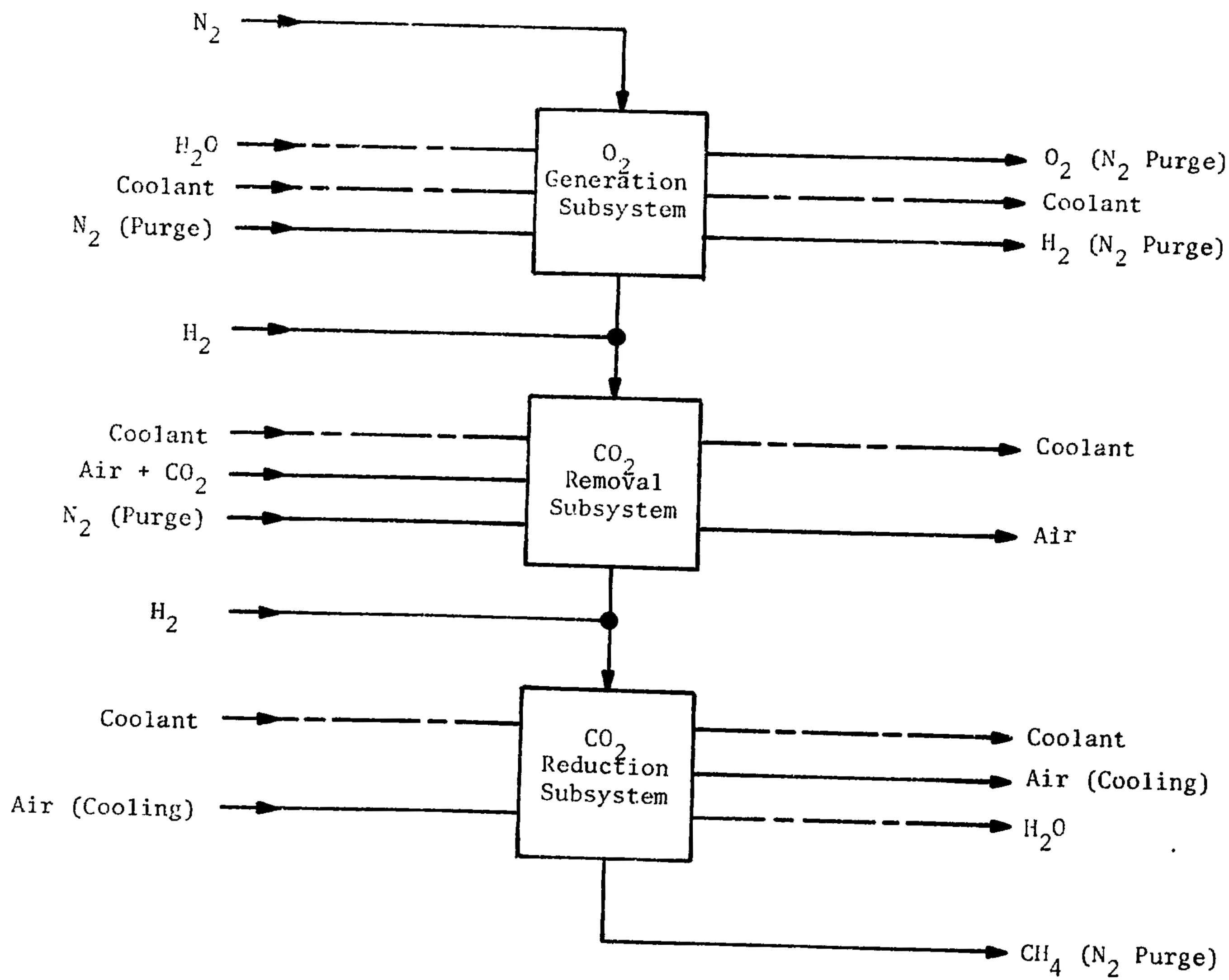

FIGURE 16 ONE-PERSON OXYGEN RECOVERY SYSTEM BLOCK DIAGRAM

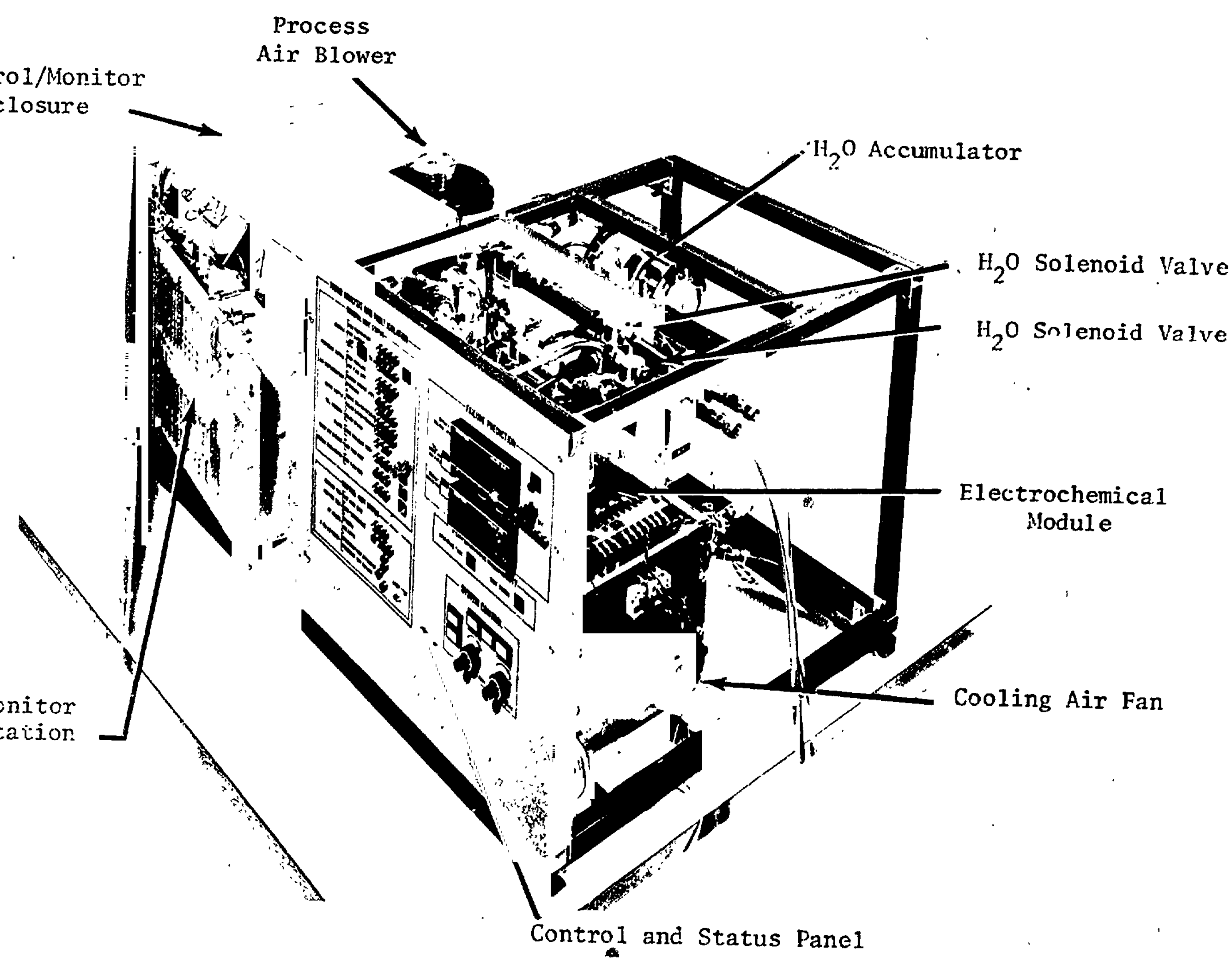

FIGURE 17 ONE-PERSON ELECTROCHEMICAL DEPOLARIZED CO_2 CONCENTRATOR

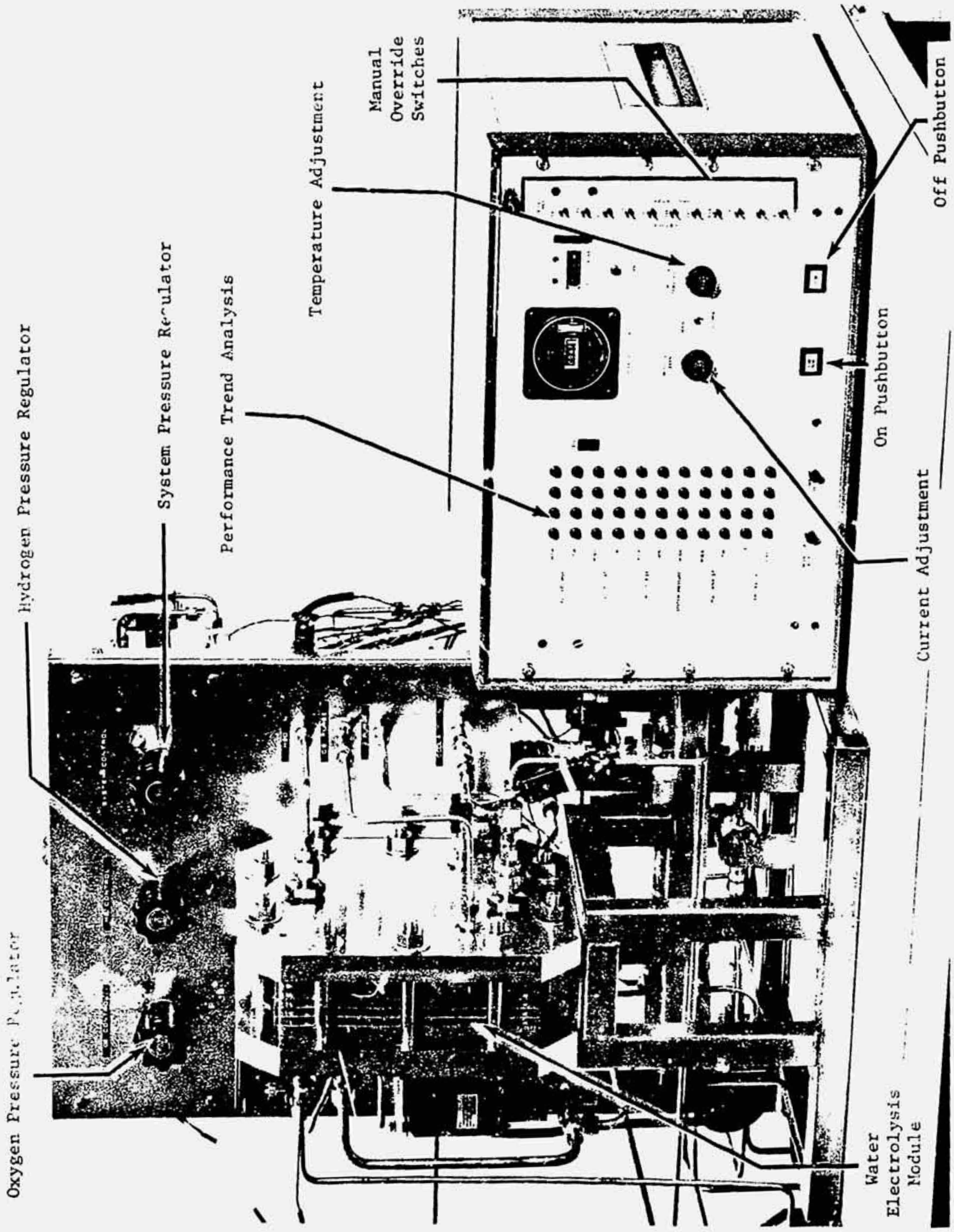

FIGURE 18 ONE-PERSON OXYGEN GENERATION SYSTEM

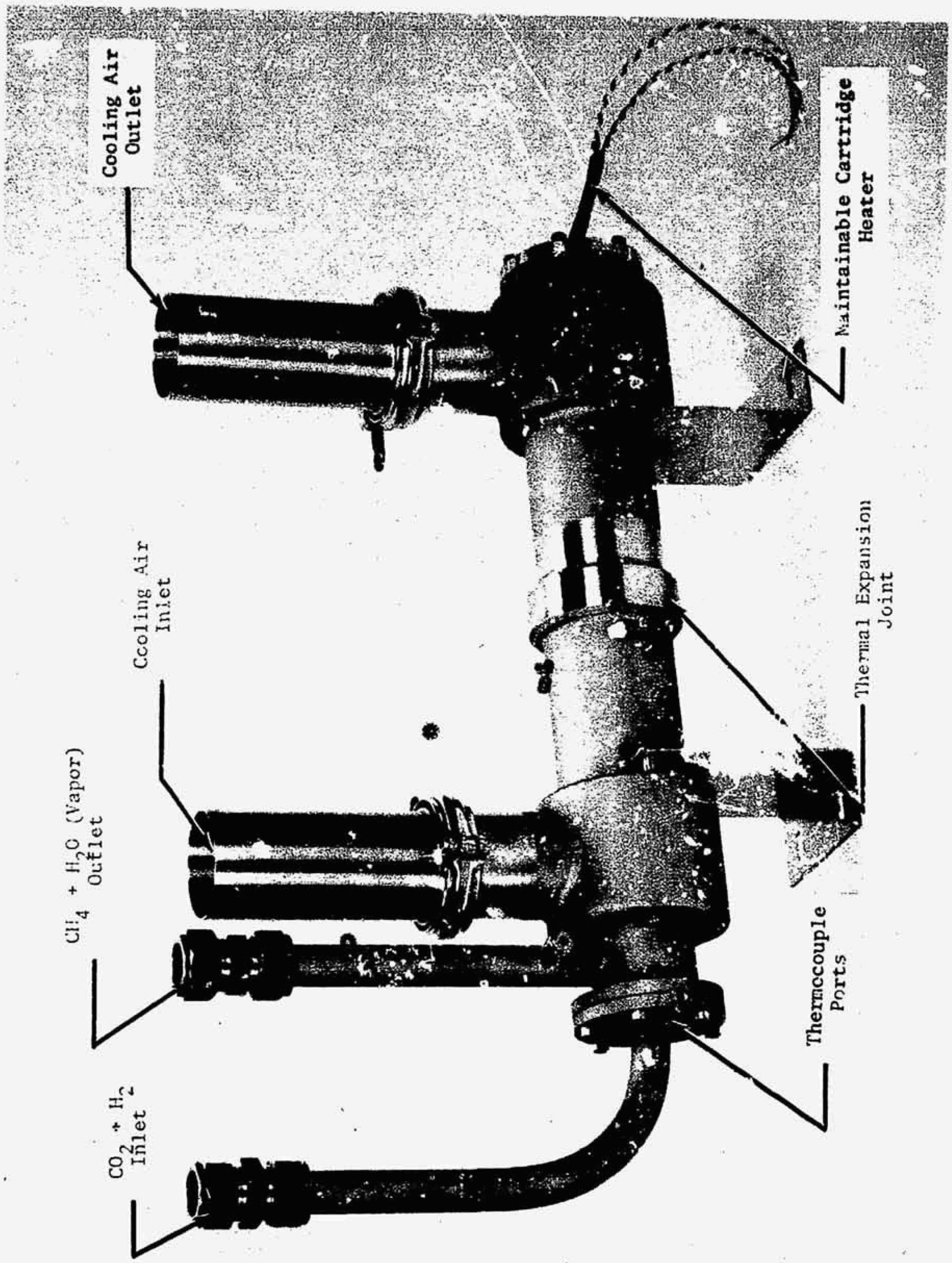

FIGURE 19 ONE- TO THREE-PERSON SABATIER REACTOR

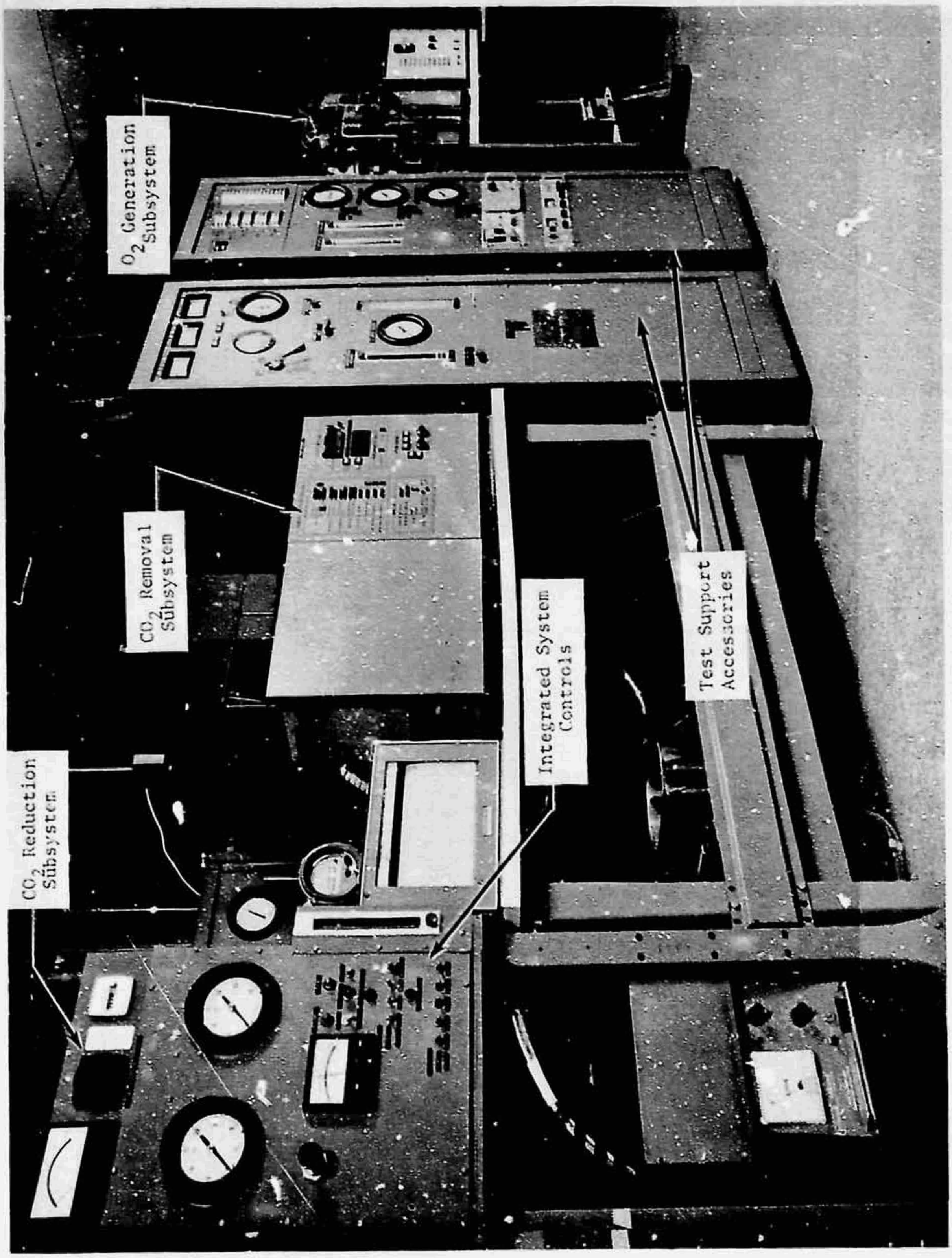

FIGURE 20 ONE-PERSON LABORATORY SYSTEM TEST FACILITY

TABLE 3 BASELINE OPERATING CONDITIONS FOR THE LBS-S/ORS-1(L)

Process Air Inlet	
pCO_2, Pa (mm Hg)	400 (3.0)
Air Flow Rate, dm^3/min (scfm)	230 (8.0)
Dew Point Temperature, K (F)	286 to 289 (56 to 60)
Dry Bulb Temperature, K (F)	291 to 294 (65 to 70)
Relative Humidity, %	61 to 84
EDC Module	
Number of Cells	5
Current, A	13.7
Current Density, mA/cm^2 (ASF)	30.1 (28)
Temperature, K (F)	292 to 298 (73 to 77)
Pressure, kPa (psia)	101 (14.7)
Cell Voltage, V	0.3
CO_2 Removal Efficiency, %	74
Power Generated, W	21
Heat Generated, W (Btu/h)	65 (220)
Water Electrolysis Module	
Number of Cells	6
Cell Current, A	19.4
Cell Current Density, mA/cm^2 (ASF)	208.7 (194)
Temperature, K (F)	333 to 339 (140 to 150)
Pressure, kPa (psia)	965 (140)
Cell Voltage, V	1.60
Power Required, W	186
Heat Generated, W (Btu/h)	14 (48)
Sabatier Reactor	
Temperature, K (F)	644 (700)
Pressure, kPa (psia)	108 (15.7)
CO_2 Reduction Efficiency, %	68
H_2 Conversion Efficiency, %	96

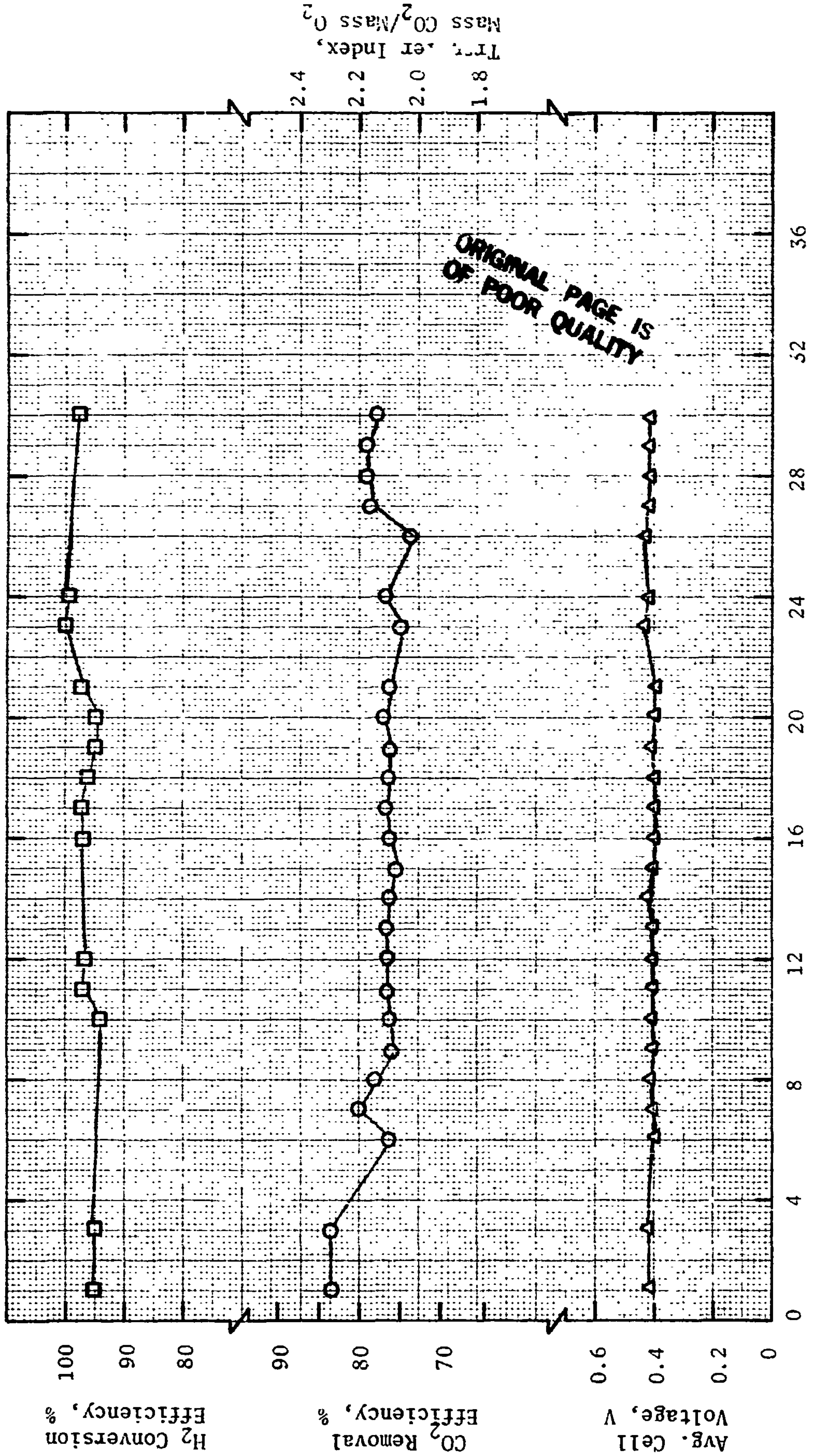

FIGURE 21 EDC AND SABATIER PERFORMANCES FOR 30-DAY INTEGRATED ENDURANCE TEST

Four-Person Laboratory Breadboard System

A four-person capacity, air-cooled EDC (CXA-4(A)) was modified and refurbished to support testing of the LBS-B/ORS-4(A) being evaluated under a separate NASA-funded program.[15,16] The overall objectives of the test were to:

- Demonstrate the compatibility of the EDC with a B-CRS primarily at the H_2/CO_2 EDC exhaust/B-CRS feed interface
- Test the EDC with OGS-generated H_2
- Extend integration technology by operating three subsystems as one ORS

Figure 22 is a block diagram showing the closed O_2 loop system with an integrated EDC, B-CRS and OGS. A previously developed six-person capacity, self-contained EDC[6] was refurbished and modified to form the CXA-4(A). Only three of the six one-person design capacity modules were used to provide the CO_2 removal capacity for four men, e.g., 4.0 kg CO_2/d (8.8 lb CO_2/d). To achieve the extra CO_2 removal rate, the modules were operated at the higher than design current density (26.9 versus 22.6 mA/cm^2 (25 versus 21 ASF)). The electrochemical cells were not of the advanced, lightweight style but were externally air-cooled 2.3 dm^2 (0.25 ft^2) cells.

The CXA-4(A) and its associated TSA were assembled to port the integrated testing program. Figure 23 is the block diagram of th BS-B/ORS-4(A) indicating the three subsystems and their TSA. The EDC TSA consisted of modifications to the existing Fluid Supply Unit (FSU) and Test Accessories Control Unit and additions of a new Coolant Supply Unit (CSU).[6] Also, a new EDC testing facility, an Air Supply Unit (ASU), was added. This TSA is further discussed below.

Table 4 lists the operating conditions and characteristics for the EDC used in testing the LBS-B/ORS-4(A). A total of 900 hours were accumulated through subsystem level and integrated system level testing. Figure 24 shows the overall performance of the EDC over the 900 hours of operating time. Shown are average cell voltage, CO_2 removal efficiency, current density and inlet air pCO_2 as a function of time. The performance is consistent with externally air-cooled 2.3 dm^2 (0.25 ft^2) cells. Successful operation of this EDC throughout the testing was in part responsible for the successful completion of the testing of the Bosch-based ORS.

One-Person Air Revitalization System

A part of this program had shown that individually developed subsystems such as an EDC, S-CRS and OGS can be successfully integrated into a laboratory breadboard ORS at the one-person level (see above). The 30 days of endurance testing of the ORS showed that the three subsystems would remove and reduce metabolically-generated CO_2 and produce the required O_2 levels for one person.

The next step in the development of the EDC for spacecraft ARS application was completed as part of the program activities. This activity was the design,

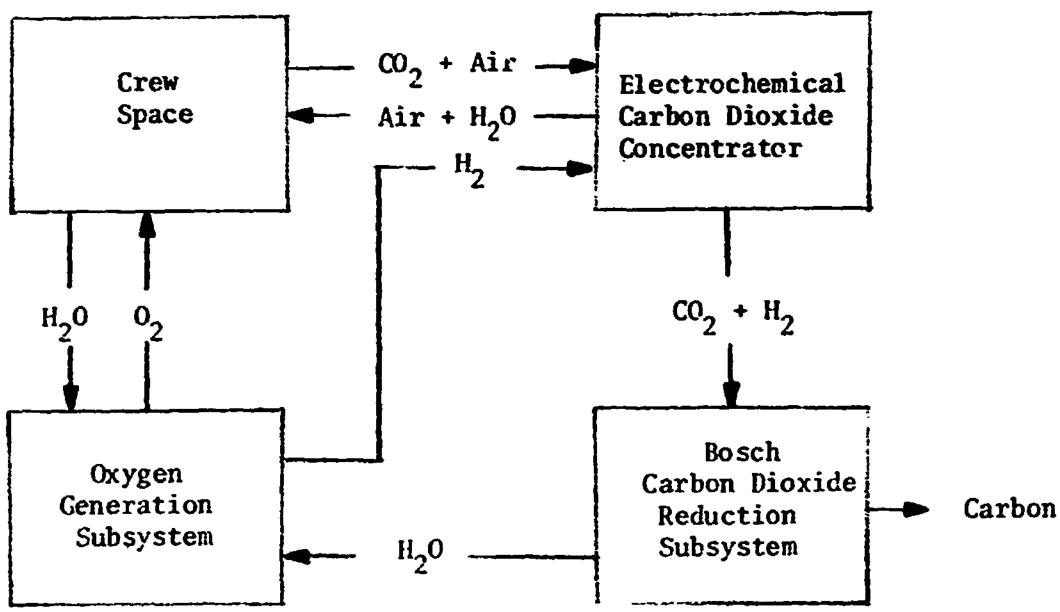

FIGURE 22 CLOSED OXYGEN LOOP WITH INTEGRATED EDC/B-CRS/OGS

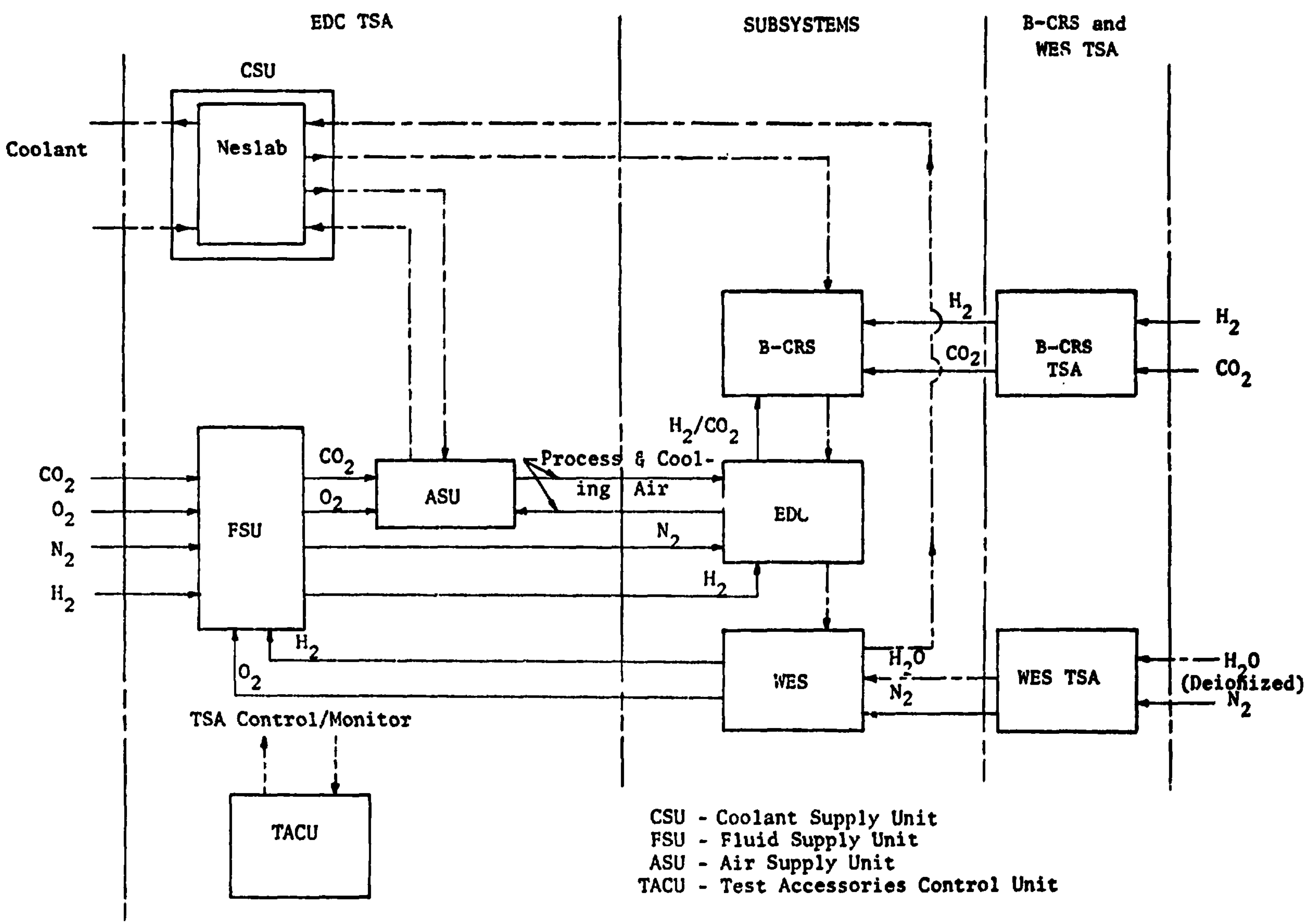

CSU - Coolant Supply Unit
FSU - Fluid Supply Unit
ASU - Air Supply Unit
TACU - Test Accessories Control Unit

FIGURE 23 LBS-B/ORS-4(A) BLOCK DIAGRAM SHOWING RELATIONSHIP BETWEEN TSA AND SUBSYSTEMS

TABLE 4 BASELINE OPERATING CONDITIONS OF THE FOUR-PERSON LABORATORY BREADBOARD EDC

Operating Time, h	900[a]
Number of Cells	45
Current Density, mA/cm^2 (ASF)	22.1 (20.5)
Current, A	5.00
pCO_2 Range, Pa (mm Hg)	306 to 466 (2.3 to 3.5)
Process Air Flow Rate, dm^3/min (cfm)	710 (25)
Process Air Temperature, K (F)	286 (56)
Process Air Dew Point, K (F)	284 (51)
CO_2 Removal Efficiency, %	73
Transfer Index	2.0
Average Cell Voltage, V	0.34
Power Generated, W	77
Heat Generated, W (Btu/h)	200 (680)

(a) Includes Familiarization, Integrated Checkout and Shakedown, Design Verification and Endurance Tests.

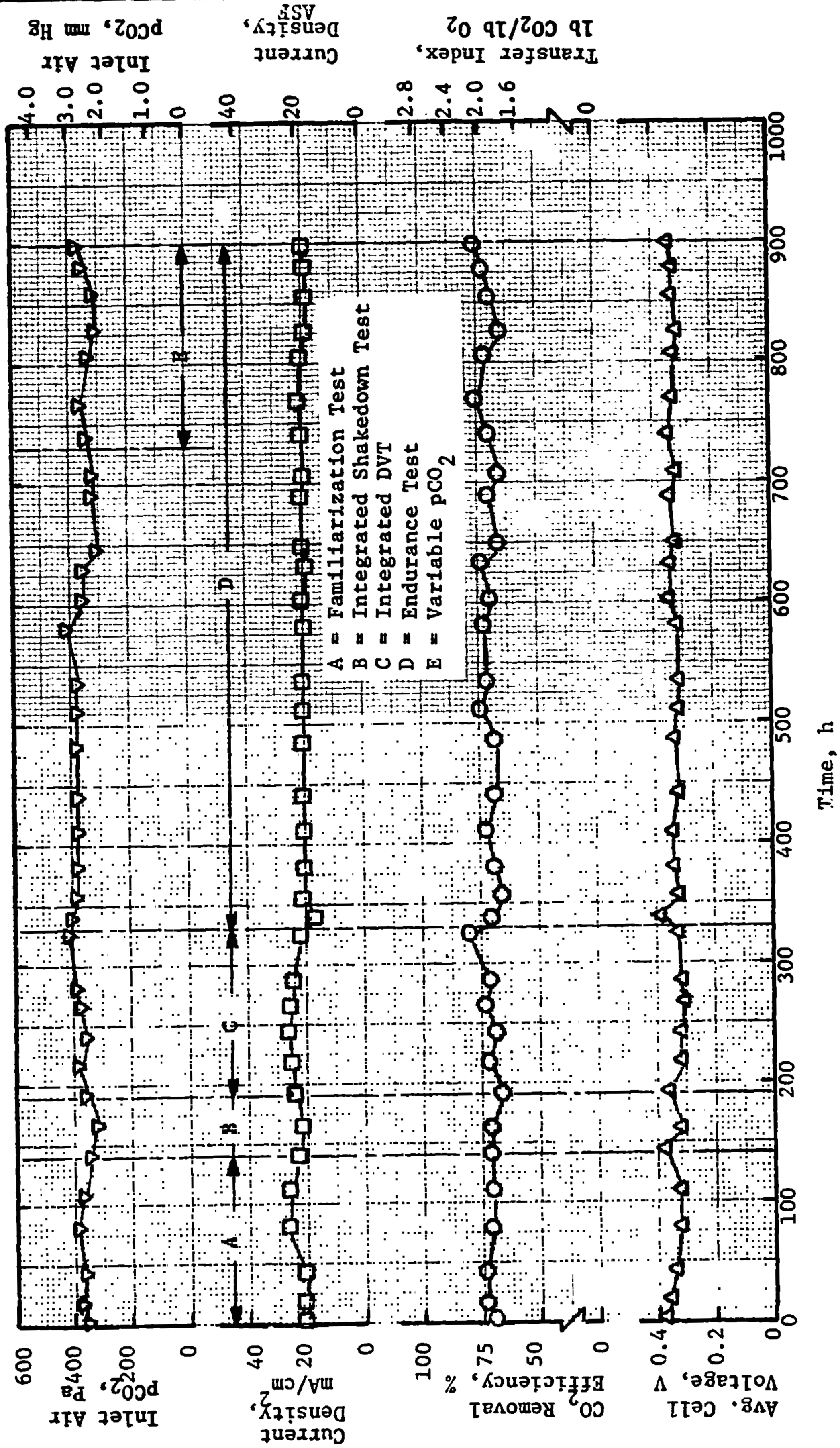

FIGURE 24 EDC PERFORMANCE DURING FOUR-PERSON INTEGRATED LABORATORY BREADBOARD TESTING

fabrication and testing of a one-person, experimental Air Revitalization System (ARX-1). The philosophy for this next-step approach was different than in the previously integrated laboratory breadboard system where each of the three subsystems (1) were self-contained, (2) had their own C/M I, (3) were started and shut down independently, (4) were tied together by appropriate interfaces and (5) contained redundant components.

The self-contained system versus subsystem approach selected for the ARX-1 was based on reducing subsystem interfaces, eliminating redundant components and utilizing the products (heat, electrical power, fluids) of one subsystem in another. Also, the C/M I was designed as a single unit that would operate all components as a single system by providing for one-button startup/shutdown of all ARS functions, automatic sequencing and control and monitoring for self-protection and safe operation.

Advantages of the integrated system approach, with specific examples, are listed in Table 5. The objective of this portion of the program activities was to demonstrate, through actual testing, the validity of the approach as well as verify the advantages, identify new ones and isolate shortcomings for future correction.

ARX-1 Concept and Hardware Definition

The concept of a self-contained ARS (at the system level) is shown in block diagram form in Figure 25. Shown are the three principal subsystems needed to remove CO_2 from and provide O_2 to the crew space. These are the EDC, S-CRS and the OGS.

Additional subsystems and components are needed to provide other air revitalization functions. An NSS using decomposition of N_2H_4 provides for N_2 lost through cabin leakage. Also, the NSS supplies extra H_2 required by the S-CRS. A Cabin Humidity Control Subsystem (CHCS) is used to supply conditioned air to the EDC at RH for optimum efficiency and to remove the metabolic- and EDC-produced moisture from the cabin air. A Water Handling Subsystem (WHS) collects, stores and distributes liquid water within the ARS. Coolant flow components (not shown in Figure 25) distribute spacecraft-provided liquid coolant throughout the ARX-1. Finally, the centralized C/M I provides for automatic, integrated operation.

Table 6 lists the design specifications and characteristics established for the ARX-1. Each of the elements of the ARX-1, with the exception of the OGS and NSS, are discussed in the following subsections. The activities associated with the development of the OGS and NSS for the ARX-1 were funded under separate NASA Ames Research Center programs.[17,18] The development associated with the S-CRS and its major components were supported by Contractor funds. Only the EDC development, TSA, general integration aspects and testing were performed as part of this contract.

CO_2 Removal/Cabin Humidity Control Subsystem Hardware. The liquid-cooled EDC concept lends itself well to the centralized ARS approach especially when integrated with a humidity control concept using a condensing heat exchanger.

TABLE 5 ADVANTAGES OF DEVELOPING AND TESTING SELF-CONTAINED SYSTEM HARDWARE

Advantage	Examples
1. Elimination of duplicate components	• Single blower supplies air to CHCS and EDC • Common shutoff, purge and isolation valves • Single regulator backpressures S-CRS and EDC exhaust gases • Water accumulators, valves and pumps for S-CRS and CHCS combined • Single blower cools S-CRS reactor and separates entrained liquid from CHCS process air • Series and parallel flow of coolant minimizes valves, lines and fittings
2. Reduction of TSA hardware, interfaces and expendables	• H_2 from OGS used in EDC and S-CRS • Water collected from CHCS and S-CRS used in OGS • Single power interface • EDC process air from CHCS instead of TSA • H_2 plus CO_2 mixture for S-CRS from EDC
3. Centralized Control and Monitor Instrumentation	• Single C/M I operator/system interface panel • One-button startup and shutdown for integrated system
4. Provides real-life test conditions	• Transient performance evaluated • Simultaneous testing of subsystems and components • Early development problems uncovered - not only major ones, but also those often overlooked, e.g., coolant and water handling • Interaction between major components identified
5. Single System philosophy provides technology base for actual flight hardware	• No surprises when adding ancillary and interface components later
6. Saves development costs	• Hardware components eliminated • Test personnel time minimized • Expendable fluids minimized

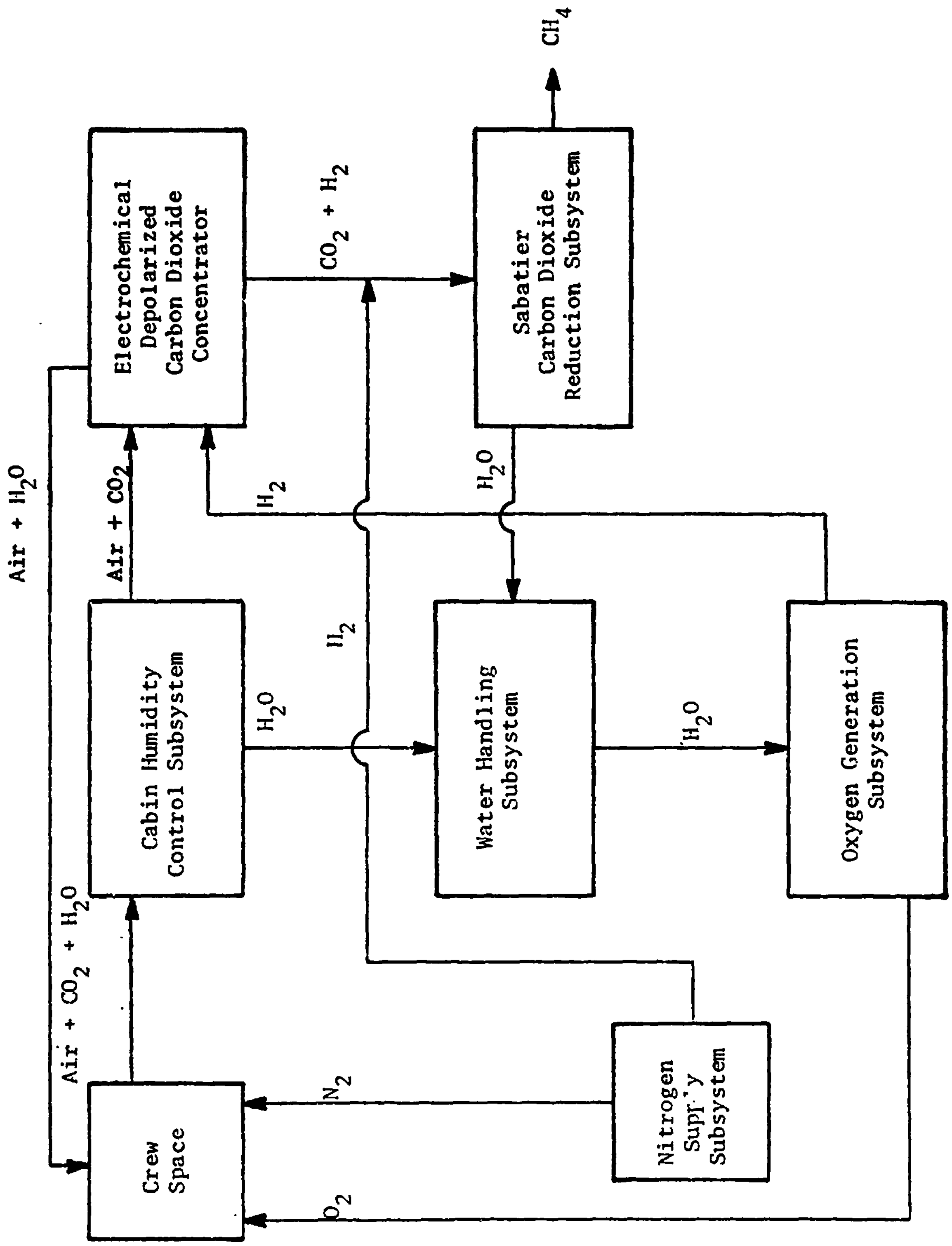

FIGURE 25 AIR REVITALIZATION SYSTEM BLOCK DIAGRAM

TABLE 6 ONE-PERSON AIR REVITALIZATION SYSTEM DESIGN CHARACTERISTICS

Crew Size	1
CO_2 Removal Rate, kg/d (lb/d)	1.00 (2.20)
O_2 Generation Rate, kg/d (lb/d)	1.03 (2.27)[a]
Water Vapor Removal Rate, kg/d (lb/d)	1.80 (3.96)
Liquid Water Production Rate, kg/d (lb/d)	1.49 (3.27)
Methane Production Rate, kg/d (lb/d)	0.36 (0.79)
Nitrogen Production Rate, kg/d (lb/d)	0.60 (1.32)

(a) Consists of 0.84 kg/d (1.84 lb/d) O_2 metabolic and 0.19 kg/d (0.43 lb/d) for leakage requirements.

As a result, the liquid-cooled EDC concept combined with the cabin humidity control function was selected for the ARX-1. Other reasons for closely grouping the CO_2 removal and cabin air moisture control are that the major components interface directly with a flowing stream of cabin air and the air processed by a condensing heat exchanger is ideally suited for achieving reliable and efficient EDC operation. Also, redundant components such as a process air fan can be eliminated.

Figure 26 is a block diagram of the combined CHCS/EDC functions. Baseline operating conditions are given in Table 7. Filtered cabin air enters a condensing heat exchanger where moisture is removed to control the cabin dew point. A portion of the air passes through the EDCM for CO_2 removal. The EDC exhaust air and the remaining process air are returned to the cabin. The moisture removed by the condensing heat exchanger, along with some cabin air, is passed to the WHS components Hydrogen required by the EDC is obtained from the OGS and is sent mixed with the CO_2 to the S-CRS. A N_2 purge of the H_2-carrying cavities of the EDC is provided. Oxygen from the OGS and makeup N_2 from the NSS are added to the air upstream of a filter prior to delivery to the cabin.

The EDCM consists of six advanced liquid-cooled cells. This module was discussed previously and shown in Figure 6.

The major component of the CHCS is the condensing heat exchanger shown in Figure 27. The one-person condensing heat exchanger design was based on the previously established concepts. Details of construction and operation of the 11.4 kg (25.0 lb) unit are discussed in a prior report.[11]

<u>CO_2 Reduction Subsystem Hardware</u>. The Sabatier-based CO_2 reduction process was selected for the ARX-1. This process is ideally suited for an ARS using a N_2H_4-based NSS which produces H_2 as a byproduct. Sufficient H_2 is then available to convert all of the metabolic CO_2 for subsequent O_2 recovery. The Sabatier process is based on the reaction of

$$4H_2 + CO_2 = 2H_2O + CH_4 + \text{heat}$$

Figure 28 is a block diagram of the S-CRS. Carbon dioxide and H_2 from the EDC enter the Sabatier reactor where the reactants undergo conversion to methane (CH_4) and water. The water is condensed in a zero-gravity compatible, liquid-cooled, porous plaque condenser/separator and is removed to the WHS. The reactor exhaust gases, primarily CH_4, are passed to an Attitude Control System (ACS) or storage. However, provisions have been made for venting the product gases minus the water to overboard vacuum. A vent to cabin, following an N_2 safety purge, is provided to depressurize the S-CRS for maintenance. The Sabatier reactor is air-cooled. The main component of the S-CRS, the Sabatier reactor, was shown in Figure 19. The operating characteristics and anticipated performance of the one-person level S-CRS are shown in Table 8.

<u>Water Handling Subsystem Hardware</u>. Water is generated and consumed at various locations in the ARX-1. For purposes of design and fabrication, the water handling components were treated as a separate subsystem. A block diagram of the WHS is shown in Figure 29. The two principal water sources are from the

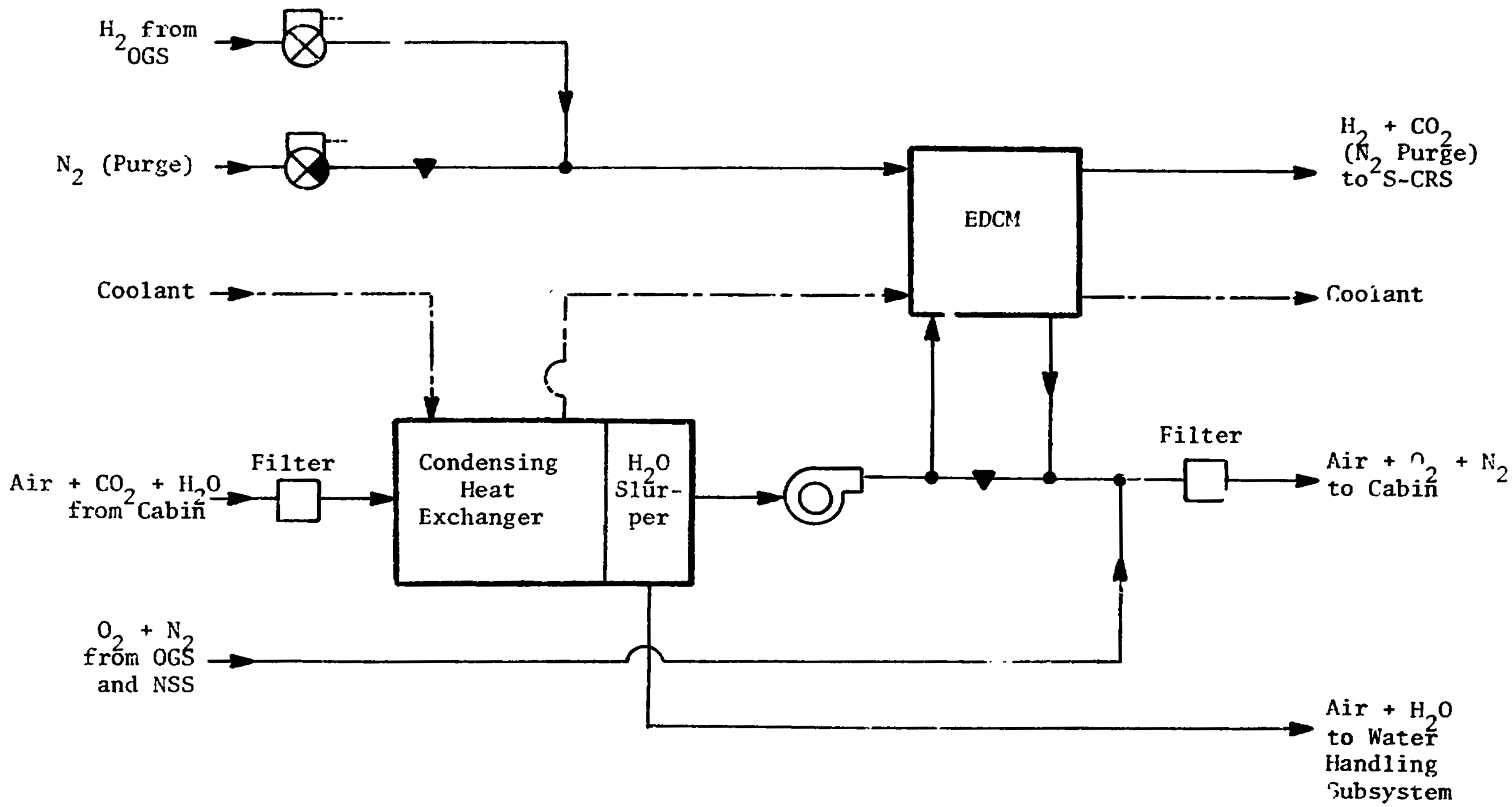

FIGURE 26 CHCS/EDC BLOCK DIAGRAM

TABLE 7 EDC/CHCS OPERATING CONDITIONS FOR ONE-PERSON AIR REVITALIZATION SYSTEM

EDC	
Number of Cells	6
CO_2 Removal Rate, kg/d (lb/d)	1.0 (2.2)
Current, A	10.3
Current Density, mA/cm^2 (ASF)	22.6 (21)
Cell Voltage, V	0.45
Air Inlet Temperature, K (F)	285 to 290 (54 to 63)
Pressure, kPa (psia)	101 (14.7)
Air Flow, dm^3/min (scfm)	270 (9.6)
pCO_2, Pa (mm Hg)	400 (3.0)
CO_2 Removal Efficiency, %	0.84
Power Generated, W	27.8
Heat Generated, W	49.4
CHCS	
Water Removal Rate, kg/d (lb/d)	2.30 (5.07)
Cabin Air Flow, m^3/min (cfm)	2.8 (100)
Cabin Air Temperature, K (F)	286 to 300 (65 to 80)
Cabin Min. Dew Point Temperature, K (F)	279 (42.5)
Cabin Max. Relative Humidity, %	70
Nominal Latent Heat Removed, W (Btu/h)	61.5 (210)
Nominal Sensible Heat Removed, W (Btu/h)	521 (1780)

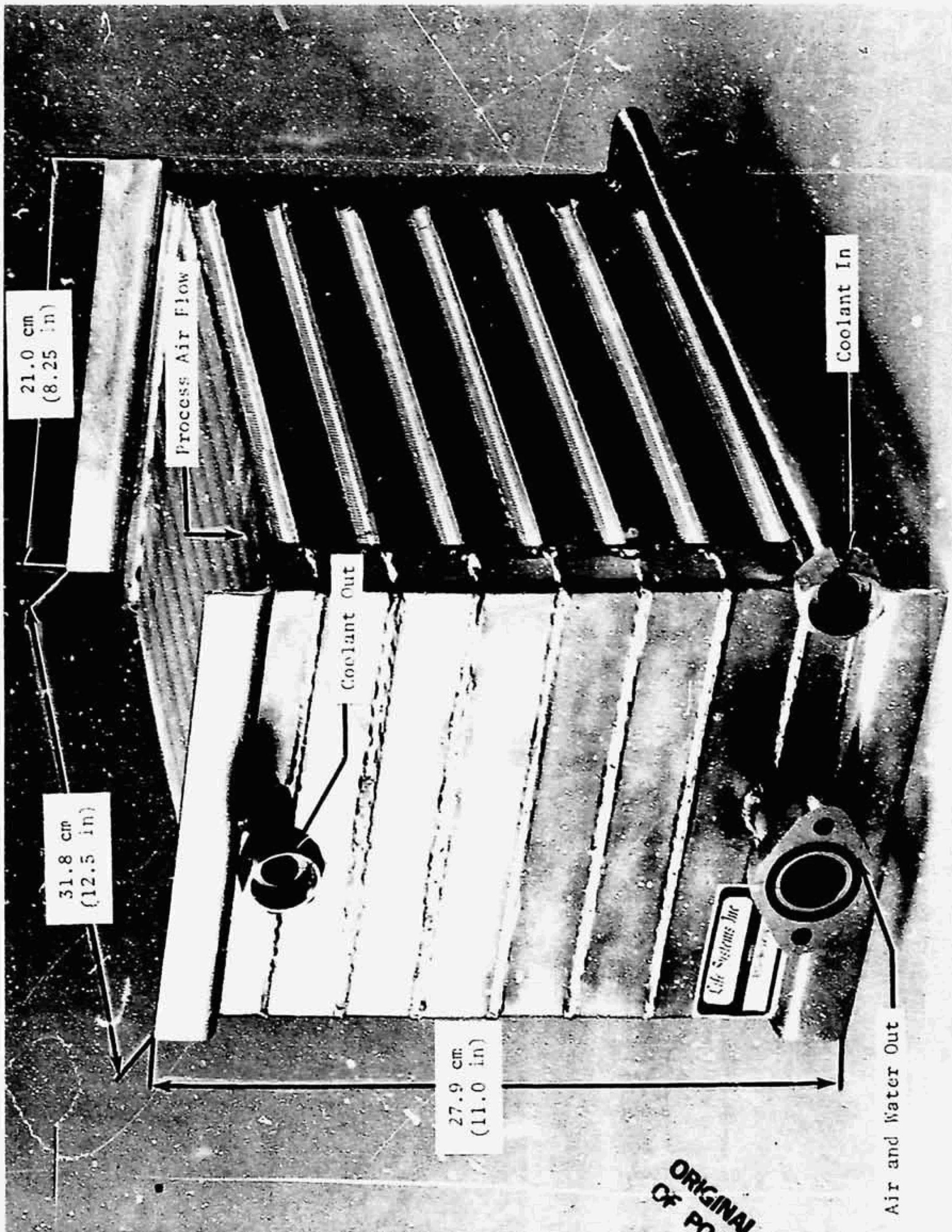

FIGURE 27 ONE-PERSON CONDENSING HEAT EXCHANGER

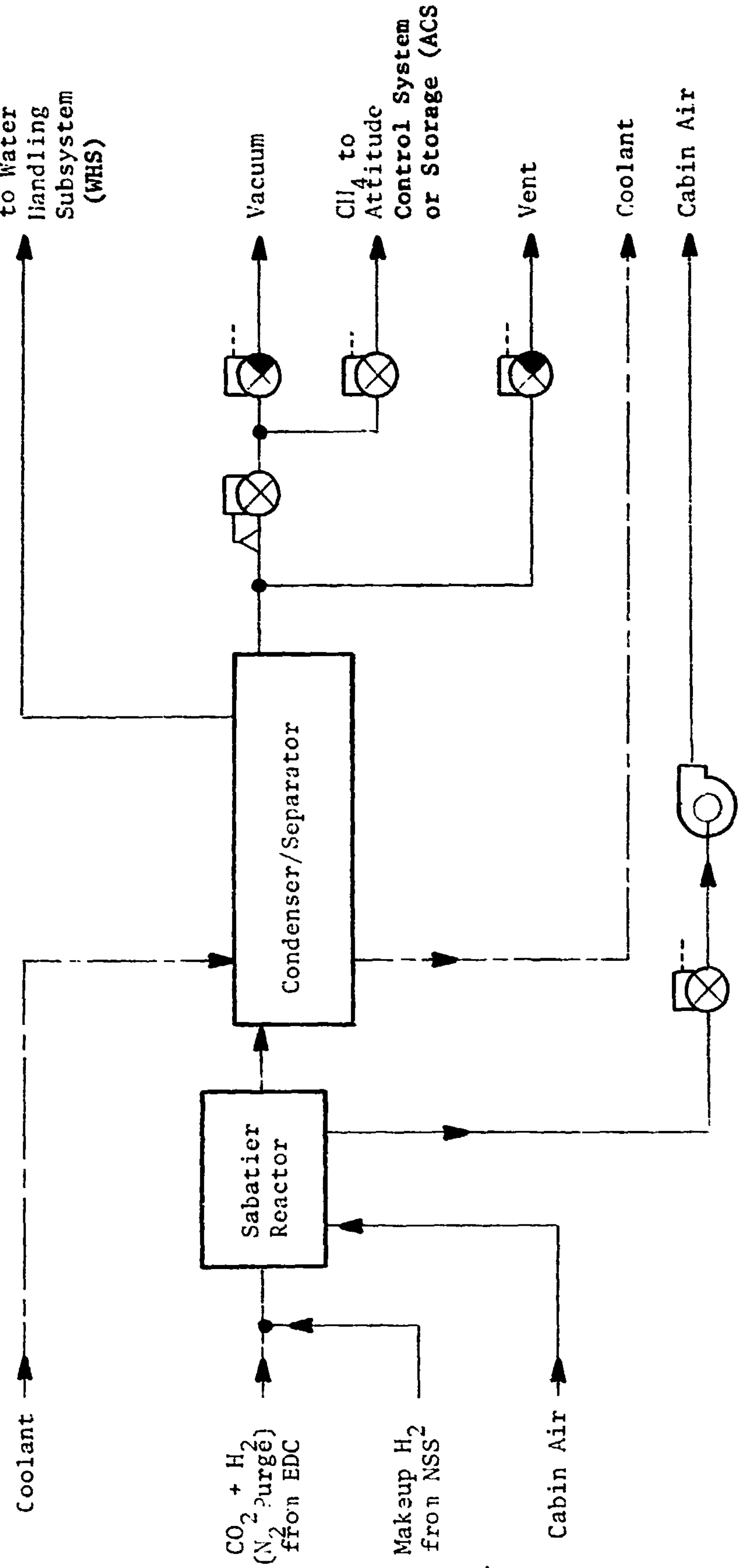

FIGURE 28 SABATIER CO_2 REDUCTION SUBSYSTEM

TABLE 8 S-CRS OPERATING CONDITIONS FOR ONE-PERSON AIR REVITALIZATION SYSTEM

H_2 Inlet Flow, cm^3/min (lb/d)	1700 (0.43)
CO_2 Inlet Flow, cm^3/min (lb/d)	380 (2.20)
Water Inlet Flow, cm^3/min (lb/d)	20 (0.05)
Inlet Volumetric Flow Ratio, H_2/CO_2	4.5
H_2 Outlet Flow, cm^3/min (lb/d)	250 (0.07)
CO_2 Outlet Flow, cm^3/min (lb/d)	19 (0.11)
CH_4 Outlet Flow, cm^3/min (lb/d)	360 (0.77)
Water Outlet Flow, cm^3/min (lb/d)	730 (1.73)
Reactor Temperature, K (F)	616 (650)
Heater Temperature, K (F)	687 to 711 (780 to 820)
CO_2 Reduction Efficiency, %	95
H_2 Conversion Efficiency, %	85

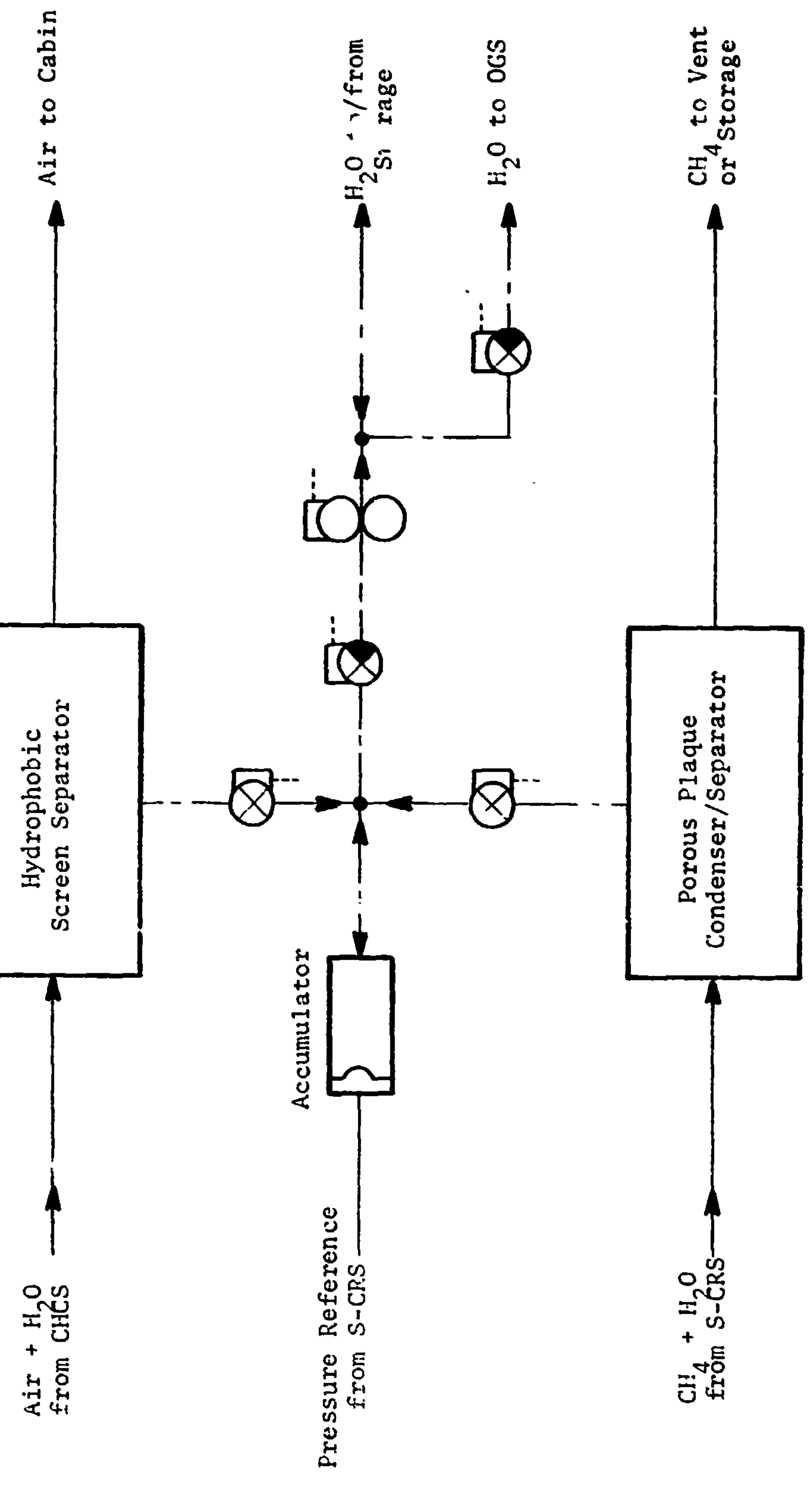

FIGURE 29 WATER HANDLING SUBSYSTEM BLOCK DIAGRAM

condensing heat exchangers in the CHCS and the S-CRS. The condensed water from the CHCS is separated from the air by a hydrophobic screen liquid/gas separator. Such a component was sized, designed and fabricated as part of this program.(11) A photograph of the separator is shown in Figure 30. The water vapor in the outlet gas stream of the Sabatier reactor is condensed and separated by a porous plaque liquid/gas condenser/separator. This unit is shown in Figure 31. The liquid outputs from these two devices flow to a water accumulator which is periodically emptied into a water storage tank. As is shown in Figures 25 and 29, this liquid water is also supplied to the OGS for conversion to H_2 and O_2, thus completing the water loop.

Coolant Loop Hardware. A distinct advantage of developing a self-contained ARS is the capability for reducing the number of components and the interfaces with the TSA. One of the principal areas where this was implemented in the ARX-1 was with the liquid coolant flow and supply.

Figure 32 shows the block diagram of the coolant loop hardware. The three principal components that interface with the coolant flow are the Sabatier condenser/separator, the condensing heat exchanger in the CHCS and the EDCM heat exchanger. A combination of series/parallel flows and secondary coolant loops was designed and implemented to provide the required coolant at the desired temperatures to the proper components. A key component that permits this approach was a coolant flow diverter valve, shown in Figures 33 and 34. This component was developed under this program and has been discussed in detail in a prior report.(11)

ARX-1 Hardware Mechanical Summary

The description of the functional concept and major components of the ARX-1 was presented above. Figure 35 is the overall schematic of the system. Figure 36 shows the major components in the packaged mechanical hardware. The total weight of this breadboard system, including all components, wiring, plumbing and frame, is 281 kg (619 lb) and occupies an envelope of 71 x 96 x 114 cm (28 x 38 x 45 in). The ARX-1 mechanical hardware with its C/M I and TSA, which comprise the test facility, is shown in Figure 37.

Control/Monitor Instrumentation

The C/M I selected for the ARX-1 was an advanced instrumentation design using minicomputer/software technologies. This C/M I, including an advanced operator/subsystem interface panel, was designed to be packaged in a separate self-contained enclosure (Figure 38). The function of the C/M I was to provide automatic mode and mode transition control, automatic shutdown provisions for self-protection, provisions for monitoring system parameters and provisions for interfacing with ground test instrumentation.

Operating Modes and Mode Transitions. The C/M I provided five operating modes: (1) Shutdown, (2) Normal, (3) Purge, (4) Standby and (5) Unpowered. These operating modes and allowable mode transitions are shown in Figure 39. In the Normal Mode the system provides the function of removing and reducing CO_2, generating O_2 and N_2, controlling cabin humidity and distributing or

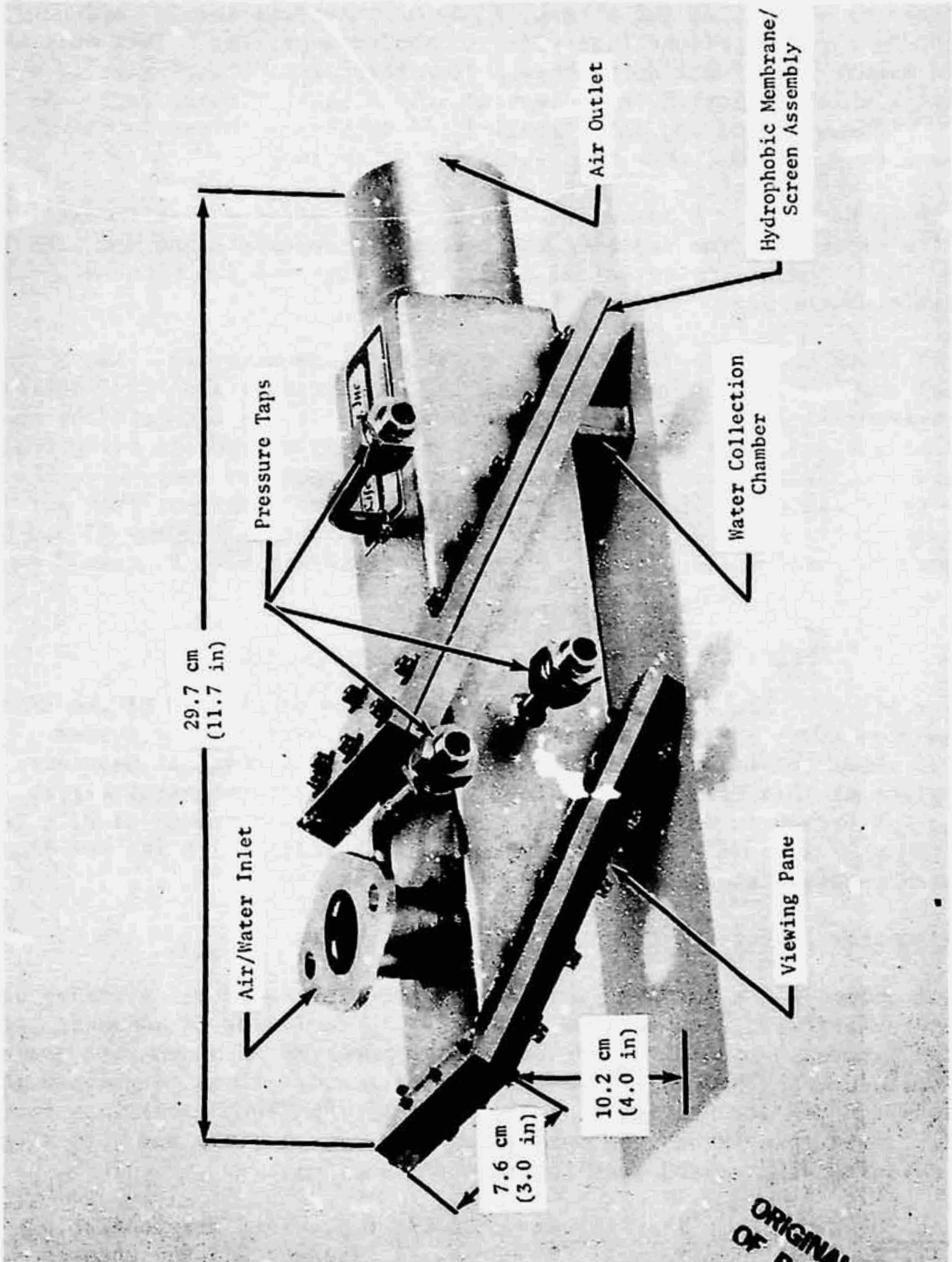

FIGURE 30 HYDROPHOBIC SCREEN LIQUID/GAS SEPARATOR

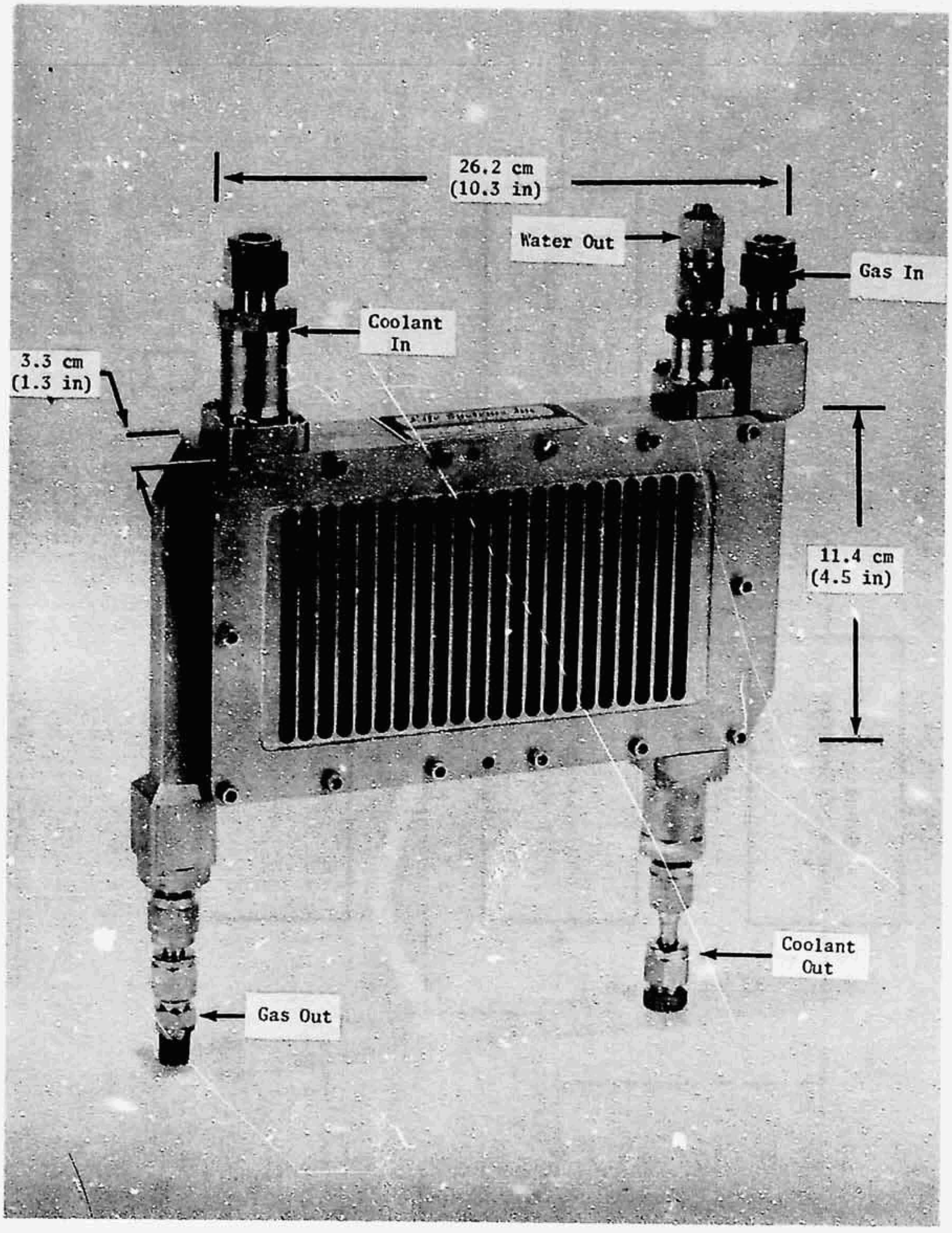

FIGURE 31 POROUS PLAQUE CONDENSER/SEPARATOR

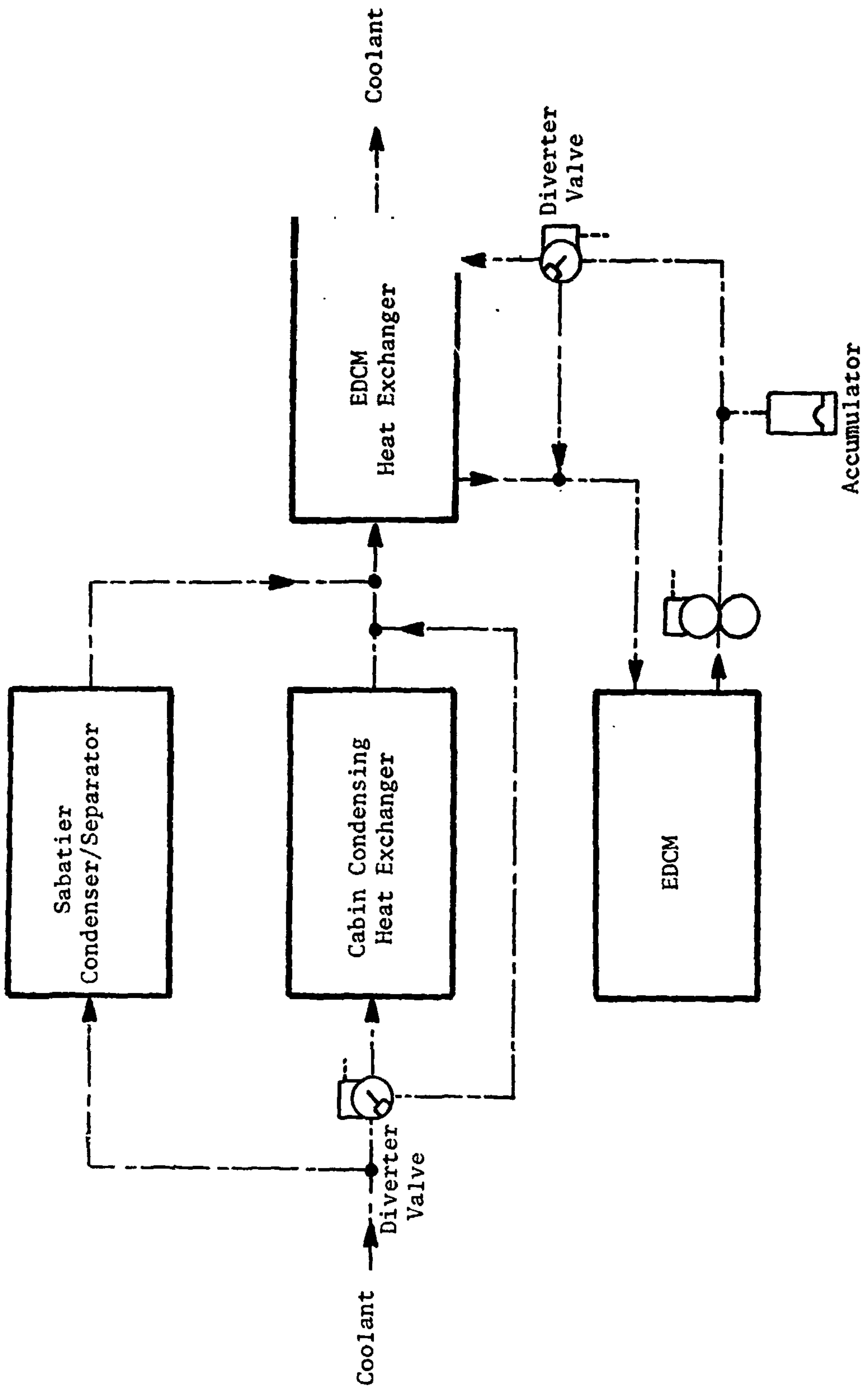

FIGURE 32 COOLANT FLOW HARDWARE BLOCK DIAGRAM

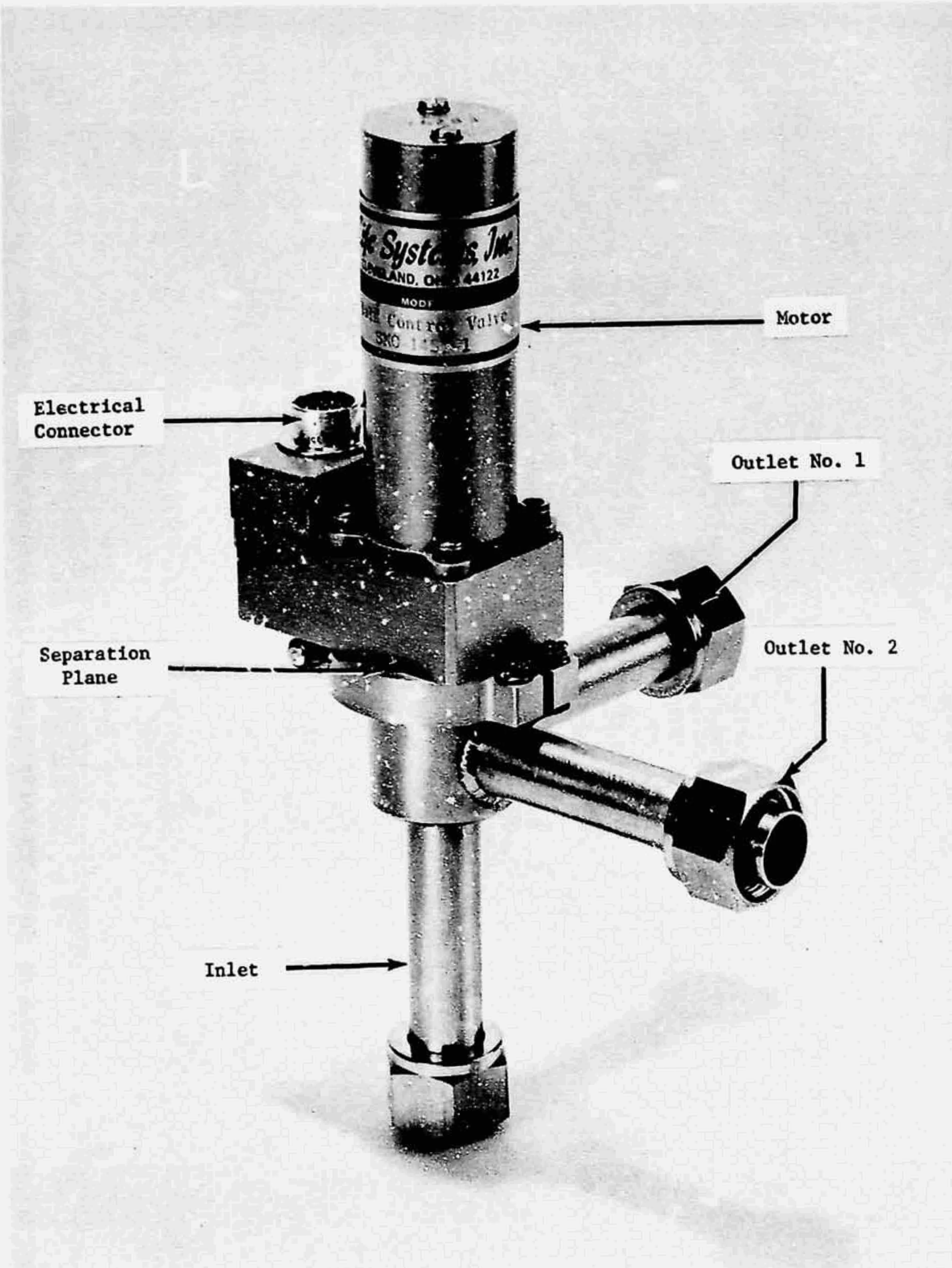

FIGURE 33 ASSEMBLED DIVERTER VALVE

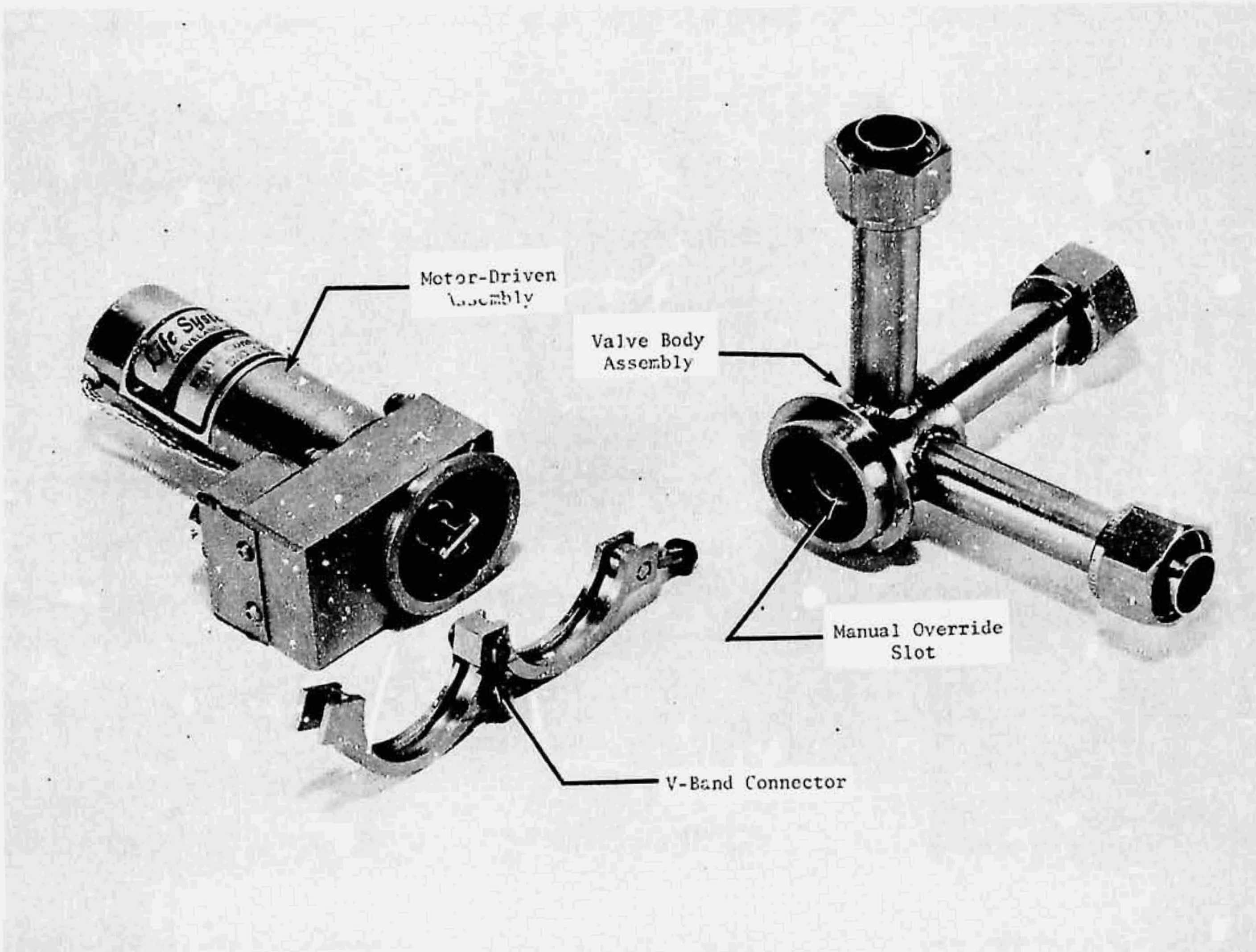

FIGURE 34 DIVERTER VALVE ILLUSTRATING MAINTAINABILITY FEATURES

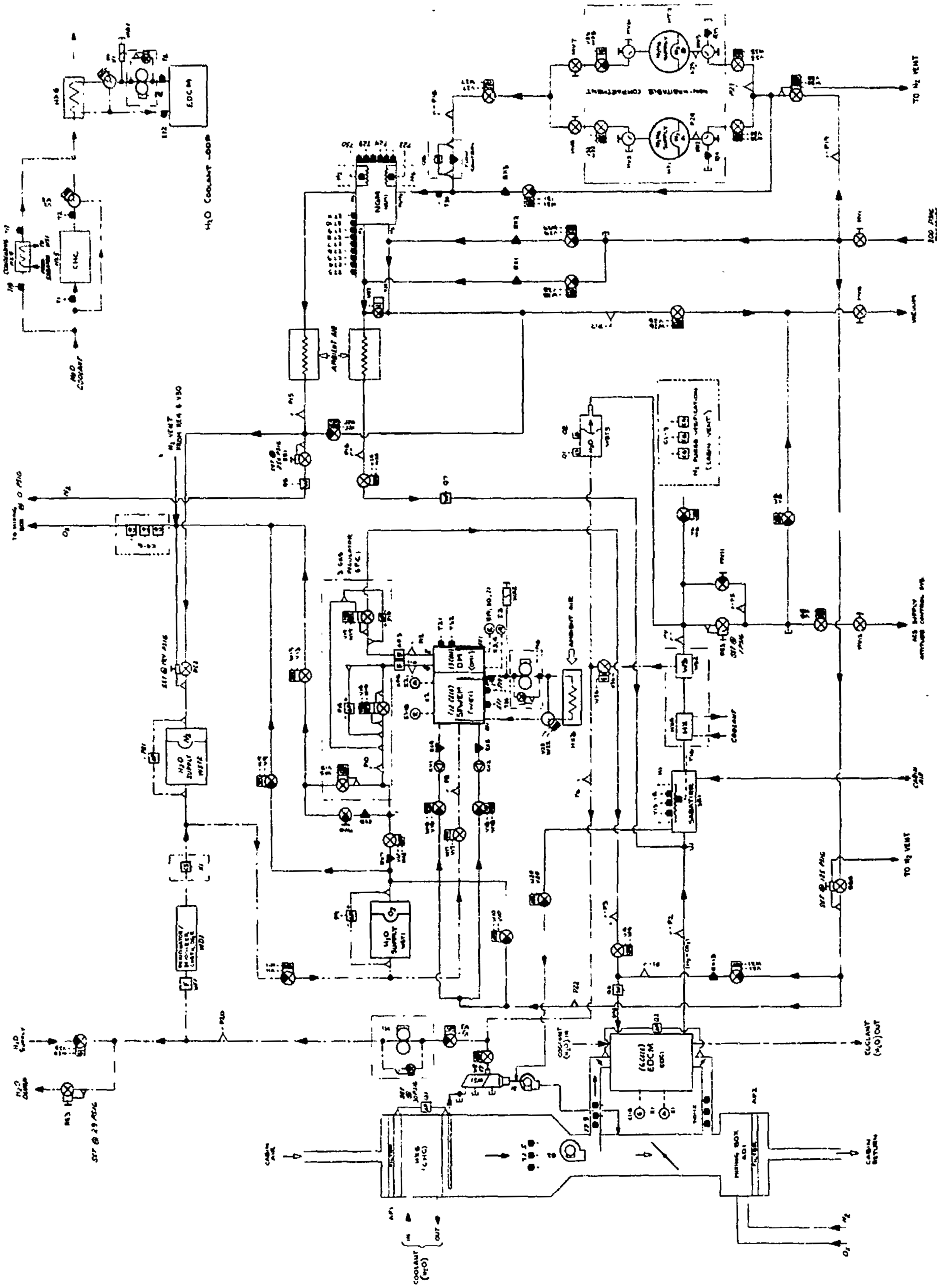

FIGURE 35 ARX-1 MECHANICAL SCHEMATIC

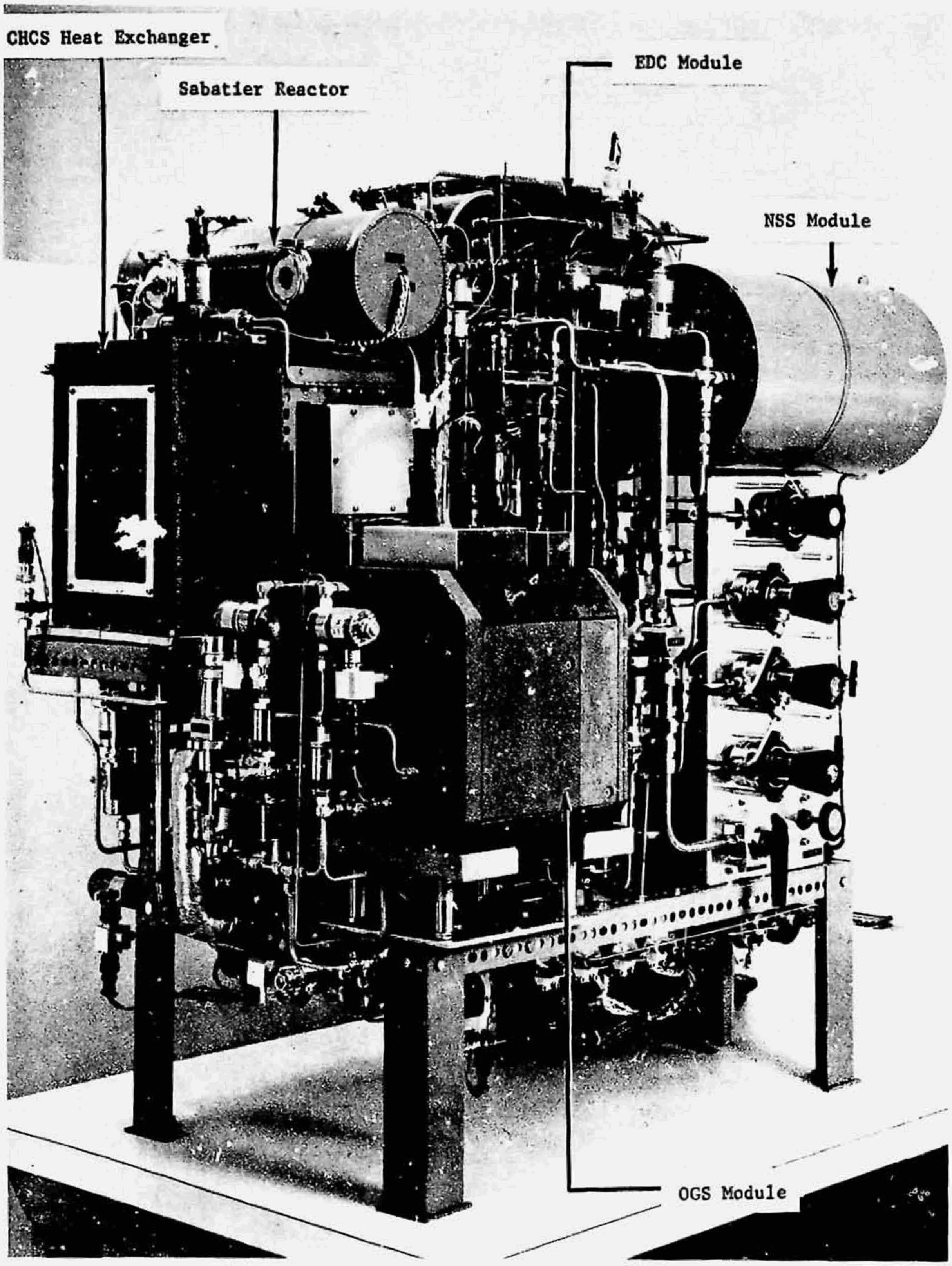

FIGURE 36 ARX-1 MECHANICAL HARDWARE

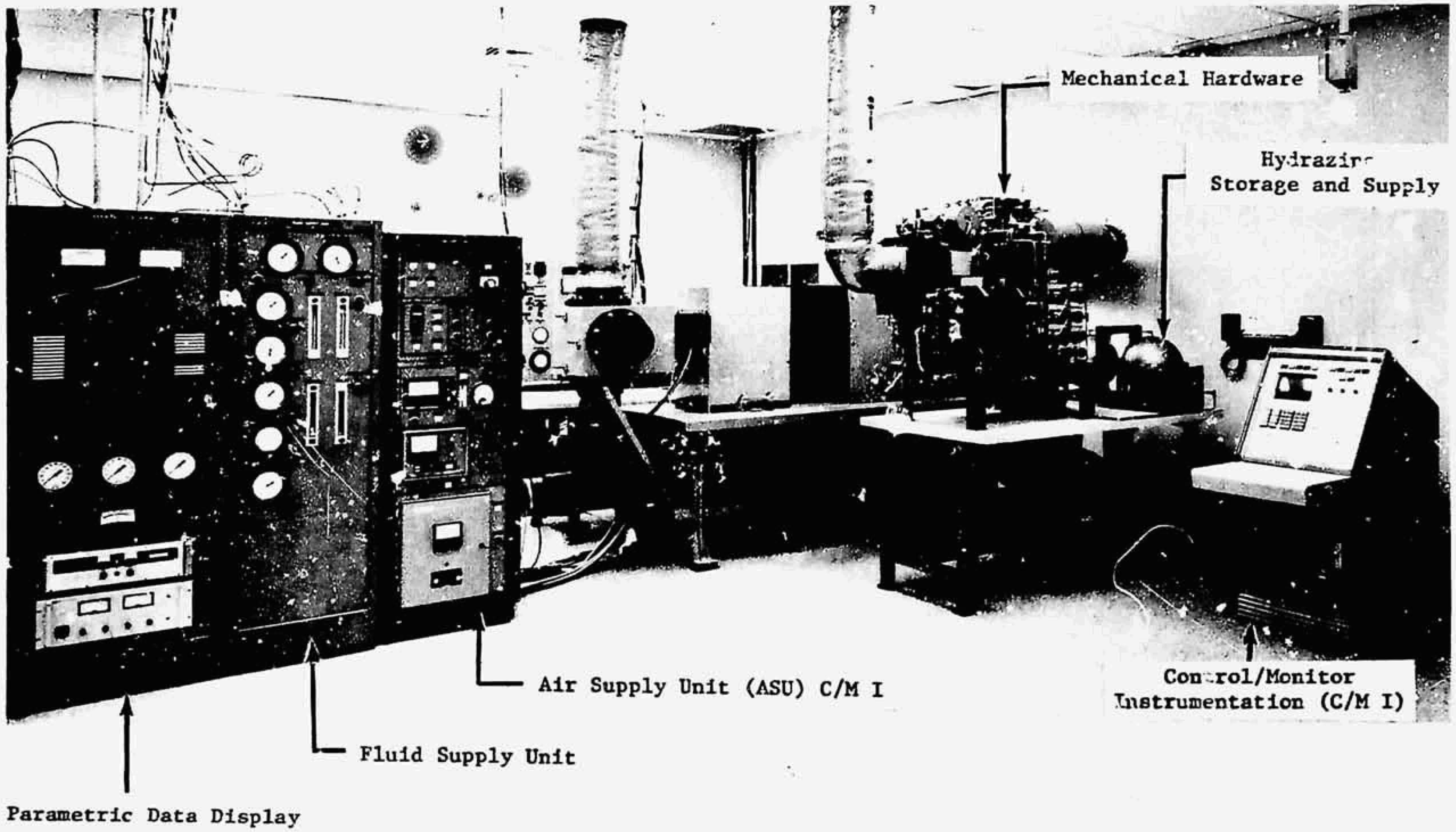

FIGURE 37 ARX-1 TEST FACILITY

FIGURE 38 ARX-1 CONTROL AND MONITOR INSTRUMENTATION

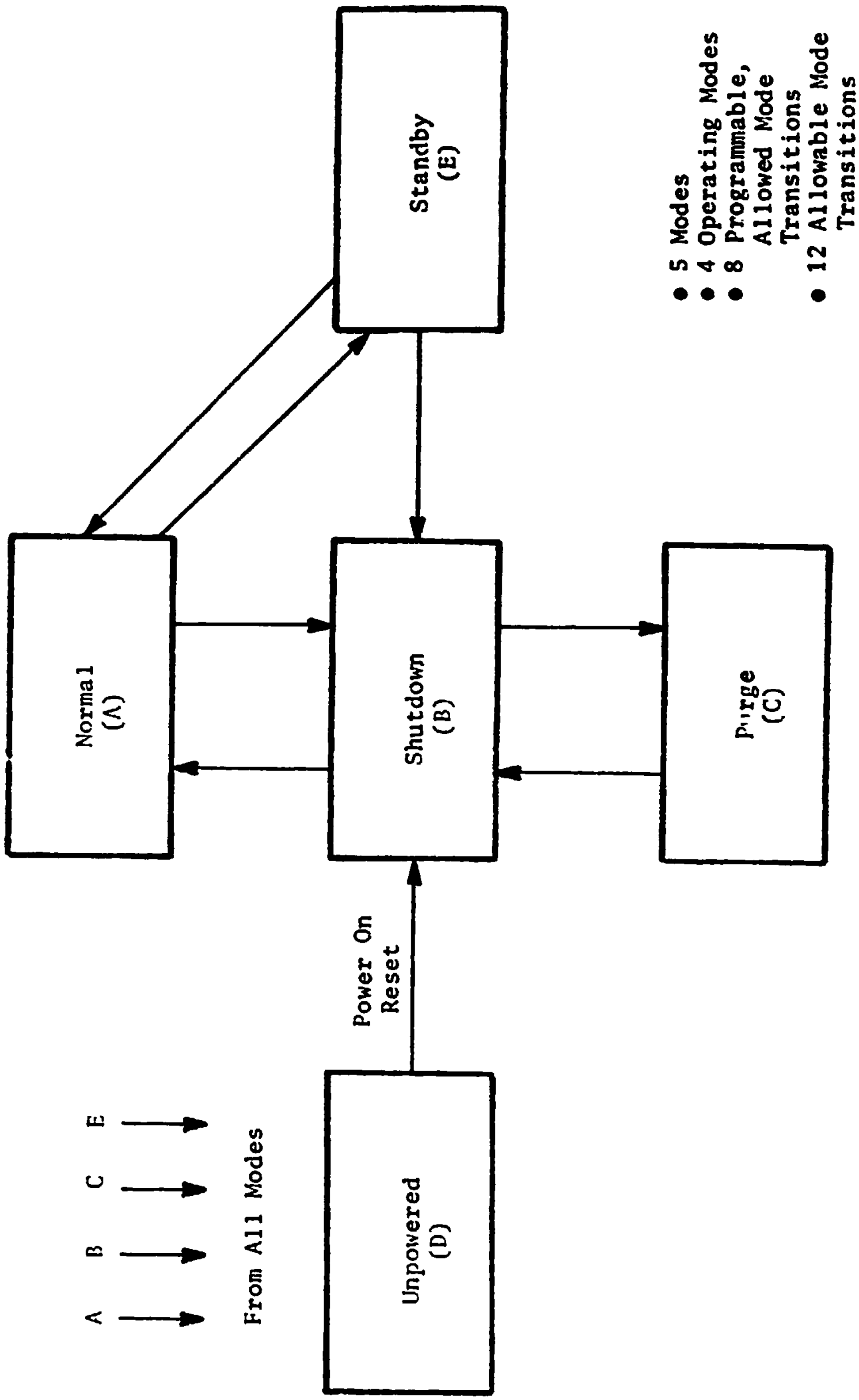

FIGURE 39 OPERATING MODES AND ALLOWABLE MODE TRANSITIONS

storing water, as required. In the Shutdown Mode these functions are inoperative but the system is powered and all sensors are working. During Purge, all H_2-carrying lines throughout the system are being purged with N_2. In the Standby Mode the system is powered and maintained at operating temperatures and pressures; however, actual conversion processes are not taking place. Finally, in the Unpowered Mode, no electrical power is applied to the system and there are no fluid flows.

System Control and Monitoring. There are 16 software/hardware controls needed to operate the hardware. These include controls for EDCM temperature and current, S-CRS temperature, CHCS temperature, water accumulator fill and/or empty, OGS temperature, pressure and current and N_2 Generation Module (NGM) pressure and temperature.

Sensors are required to interface with the C/M I to provide for control and monitoring of subsystem parameters and performance. Over 100 sensors are implemented in the ARX-1. These monitor flows, pressures, temperatures, currents, voltages, liquid levels, combustible gas presence and valve positions.

Operator/System Interface. The operator/system interface of the C/M I is shown in Figure 40. The operator can communicate with the ARX-1 through this interface panel. The panel is subdivided into three major areas: System Status, Operator Commands and System Control.

Overall system status is provided in the upper left-hand portion of the panel. The status summary is given as Normal, Caution, Warning or Alarm and is determined by the worst case condition for any critical parameter. A Reset button is provided to clear the status summary and reset the subsystem monitoring functions. Messages and information concerning the system are displayed on a CRT located below the status summary indicators. The CRT is used to display fault diagnostic messages, present status and values of selected sensors, operator/system input/output data, operator-to-system communications, elapsed times and system-to-operator communications.

The operator commands section in the lower left-hand corner provides the capability of the operator to communicate with the C/M I. Capability exists for entering data, examining current values, updating scale factors, modifying setpoints or allowable ranges and control of the CRT.

Manual initiation of the four operating modes (Normal, Standby, Purge and Shutdown) is provided in the upper right-hand corner of the panel. The controls automatically prevent the operator from initiating an illegal mode transition, e.g., Normal to Purge. The subsystem will not respond to an illegal mode transition command. Accidental mode initiation is prevented by providing a Mode Change Permit button which must be simultaneously depressed with the desired mode button.

The control status is located directly below the operating mode/commands section. Three lights are provided to indicate whether one of the automatic protection overrides or an actuator override has been activiated. A light is also provided to indicate when the panel switches have been disabled, a condition used to prevent unauthorized personnel to activate any button.

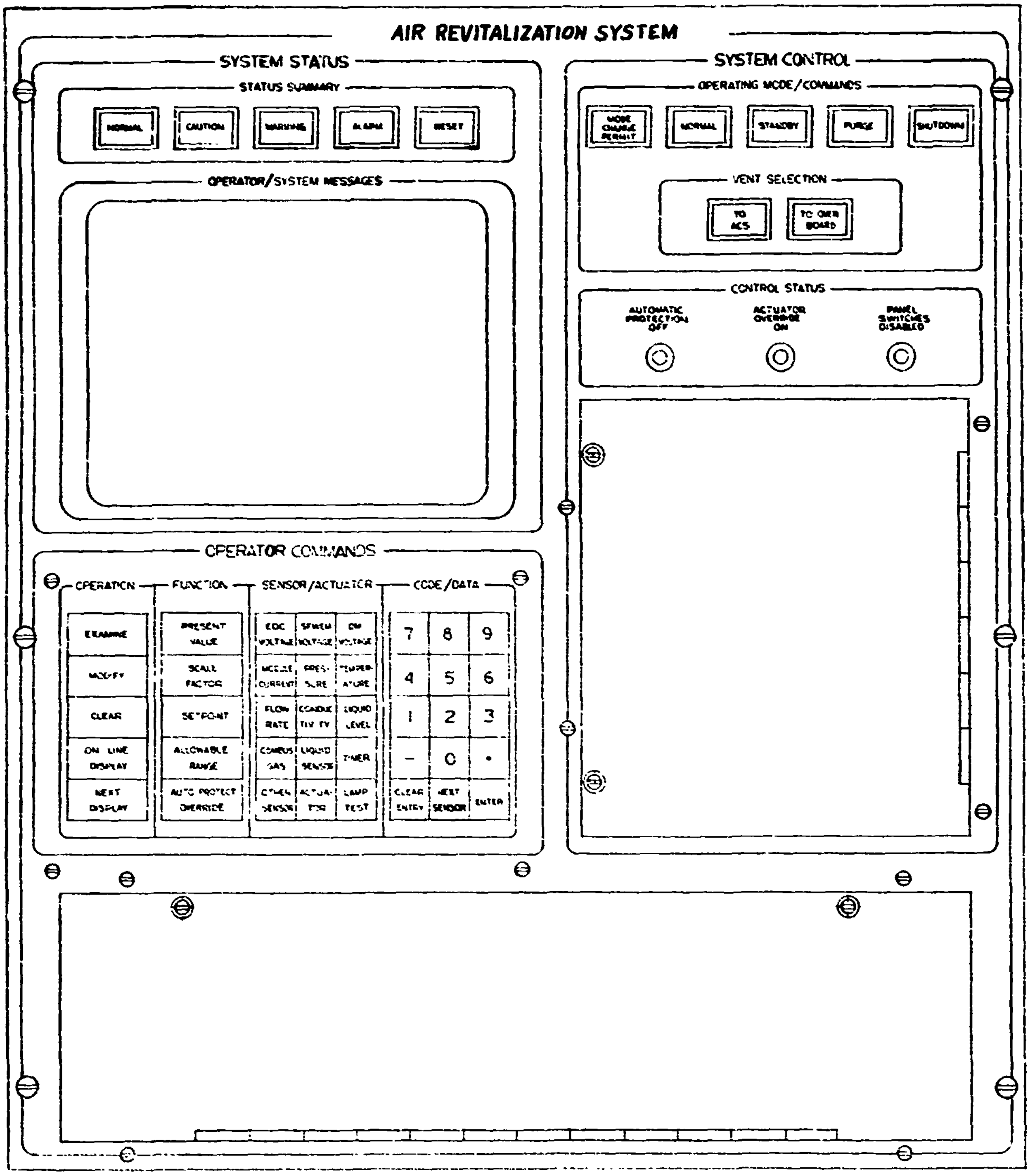

FIGURE 40 ONE-PERSON AIR REVITALIZATICN SYSTEM OPERATOR/SYSTEM INTERFACE PANEL

Manual controls, designed primarily for use during system debug or off-design operation, are provided behind an access panel located immediately below the operator commands and system control sections. Overrides are provided for all actuators in the form of toggle switches. The actuator overrides must be placed in an automatic position for the system to operate normally. Also, manual adjustments are provided for adjusting certain setpoints such as EDCM current and Sabatier reactor temperature. The access panel is normally closed to prevent unauthorized actuations.

ARX-1 Testing

The ARX-1 testing was conducted for a period of 120 days and included testing at the component, subsystem, C/M I (hardware and software) and total system levels. Specific testing activities which occurred during the checkout, shakedown and endurance phases are shown in Figure 41.

A total of 480 h (20 d) of successful integrated operation in the Normal mode was achieved. Normal mode excludes the time required for the transitions Shutdown to Normal and Normal to Shutdown. These transitions typically require 0.5 h each and primarily involve the pressurization or depressurization of the OGS. Of the total normal operation, two seven-day periods of continuous operation were achieved.

The overall system performance is shown in Figure 42. It is seen that the ARX-1 removed CO_2 at greater than the one-person level and generated O_2 above the design level which accounted for one person's metabolic consumption plus an allowance for overboard leakage. The curve for net water recovered is the algebraic total of the water (1) removed by the CHCS from the simulated cabin atmosphere, (2) removed by the S-CRS condenser/separator and (3) supplied to the OGS. The majority is that removed by the CHCS.

While Figure 42 presents the performance of the overall ARX-1 system, individual subsystem performances for the EDC, CHCS and S-CRS are given in Figures 43, 44 and 45, respectively. The six-cell, liquid-cooled EDCM performed exceptionally well with an average cell voltage of 0.46 V and CO_2 transfer efficiency of 82%. The CHCS reliably controlled dew point to the EDC at 286 K (56 F) in response to varying inlet RH conditions. The S-CRS maintained H_2 conversion efficiencies consistently near 100%. This was to be expected since the H_2/CO_2 mole ratio at the S-CRS inlet was about 2.6 instead of the 4 required for stoichiometric operation.

In summary, the ARX-1 testing demonstrated the following: (1) duplicate subsystem interface components can be eliminated by treating the hardware from a single system viewpoint, (2) TSA and expendable usage can be reduced (e.g., OGS H_2 used by EDC), (3) a single integrated C/M I can simplify the collection and display of engineering data, (4) single one-button startup of several subsystems can be achieved, (5) the system provides real-life test conditions by determining the effects of changes in the cabin simulator on the system as a whole and (6) development and testing costs were saved. To illustrate the last point, Figure 46 shows the total test time accumulated on the major subsystems and components of the ARX-1. Over 10,000 hours of testing have

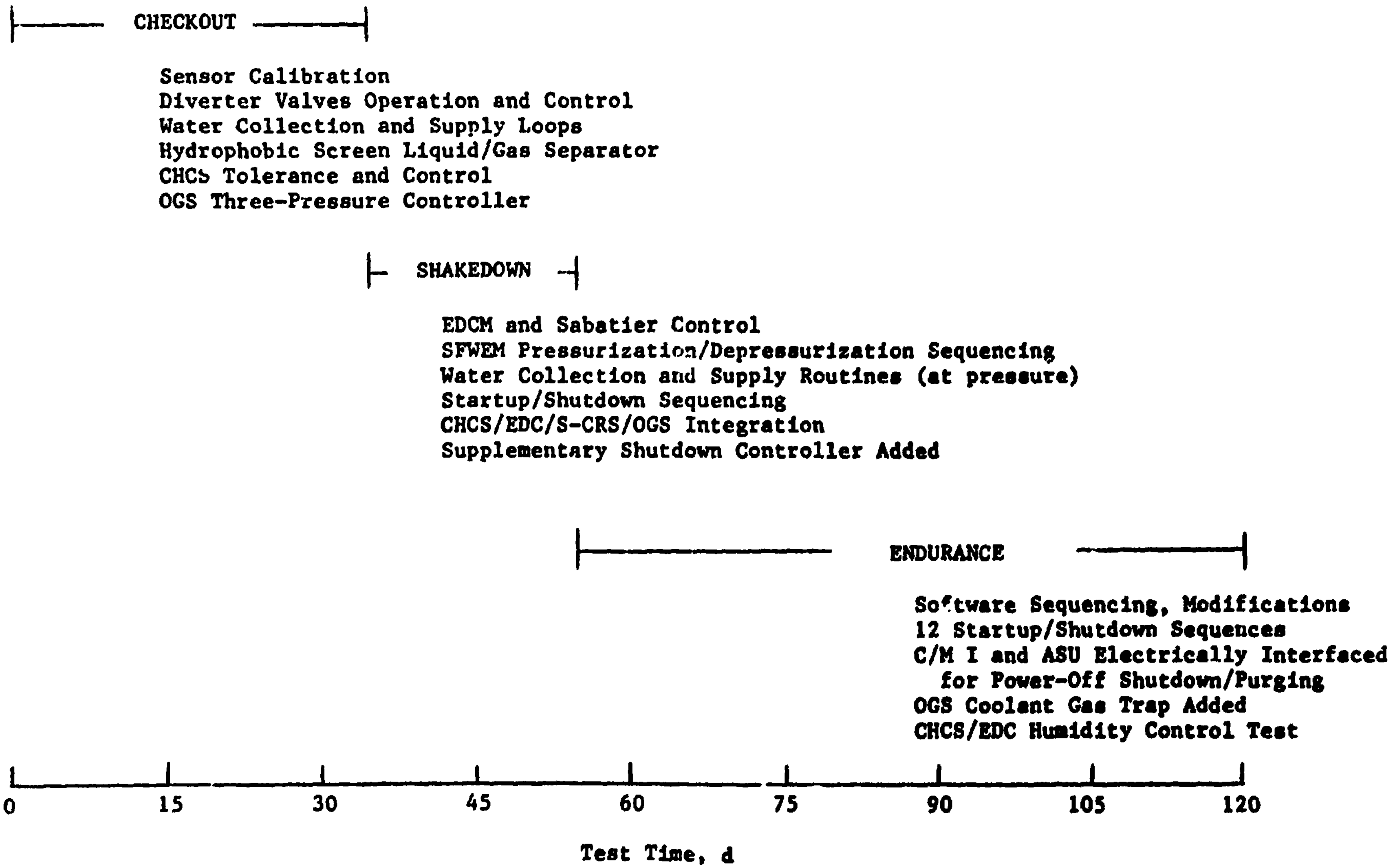

FIGURE 41 ARX-1 TEST OVERVIEW

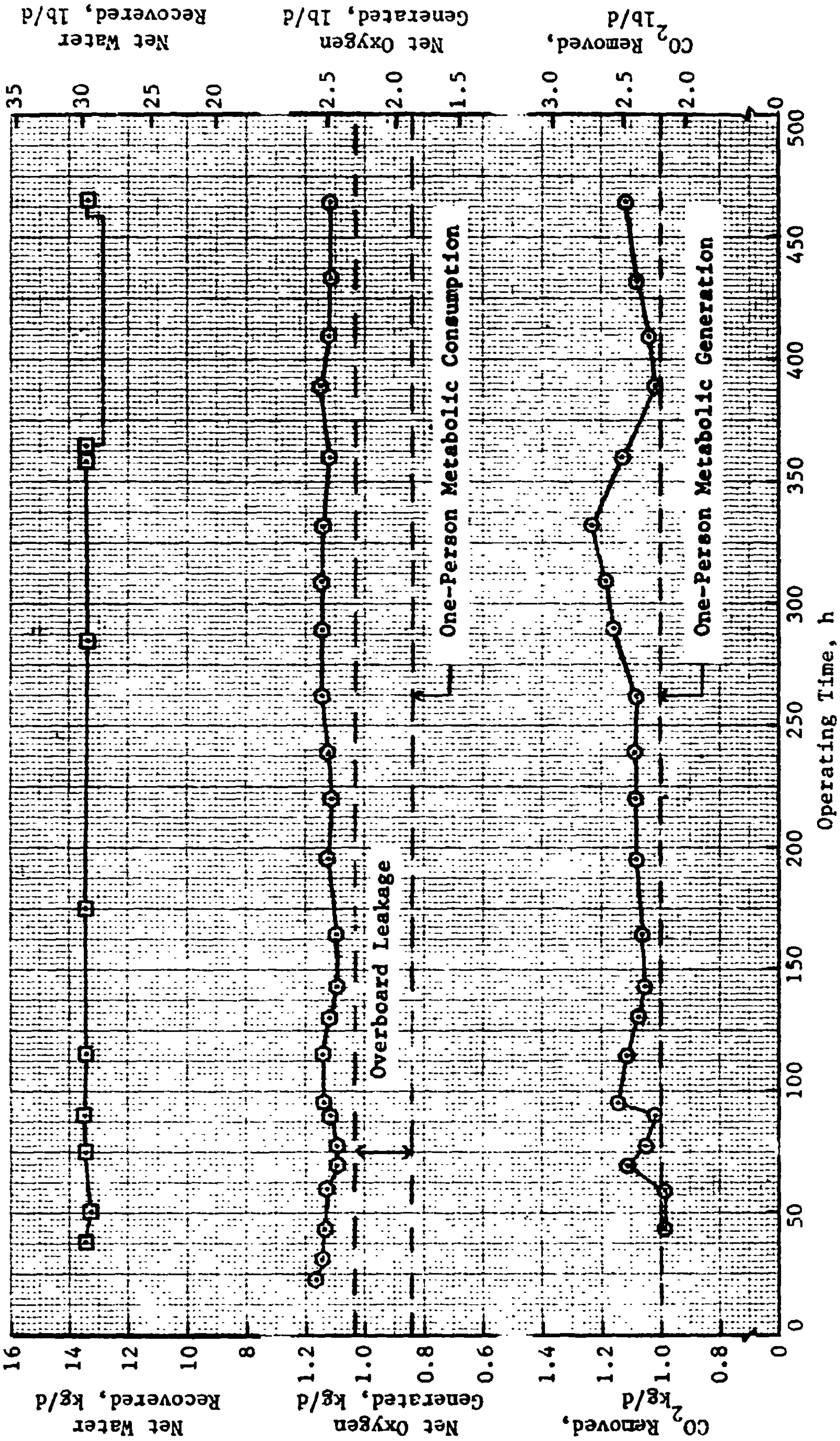

FIGURE 42 ARX-1 SYSTEM PERFORMANCE

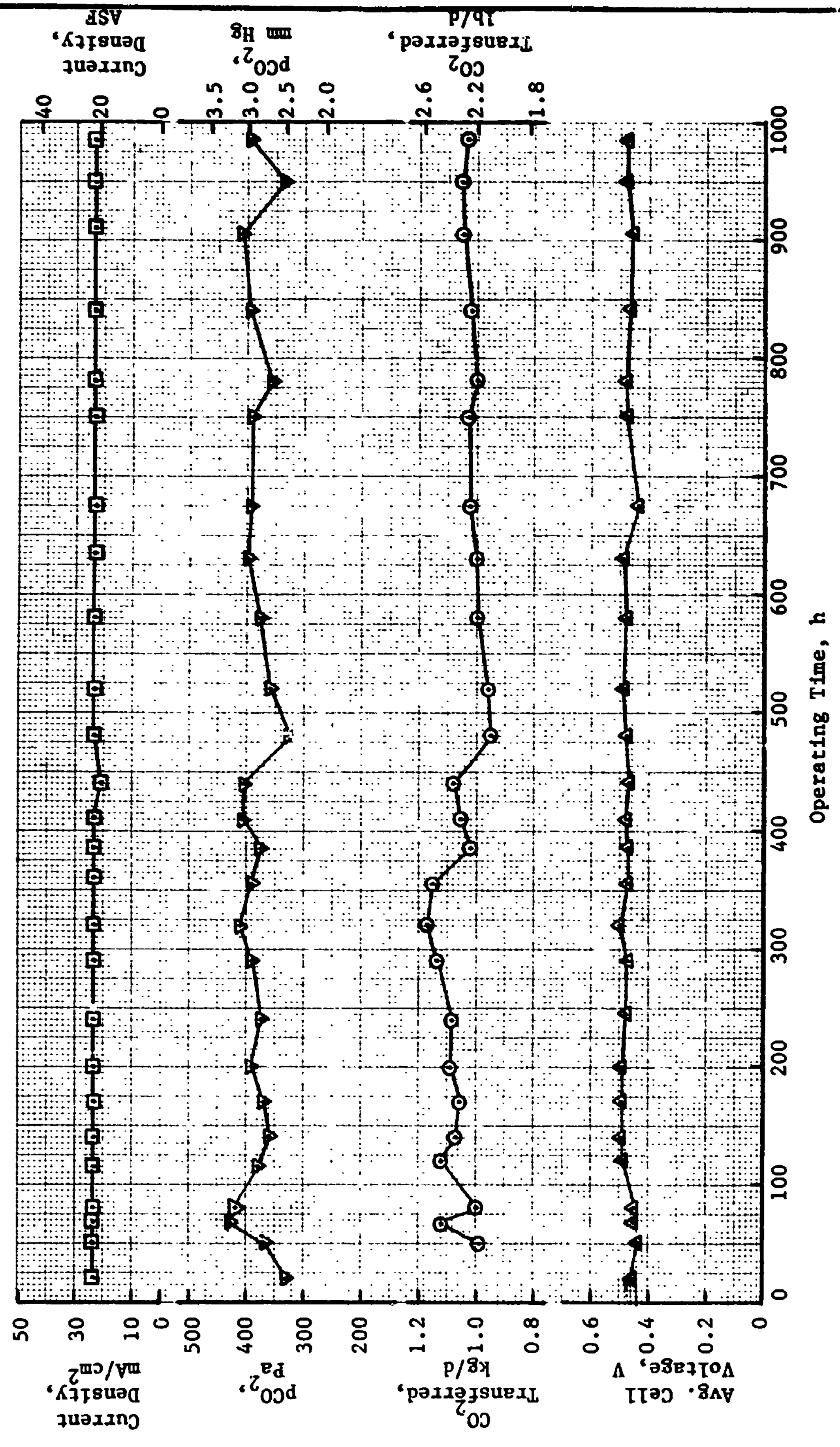

FIGURE 43 ARX-1 EDC PERFORMANCE

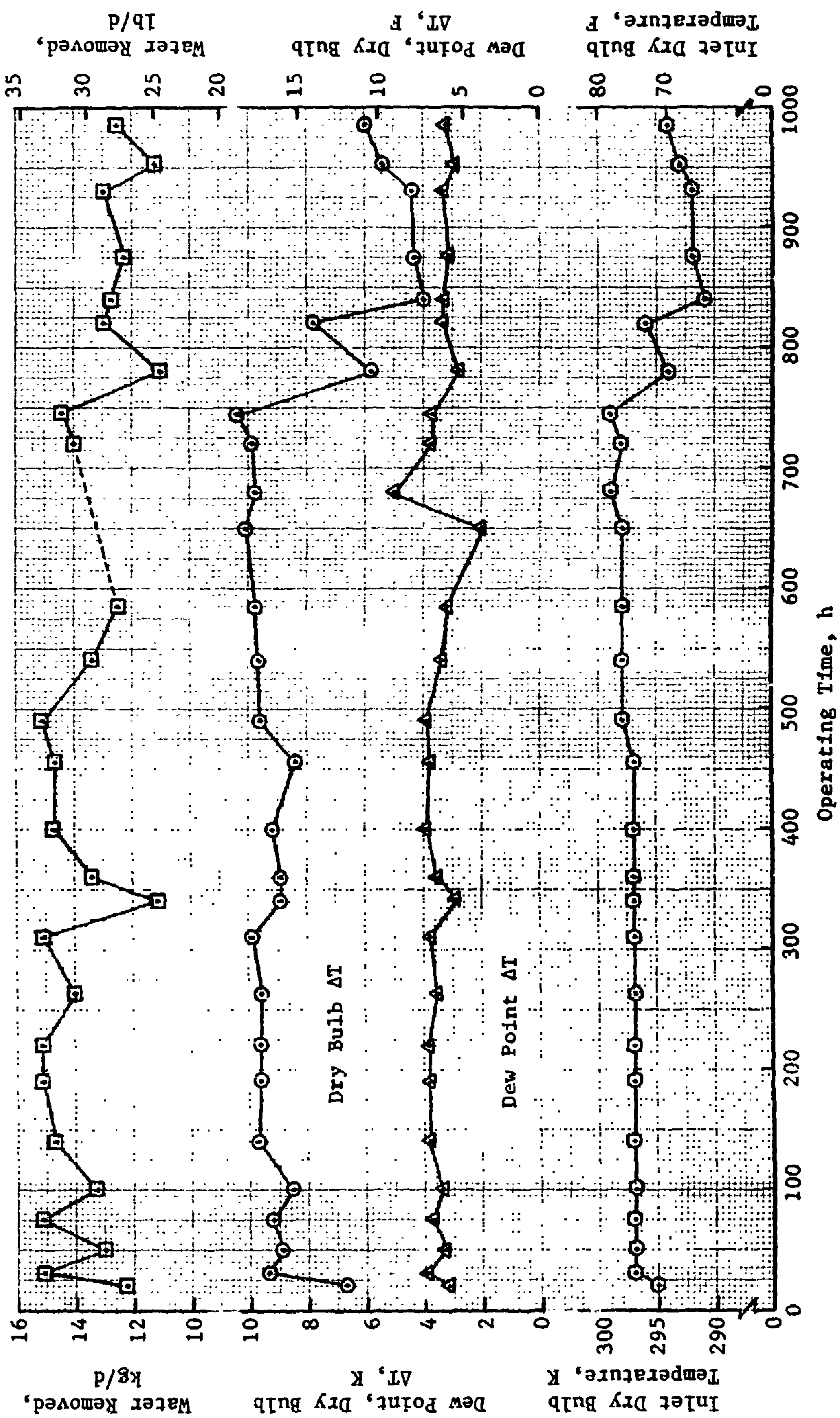

FIGURE 44 ARX-1 CHCS PERFORMANCE

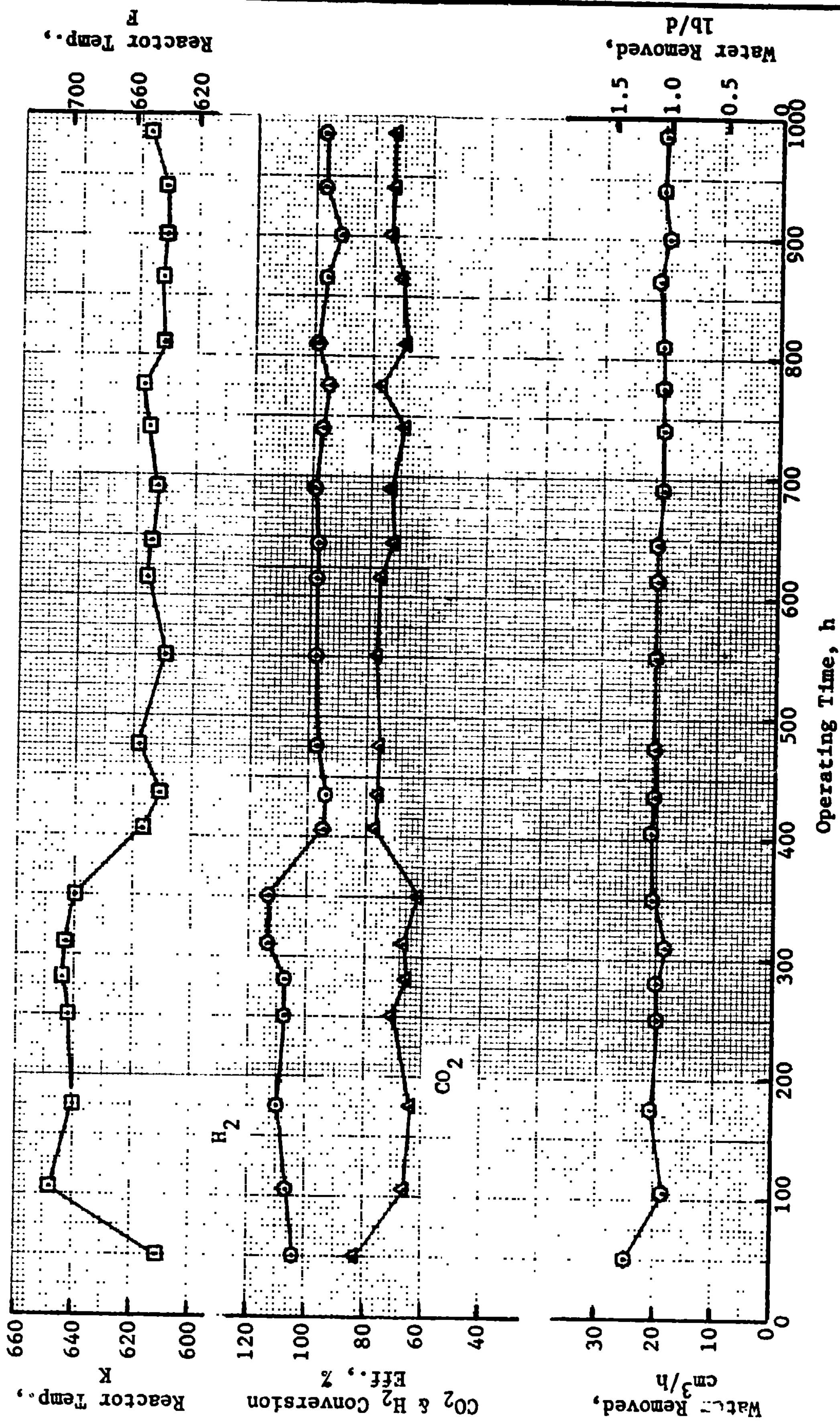

FIGURE 45 ARX-1 S-CRS PERFORMANCE

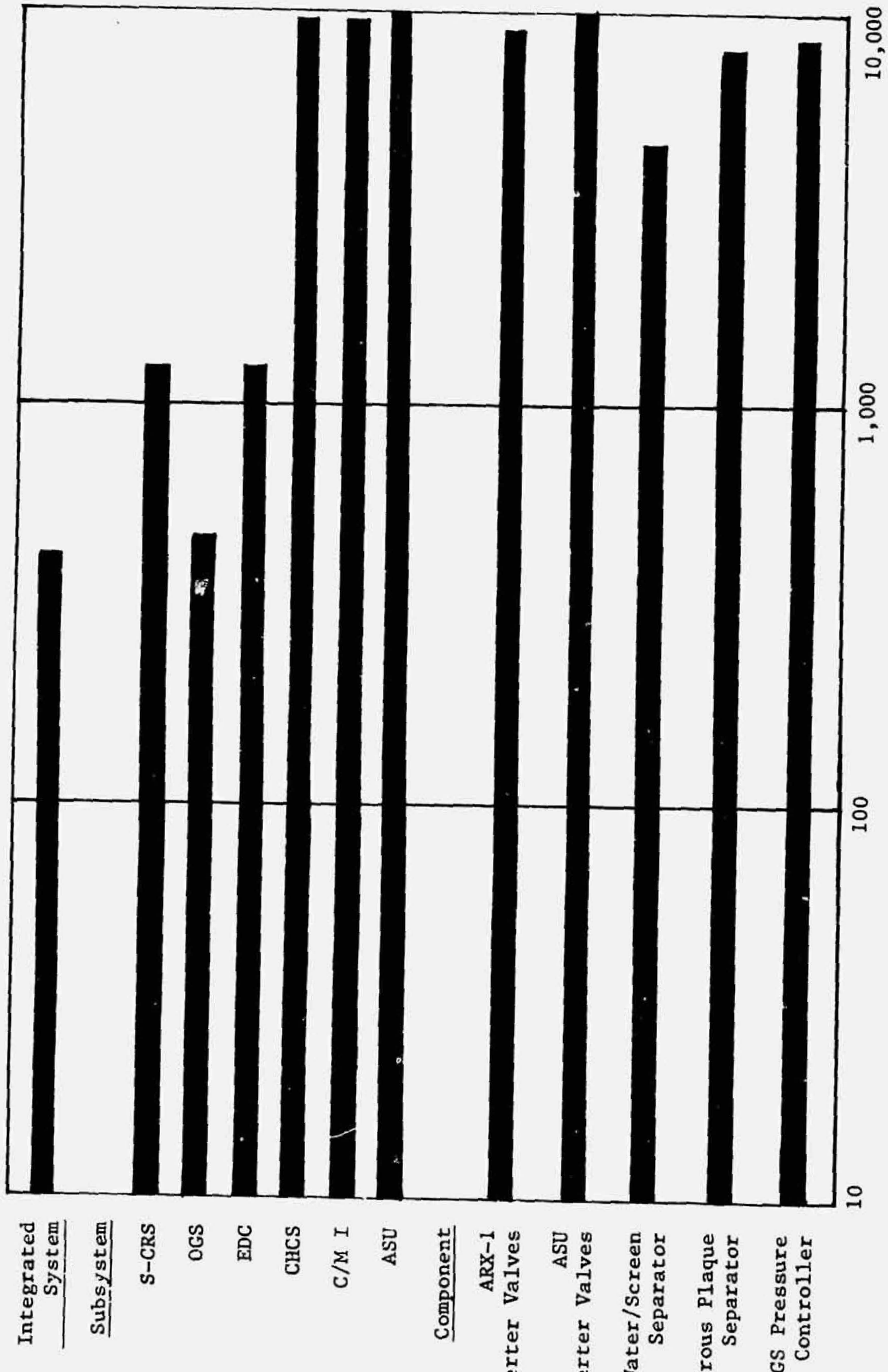

FIGURE 46 LIFE TESTING OF ARX-1 COMPONENTS/SUBSYSTEMS

been achieved for some components using the ARX-1 as a test bed. Development of the ARX-1 as a system permitted parallel testing of key hardware elements.

TEST SUPPORT ACCESSORIES DEVELOPMENTS

Test Support Accessories were designed and developed to support the test objectives of single cell, subsystem and integrated system EDC tests. Single cell TSA supported the advanced performance level (B level) testing. Subsystem TSA was developed for the CS-3. The integrated system EDC TSA focused on (1) developing an EDC ASU which was used to simulate a spacecraft cabin environment for EDC subsystem testing now and in the future and (2) developing the TSA to support the ARX-1 testing.

Single Cell Test Stands

As part of the overall TSA support activities, previously fabricated, multi-position single cell test facilities were refurbished and upgraded. Two phases of refurbishment activities were performed: initial upgrading and final refinement to meet the requirements for advanced performance level (B level) testing.

Initial Refurbishment and Upgrading

The single cell, three-position test stand previously fabricated[5] was refurbished and upgraded to replace worn components and to increase the level of control and monitor sophistication consistent with the advancement in EDC technology.

The initial test stand had a capability to simultaneously test three different individual single cells. One of the test positions was eliminated to allow for the addition of the components and parts needed to incorporate desired improvements. Each of the two remaining positions, however, were upgraded to allow testing at the submodule level, e.g., stacking from one to five cells between one set of end plates.

The major improvement incorporated into the test facilities included upgrading the current controllers to allow for higher current operating ranges consistent with the advanced cells, addition of provisions to allow for internally air-cooled cells and incorporation of positive feedback control of inlet process air humidity, as well as module temperature differentials (inlet dew point to outlet dry bulb temperature differential). In addition, safety shutdowns for H_2 backpressure, as well as humidity and temperature differential bands were added to the already existing cell voltage monitoring capability. Table 9 is a summary comparison of the updated test stand compared to its previous capabilities.

Advanced Level Technology Test Capability

To prepare for the advanced performance level single cell testing (described further below), additional improvements were added to the two submodule test facilities. In addition, a separate test facility was fabricated to allow for simultaneous parametric testing in parallel with single cell endurance testing at the original two test positions.

TABLE 9 SUMMARY OF SINGLE CELL TEST STAND IMPROVEMENTS

		Original Stand	Updated Stand
1.	Increased current capability	0 to 10 A	0 to 25 A
2.	Increased voltage range, negative and positive	-1.9 V to +4.5 V	-7.5 V to +7.5 V
3.	Replacement of temperature controllers	Mechanical Relays	Solid State
4.	Improved liquid coolant temperature stability	Dependent Control	Independent
5.	Addition of air cooling capability	Nonexistent	2 of 3 Positions
6.	Replacement of all liquid pumps	H_2O Submergible	Nonsubmergible
7.	Relocation and rewiring of electronics	Table Top Mounting	Above Test Bed Area
8.	Relocation of electrical module connections	Table Top Mounting	Above Test Area
9.	Addition of anode gas pressure shutdowns	None	1 of 3 Positions
10.	Replacement of worn valves, heaters and relays	Functional	Improved Reliability
11.	Updated process air heat exchanger	Coolant and Tape Heaters on Copper Pipe	In-line Cooling and Heating (Feedback Controlled)
12.	Improved control of process air dry bulb temperature	None	ΔT Control (Dry Bulb-Dew Point) or Constant Level
13.	Improved module temperature control	Constant Level	ΔT Control (Dry Bulb-Dew Point) or Constant Level
14.	Improved temperature sensors for control and monitor	Thermocouples	Resistance Temperature Sensors
15.	Dew Point temperature readout	None	Digital

The requirements of the advanced performance level testing (B level) were established to meet the needs of the test program and are listed in Table 10. As Table 10 shows, the operating ranges selected are consistent with application of the EDC to projected spacecraft environments. Also, special emphasis was placed on defining and implementing automatic protection, feedback controls and operating parameter monitoring. Design and fabrication of the test facilities were completed and all requirements incorporated.

Three-Person Preprototype EDC Subsystem

The TSA developed for the CS-3 supplied process and cooling air, H_2, N_2 purge, vent for the H_2/CO_2 exhaust stream, electrical power (60 and 400 Hz power), provisions for parametric data display and provisions for collection of parametric data via a 24-hour DAS. To perform the fluid supply and vent functions, as well as parametric data display and electrical power, existing TSA previously used with the CX-1 was modified to meet the requirements for the CS-3 testing. Modifications consisted primarily of increasing the capacity from the previously used one-person to the three-person level. A separate temperature controlled cooling air stream, including a liquid/air heat exchanger, was provided.

A data collection and storage capability was developed in terms of a 24-hour DAS. This unit was designed to collect out-of-range parametric values from all the sensors of the CS-3 and store them on a floppy disk memory. Recall and display in engineering units was provided to a CRT. Data was collected by exception, i.e., any parameter falling out of present but controllable limits were stored for later retrieval. The capacity of the 24-hour DAS was such that all sensors of the CS-3 could be recorded at two-minute intervals and their values stored for a 24-hour period. Figure 47 is a photograph of the 24-hour DAS showing its minicomputer, dual floppy disks, CRT display unit, standard alphanumeric operator keyboard and line printer. The line printer permitted hard-copy record keeping of the out-of-tolerance or, if desired, normal sensor data.

Air Supply Unit

The ASU of the EDC TSA is a closed-loop air supply and conditioning system designed to simulate the various air temperature, gas composition and humidity conditions that could be encountered in a spacecraft cabin. The ASU is used primarily to supply process and cooling air to the EDC; however, it can also be used for numerous other air treatment and air control tests.

The design approach taken was similar to standard air conditioning practice. The heart of the ASU is the contractor-provided, six-person, liquid-cooled condensing heat exchanger. Process air at a dew point temperature higher than that desired is chilled to the desired dew point and subsequently post-heated to obtain the dry bulb elevation, i.e., desired RH. In order to have the process air dew point above the desired level before entering the heat exchanger, water is sprayed into the loop. The ASU is a closed loop system so that all of the air is first chilled, then heated during each pass around the loop.

TABLE 10 B LEVEL TSA REQUIREMENTS

Number of Test Positions (Single-Cell)	Three (One for Checkout and Parametric Tests and Two for Endurance Tests)
Cell Hardware	Advanced Configuration
Cooling	Liquid or Air
Operating Ranges	
Current, A	0 to 20
pCO_2, Pa (mm Hg)	Ambient to 1330 (Ambient to 10)
RH, %	26 to 80
Temperature, K (F)	291 to 300 (65 to 80)
H_2 + CO_2 Backpressure, kPa (psig)	0 to 68.9 (0 to 10)
Air Flow per Cell, dm^3/s (scfm)	0 to 0.94 (0 to 2)
Automatic Protection	Low Cell Voltage High Temperature High Backpressure Low Backpressure
Controls	Constant Current Cell Temperature Inlet/Outlet Dew Point Automatic Saturator Refill
Monitor	Current Voltage Inlet/Outlet Dew Points (Air) Inlet/Outlet Temperatures (Air) Inlet/Outlet pCO_2 (Air) Outlet pCO_2 (H_2) Air Flow H_2 Flow H_2 + CO_2 Flow CO_2 Flow Inlet/Outlet Temperature (Coolant)

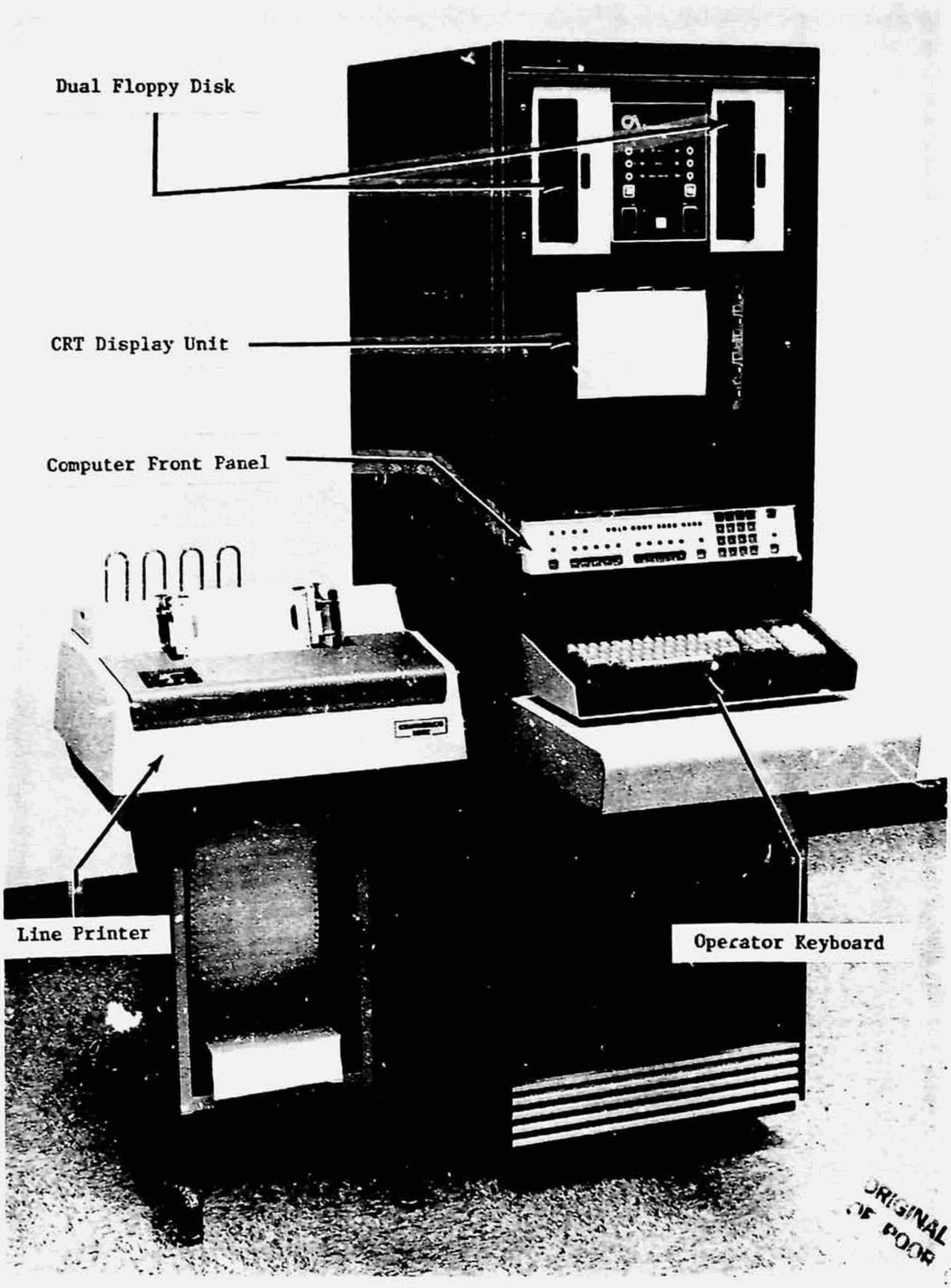

FIGURE 47 CS-3 DATA ACQUISITION SYSTEM

The principal components of the ASU are shown schematically in Figure 48. Physically, the ASU is divided into two parts. The first, the air processor, includes the condensing heat exchanger, circulation blower, spray chamber, spray pump, water reservoir, air heater and associated ducting, piping and support structure. These components are pictured in Figure 49. The ASU design specifications are listed in Table 11. The flow is established by the constant speed blower and the setting of the damper valves. While total circulation may be 17.0 m^3/min (600 cfm), it is possible to draw off the desired quantities of process and cooling air to the EDC. As shown in the schematic, the ASU has the capability of supplying two systems under test simultaneously.

The water is supplied to the air through a pump and spray nozzle. Excess and condensed water is gravity returned to the reservoir. The 5000 W electric heater can give a 12 K (20 F) elevation in dry bulb temperature at a nominal flow rate of 14.2 m^3/min (500 cfm).

Aside from the sensors, all instrumentation is housed in the ASU control and monitor cabinet pictured in Figure 50. This includes the controls to operate the blower, water pump and heater; the instrumentation and sensors to monitor and control temperature, pressure, humidity, CO_2 and O_2 levels; and the capability to periodically calibrate the instruments. In addition, shutdown capability both within the ASU and to and from other subsystems exists. The shutdown parameters are dry bulb and dew point temperature, air flow, H_2 concentration and an external signal.

The ASU was tested extensively and met or exceeded all design specifications. Air flow capability was from 0 to 20 m^3/min (750 cfm). Dew points were maintained from 279 to 301 K (42.5 to 82 F) and dry bulb temperatures from 279 to 302 K (42.5 to 85 F). Resulting RH levels ranged from 26% to 100% saturation. The ASU was operated for more than 900 hours in support of the LBS-B/ORS-4(A) testing and for over 8,000 hours in support of the ARX-1 testing.

One-Person Air Revitalization System

Test Support Accessories were developed to support the test program of the ARX-1. A block diagram of the total TSA servicing the one-person ARS with its C/M I and N_2H_4 Supply, is shown in Figure 51. Some of the TSA hardware was developed or refurbished as part of this program; other hardware was provided from prior programs and modified. This hardware included part or all of the FSU, the ASU and its control, the CSU, the water source with liquid level monitoring, the vent/vacuum source, the high N_2 pressure supply for purging, the DAS and the Parametric Data Display.

A major portion of the TSA activities was involved with the development of the Parametric Data Display. The total unit, packaged in a separate cabinet, is shown in Figure 52. It services all of the functions of the ARX-1. Specifically, it contains displays for temperatures, cell voltages and currents, flows and pressures. Also shown in the lower portion of the cabinet are power supplies required for operation of the parametric data display cabinet and the ARX-1.

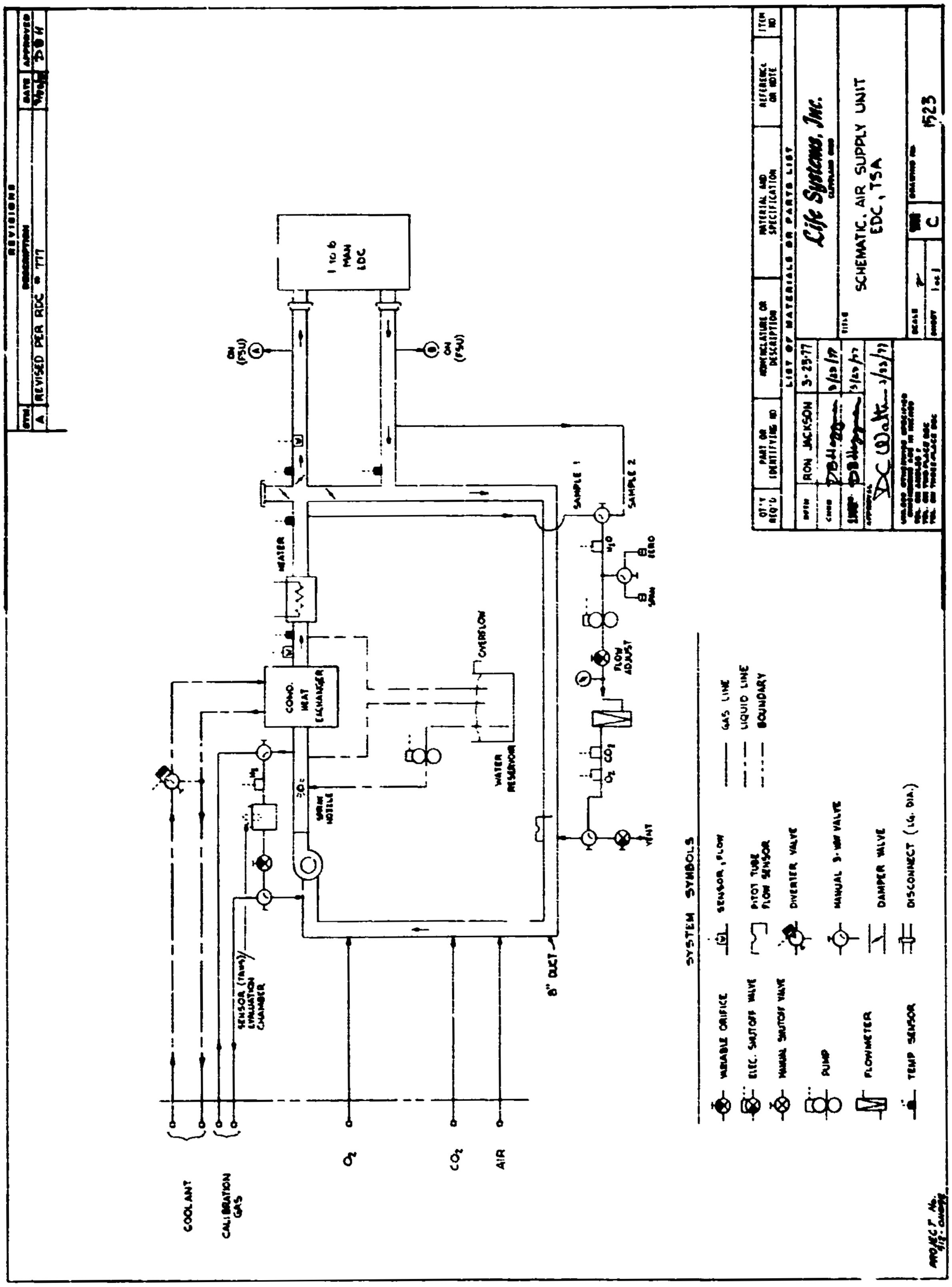

FIGURE 48 AIR SUPPLY UNIT SCHEMATIC

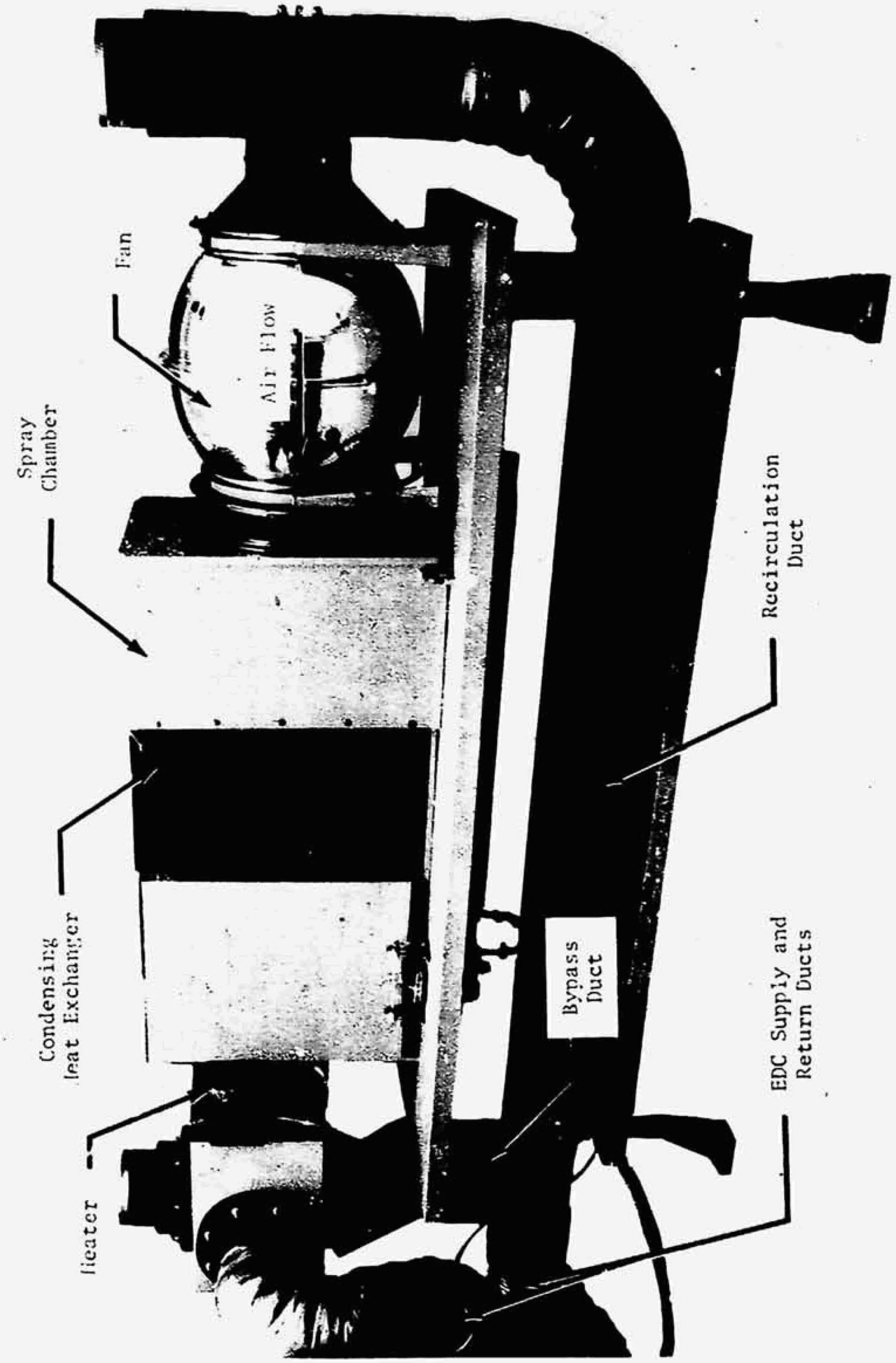

FIGURE 49 AIR SUPPLY UNIT

TABLE 11 ASU DESIGN SPECIFICATIONS

Crew Size	6
Processed Air	
Flow Rate, m^3/min (cfm)	0 to 17.0 (0 to 600)
Dew Point Range, K (F)	279 to 301 (42.5 to 82)
Dry Bulb Range, K (F)	279 to 302 (42.5 to 85)
Humidity Range, %	26 to 100
Condensing Heat Exchanger	
Heat Removal Capacity, kJ/s (Btu/h)	6.0 (20,500)
Effectiveness	0.905
Coolant	
Flow Rate, dm^3/s (gpm)	0.4 (6)
Temperature, K (F)	277 (40)
System Pressure	
Nominal, kPa (psia)	101 (14.7)
Deviation, kPa (in H_2O)	±0.74 (±3)
Nominal Gas Composition, kPa (mm Hg)	
O_2	21.3 (160)
CO_2	0 to 0.93 (0 to 7)
H_2	0.76 (5.7)
N_2	Makeup
Physical	
Air Processor	
Size, WxDxH, m (ft)	3.4 x 0.91 x 1.8 (11 x 3.0 x 6.0)
Envelope Volume, m^3 (ft^3)	5.7 (200)
Weight, kg (lb)	270 (600)
Power, W	6500
Control and Monitor Cabinet	
Size, WxDxH, m (ft)	0.55 x 0.67 x 1.8 (1.8 x 2.2 x 6)
Envelope Volume, m^3 (ft^3)	0.65 (23)
Weight, kg (lb)	114 (250)
Power, W	1000

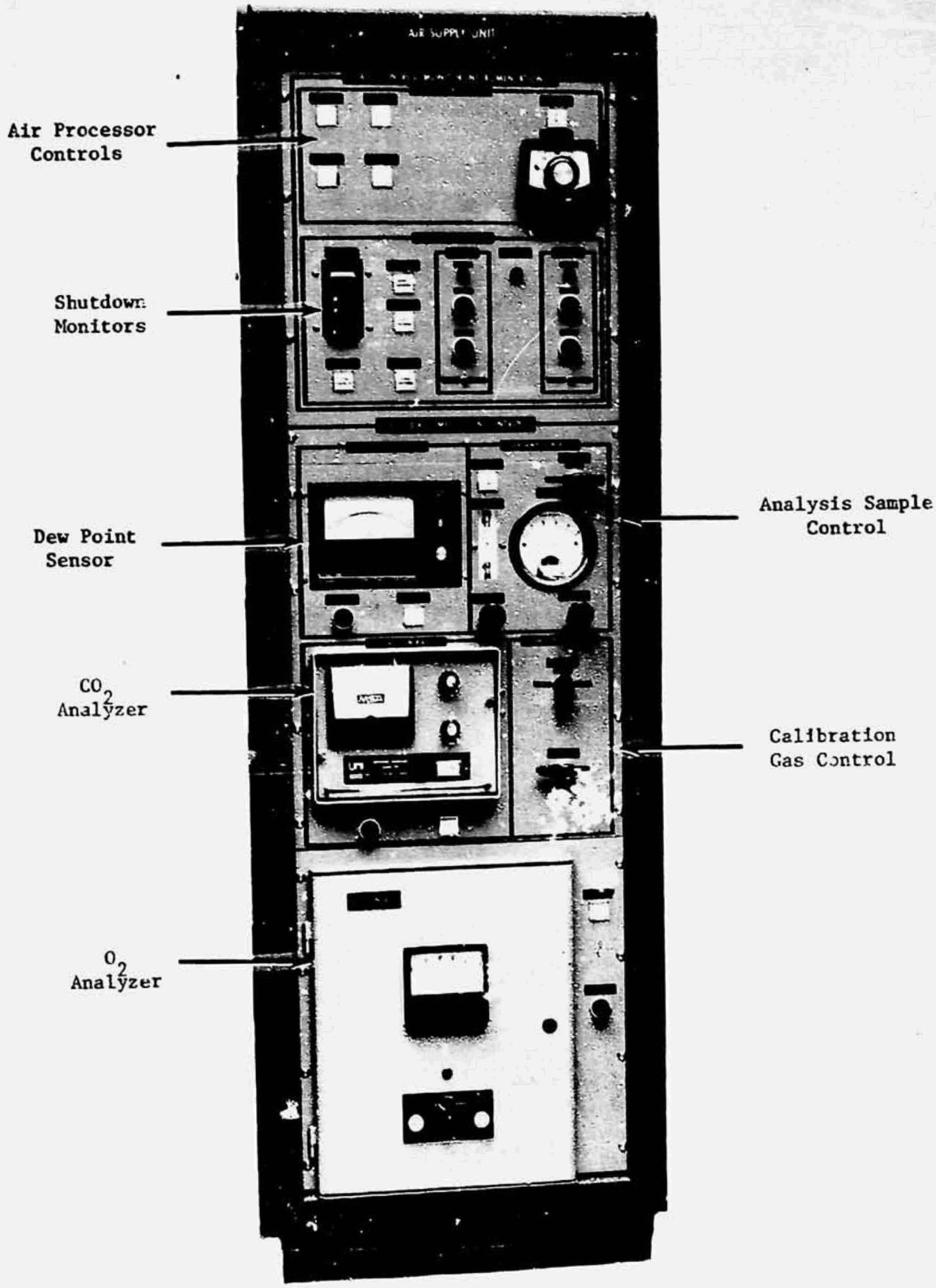

FIGURE 50 ASU CONTROL AND MONITOR INSTRUMENTATION

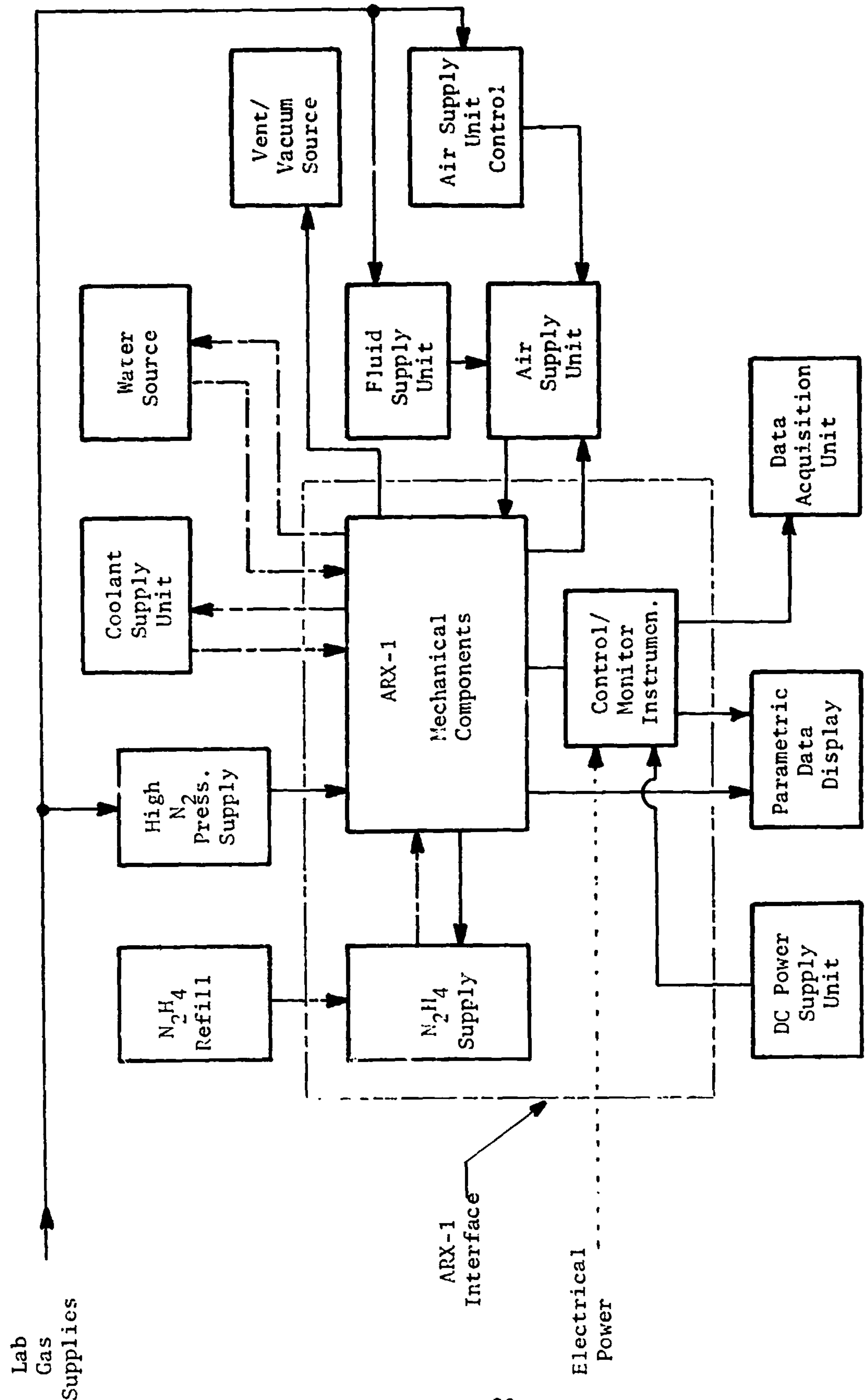

FIGURE 51 ONE-PERSON AIR REVITALIZATION SYSTEM TSA BLOCK DIAGRAM

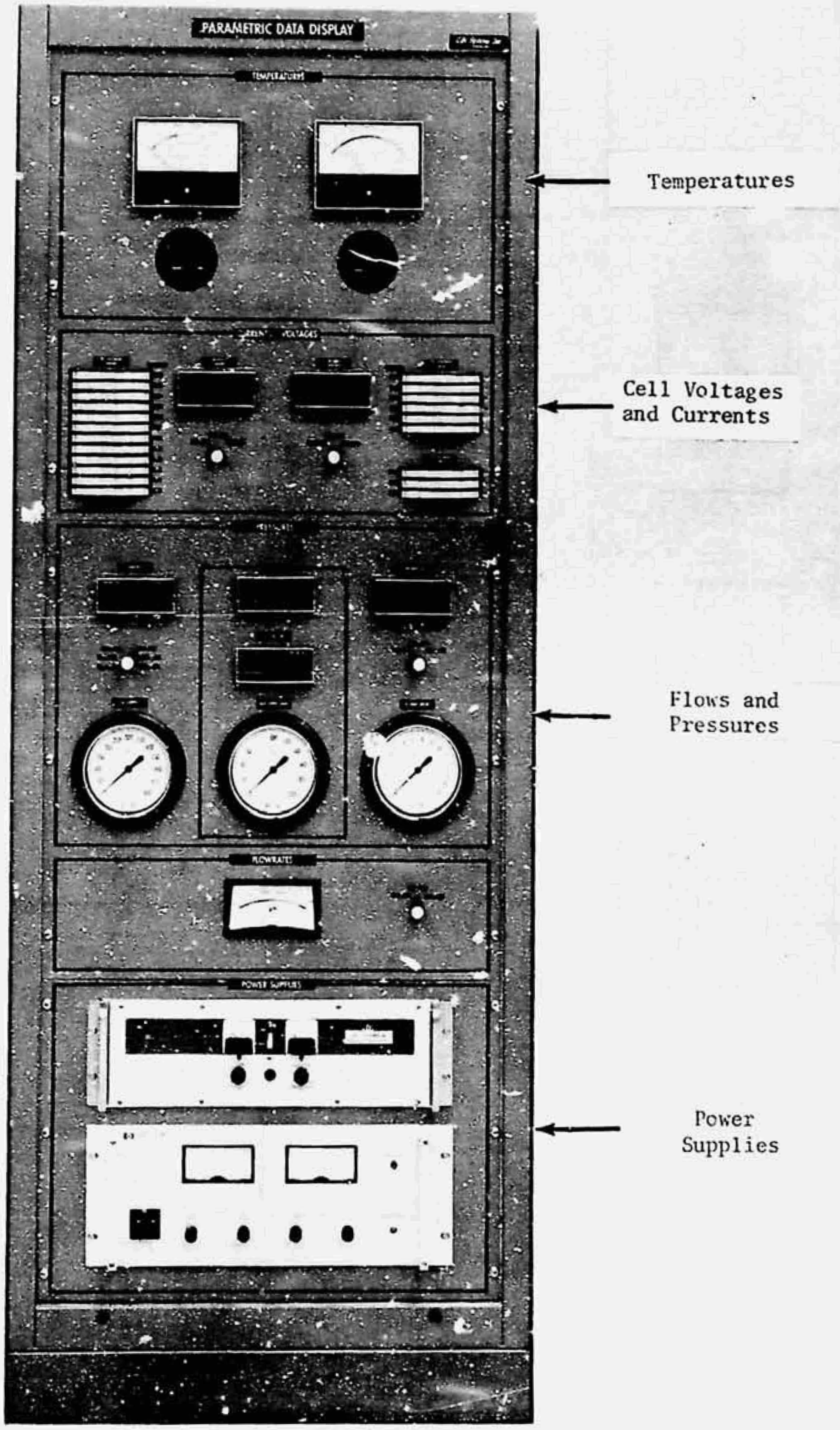

FIGURE 52 ONE-PERSON AIR REVITALIZATION SYSTEM
PARAMETRIC DATA DISPLAY CABINET

MINI-PRODUCT ASSURANCE PROGRAM

A mini-Product Assurance Program was established, implemented and maintained throughout all phases of contractual performance including design, purchasing, fabrication and testing.

Quality Assurance

Quality Assurance activities were included during the design studies, interface requirement definitions and during inspection of fabricated and purchased parts. The objective was to search out quality weaknesses and provide appropriate corrective action. Also, a quality assurance effort was involved in the preparation of the Final Report with the objective of identifying and resolving deficiencies that could affect the quality of future equipment.

Reliability

Reliability personnel participated in the program to ensure (1) proper calibration of test equipment and TSA instrumentation, (2) adherence to test procedures and (3) proper recording and reporting of test data and observations. A survey of the component, subsystem and TSA designs was performed to determine the calibration requirements for testing. Appropriate components were calibrated during assembly and after installation.

A test procedure was established to ensure that all critical parameters were properly monitored and that the testing conformed to the program's quality assurance and safety procedures. All major testing required that a test plan be completed and reviewed.

Safety

A Safety Program was initiated to ensure adherence to safety standards and procedures essential to protect personnel and equipment. The program consisted of identifying possible adverse subsystem and TSA characteristics, reviewing designs and design changes for potential safety hazards, reviewing NASA Alerts for safety information and incorporating the equipment's protective features.

Materials Control

A mini-Materials Control Program was initiated to provide assurance that the CS-3 and ARX-1 hardware did NOT preclude the efficient application of a more detailed materials control program during subsequent developments. As a goal, materials of construction were selected to comply with projected spacecraft material specifications.

Configuration Control

A mini-Configuration Management Program was established, implemented and maintained. This program provided for documentation concerning interface requirements for the ARX-1 testing and the CS-3 development and test as a part of the RLSE Program. The program was implemented with a primary goal to provide assurance that the efficient application of a more detailed configuration management program can be applied during subsequent development of ARX hardware.

TECHNOLOGY ADVANCEMENT STUDIES

As part of the contractual effort several studies were completed that were directed toward the advancement of the EDC technology. The studies were grouped into nine different areas. A short description and major results of the studies are listed in Table 12 and further described below. These studies provided valuable information which led to improved EDC cell hardware and performance and subsystem operation, as well as the establishment of further technology goals.

Electrode Teflon Loading Study

The Teflon loading, i.e., the percentage of Teflon in the catalyst binder on the EDC electrode surface, significantly affects CO_2 removal efficiency and cell voltage. The Teflon loading of the electrode controls the hydrophobic nature of the electrode and results in altering the electrode gas diffusion layer thickness and the number of available reaction sites. A study was conducted to determine if improvements in EDC performance were possible by altering the Contractor's baseline electrode Teflon loading.

Three cathodes with varying amounts of Teflon were fabricated and tested. Of the three electrodes, one contained the previously established Contractor's baseline Teflon composition, one contained a 10% lower than baseline loading, while the third contained a 10% higher than baseline Teflon composition. The electrodes were mounted and parametrically tested in standard 2.3 dm^2 (0.25 ft^2) LDC single cells with internal air cooling.

The results of the testing are shown in Figures 53 and 54, showing CO_2 removal and voltage performance of the three cathodes as a function of inlet pCO_2 level and current density, respectively.

The 10% higher than baseline Teflon electrode exhibited poor CO_2 removal efficiency and extremely poor electrical performance, failing to maintain a positive voltage and caused an early termination of the test. The 10% lower than baseline Teflon electrode, while exhibiting a CO_2 removal efficiency slightly less than baseline, did show a higher than normal cell voltage.

From these tests it was concluded that the optimum Teflon loading for CO_2 removal occurs at the baseline loading while an electrode (cathode) more optimized for power output (higher cell voltage) would require a composition slightly less than baseline.

Alternate Anode Current Collector Design

A development effort was conducted to select an alternate technique to apply the anode current collector to advanced EDC cell frames. The objective of this study was to identify and demonstrate a technique that would prevent

TABLE 12 TECHNOLOGY ADVANCEMENT STUDIES SUMMARY

Title	Description	Result
Electrode Teflon Loading	Determine effects of Teflon loading on CO_2 removal efficiency and cell voltage	Optimum Teflon loading for CO_2 occurs at baseline loading but slightly higher cell voltages occur at decreased loading level.
Alternate Anode Current Collector	Find alternate technique that has no adverse effects on polysulfone when applying the anode current collectors to cell frames	Metal foil can be inlaid and electron-beam welded to the current collector tabs; reduced internal resistance observed
Matrix Fabricator	Fabricate hardware to implement LSI's technique to produce high strength matrices	A procedure for fabricating fixture for matrices from raw asbestos fiber was assembled
Combined Humidity/ CO_2 Control Concept	Combine the functions of water and CO_2 removal within an EDC or CHCS/EDC	Combined water and CO_2 removal concept demonstrated with ARX-1 CHCS/EDC
Performance Deviation	Investigate subnormal CO_2 removal and electrical efficiencies	Electrolyte precipitation causes partial masking of the area to current transport; automatic control and monitoring and a new electrolyte prevent precipitation
Optimum EDC Current Density	Determine the optimum EDC current density and lowest weight when using EDC-generated power configurations	Optimum current density/equivalent weight occurs slightly below the current density that maximizes CO_2 removal efficiency
Electrolyte Mixture	Extend EDC operation to low process air RH's by altering electrolyte composition	Effects on performance are negligible for mixed electrolytes compared to baseline electrolytes within the nominal operating ranges of an EDC
Hydrated Salt Electrolytes	Improve EDC cell voltage performance by operating at elevated temperatures	Hydrated salts for the desired temperature range are not suitable; penalties to preheat air are excessive.
B-Level Performance	Test and analyze hardware which promises improvements in performance	A high moisture tolerance and an internal electrolyte reservoir cell design demonstrated the most improvement in performance

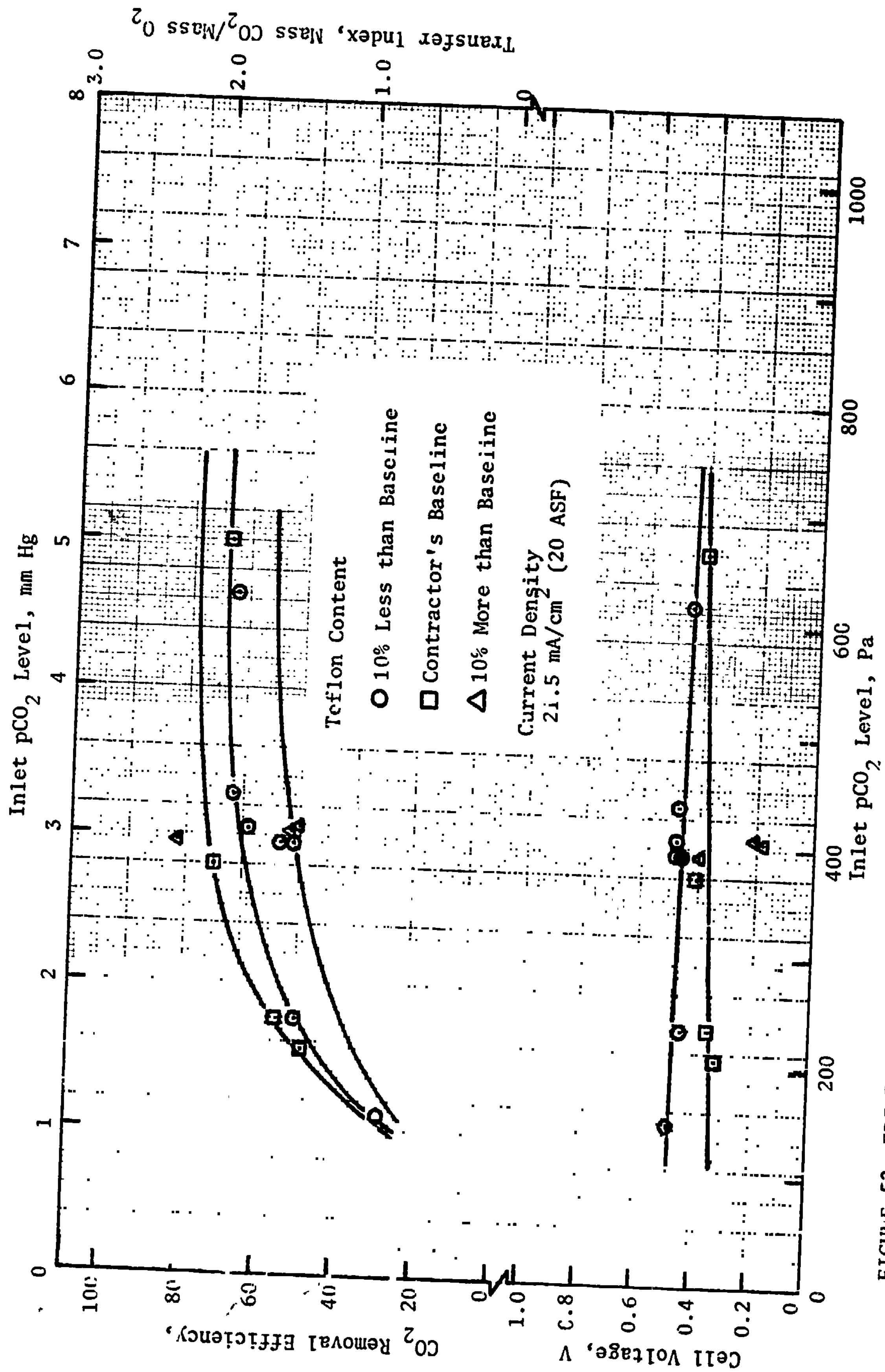

FIGURE 53 EDC PERFORMANCE AS A FUNCTION OF PROCESS AIR pCO_2 FOR VARIABLE TEFLON LOADING LEVELS

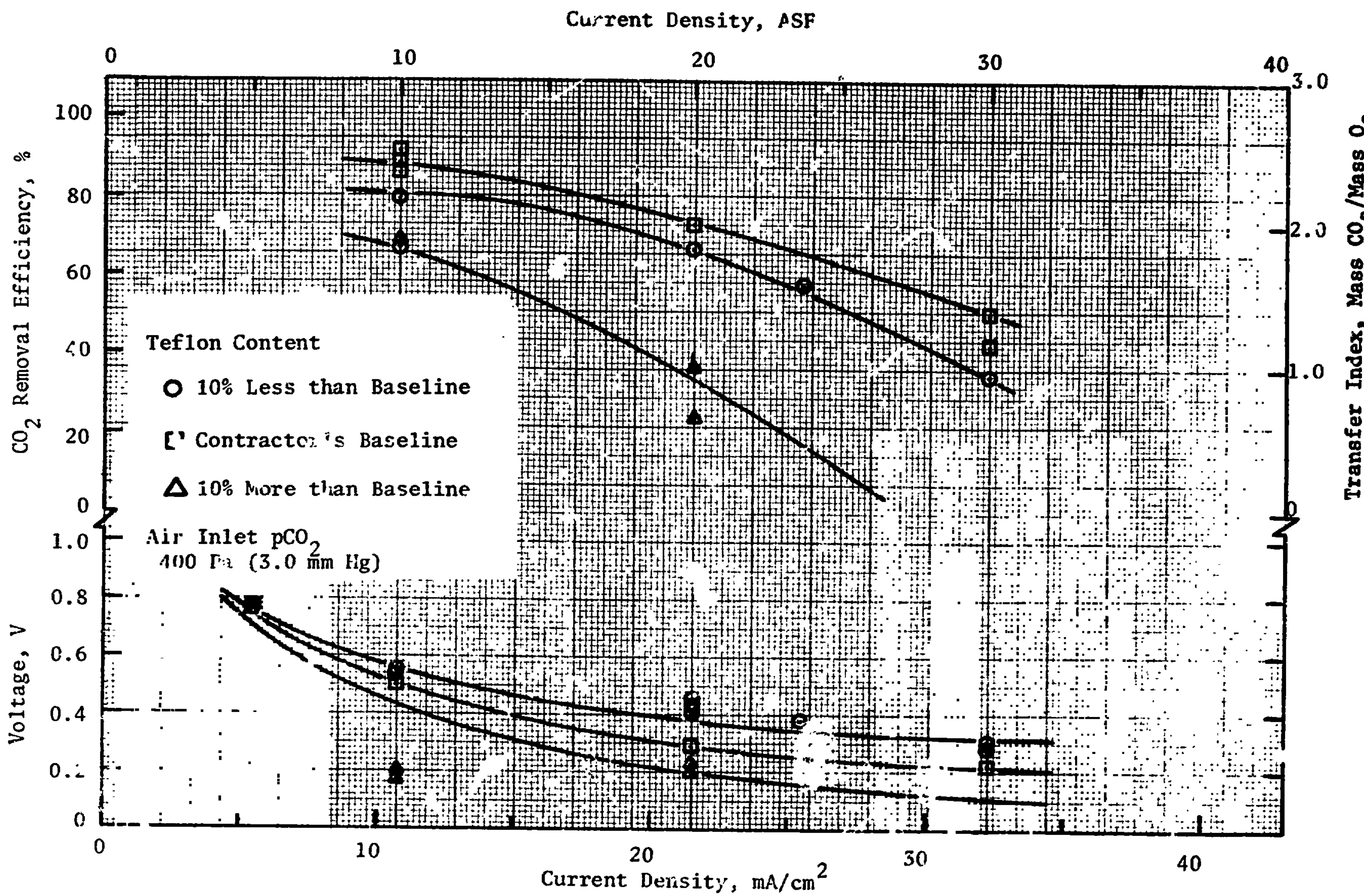

FIGURE 54 EDC PERFORMANCE AS A FUNCTION OF CURRENT DENSITY FOR VARIABLE TEFLON LOADING LEVELS

polysulfone crazing, occasionally observed after extended times (greater than one year) with the presently used plating process. In addition to crazing, the unit cost per frame was also high. The baseline design incorporated plating of the anode current collector directly onto the polysulfone cell frame. This process consisted of a series of steps including electroless nickel plating followed by silver and gold plating.

Three alternate techniques for applying anode current collectors to the cell frames were investigated. One, called ion deposition plating, was evaluated and was found to be inadequate due to the brittleness of the resulting plating. A second plating technique, called plasma deposition, was found to be unacceptable due to difficulty in achieving the required thickness and uniformity.

The third technique evaluated proved acceptable and is presently projected for the fabrication of future EDC cells. The design uses thin metal foil, sized for the required current conduction, inserted into the anode cavity of the cell and electron-beam welded to the current collector tabs. Modifications to the polysulfone frame design were made to accept the metal foil, and the injection mold for the frames was modified to be compatible with the new process.

Electrical resistance checks were made from the external tabs to the internal foil. A reduction of one order of magnitude in internal resistance losses was obtained compared to the plated design. Also, while materials costs are similar, the electron-beam welding process is substantially lower in total cost than plating.

Matrix Fabricator

Previously used fuel cell grade asbestos matrices are no longer commercially available. For this reason LSI had previously defined a step-by-step procedure for fabricating reconstituted fuel cell grade asbestos matrices from commercially available raw asbestos fibers. A matrix fabricator was required to verify the procedure at the scaled-up level required by full-sized EDC cells.

Based on the existing matrix manufacturing procedure and requirements, a new asbestos matrix fabricator was designed. The unit is of a welded aluminum construction to resist deterioration due to fluids used during the matrix fabrication procedures. The fabricator utilizes a rubber gasketed porous nickel plaque to support the matrix material during the vacuum deposition phase.

Combined Humidity/CO_2 Control Concept

During normal operation of an EDC, the water produced by the electrochemical reaction is transferred into the process air stream and exhausts into the cabin atmosphere for subsequent removal by a separate humidity control subsystem. For long-term space missions the water generated by the crew and by the reactions of the CO_2 removal process must be reclaimed for use within the spacecraft. This suggests a concept of combining the humidity control function with the CO_2 removal function by removing both water and CO_2 from the process air

C-2

stream taken from the cabin. The combined concept could potentially result in overall system weight and volume savings. Two different approaches of combined humidity/CO_2 control were investigated.

One approach is modification of the baseline EDC cell to incorporate hardware to simultaneously remove water and CO_2. This concept was extensively discussed in a prior report.(10) A water removal cavity is located adjacent to the cathode air compartment. The pressure in this compartment is maintained by vacuum vent at the vapor pressure corresponding to the desired cabin air dew point. Tests showed that the concept is feasible but was limited due to (1) difficulty in maintaining the absolute pressure levels in the 1.06 to 1.60 kPa (8 to 12 mm Hg) range which corresponds to dew points in the 281 to 287 K (45 to 57 F) range, (2) structural constraints on the cell hardware design and (3) overboard loss of water. Any advantage obtained in combining water and CO_2 removal within the cells is offset by increased size and complexity of the EDCM.

The second approach is the combined CHCS/EDC concept similar to that developed for the ARX-1. Two separate components, the CHCS heat exchanger and the EDCM, perform the desired functions of humidity and CO_2 removal. The CHCS is designed to control to the desired dew point level and yet maintain the proper RH conditions to the EDC.

The ARX-1 hardware permitted testing of this concept. Figure 55 shows the results of varying the RH of the inlet to the CHCS in terms of the EDC average RH response. The average RH is computed from the process air inlet and outlet RHs. It is seen that this parameter was maintained fairly constant (desired value is 80%) over the range of CHCS inlet RHs tested. The test was conducted over 30 days of operation with both CHCS and EDCM coolant temperature setpoints maintained at the baseline levels. The results indicate that both CO_2 and moisture removal was achieved with the hardware arrangement tested and that altering inlet conditions to the CHCS had minimal effect on the EDC operating conditions.

Performance Deviation Study

During past EDC developments certain cells exhibited deviations from the expected baseline performance, i.e., subnormal CO_2 removal and electrical efficiencies. These same cells also exhibited maldistributions of CO_2 removal, water evolution and dry bulb temperature increases over the surface area of the electrode. A performance deviation study was conducted to analytically and experimentally investigate the observed maldistributions. The study examined previous test data, then analyzed the data to identify a possible cause(s) for the subnormal CO_2 removal and electrical efficiencies.

The reason for low performance was traced to current maldistributions caused by electrolyte (Cs_2CO_3) precipitation. Start of precipitation is normally caused by out-of-tolerance interface conditions (process air RH, coolant temperature, H_2 or N_2 RH, etc.) or lack of automatic controls (module temperature, cooling air flow, etc.). Reversal to baseline performance is not possible once precipitation has occurred. As a result of the study, provisions were

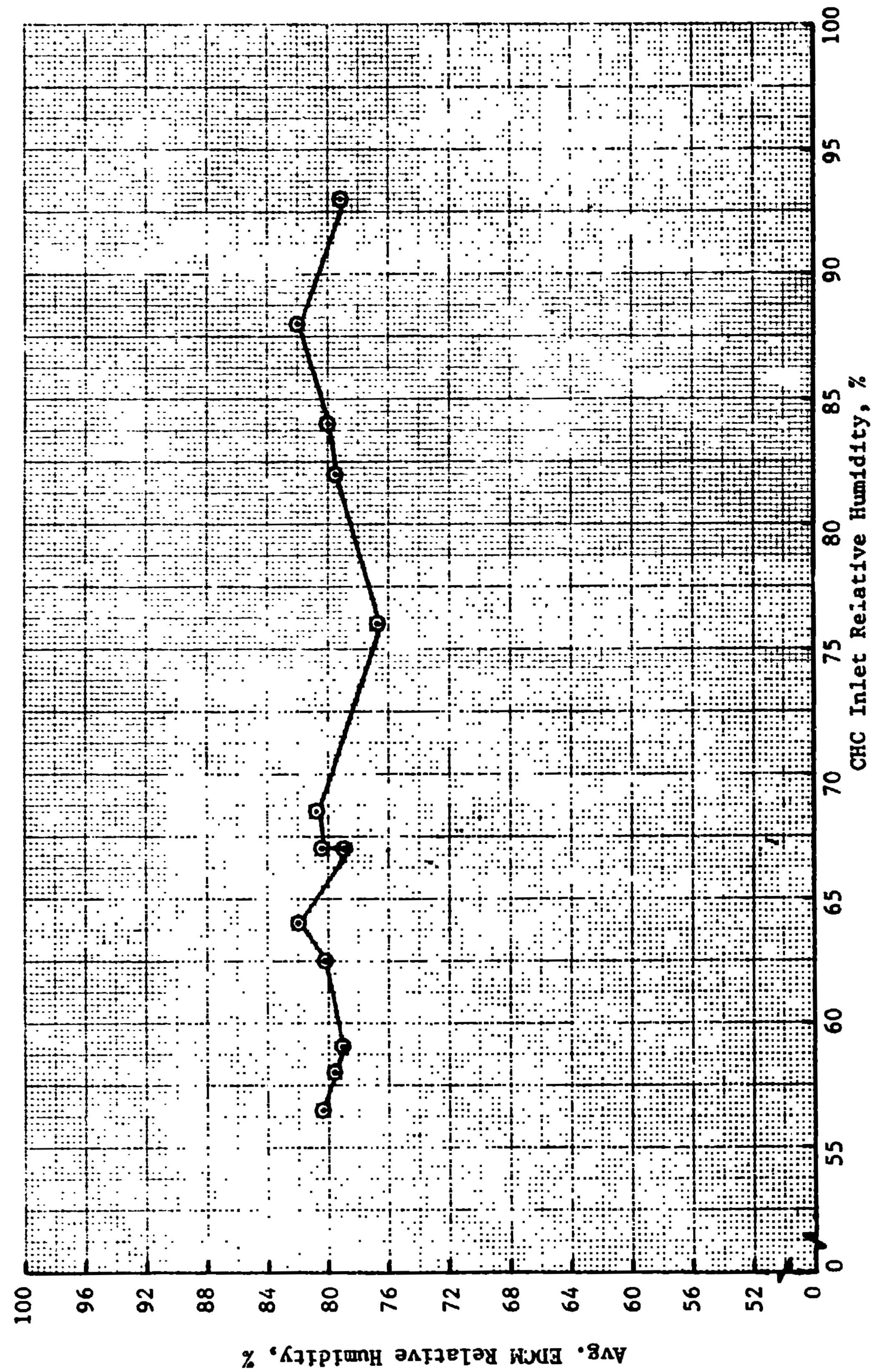

FIGURE 55 AVERAGE EDCM RH VERSUS CHC INLET RH

were included in the C/M I's of EDC's (such as the CS-3 and ARX-1) to monitor for out-of-tolerance interfaces and operating conditions and automatic shutdown of the EDC should preset limits be exceeded. Also, an advanced electrolyte (LSI-D) has been developed by LSI to increase tolerance to low RH process air streams.

Optimum EDC Current Density

A study was conducted to determine the optimum EDC current density that would result in the lowest total equivalent weight for spacecraft application when the EDC was used as a power generator as well as a CO_2 remover.

A computer program was written to facilitate calculation of total equivalent weights based on given input parameters. The equivalent weight was determined from several factors. These included CO_2 removal rate or capacity which related to fixed hardware weight. Also, weight penalties incurred because of the power used, heat rejected and the O_2 consumed by the EDC were included.

Computer results of total equivalent weight versus current density curves for 1-, 3-, 6- and 12-person EDCs are shown in Figure 56. In these and other test cases, the optimum current density for the lowest total equivalent weight occurred slightly below the current density that maximized CO_2 removal efficiency. Using the EDC generated power in other electrochemical subsystems of an ARS reduces overall power but has only a small impact on optimum EDC current density. In general, a slightly lower current density than that for optimum CO_2 removal results.

Electrolyte Mixture Study

To expand the capability of EDCs to operate efficiently at the low process air RHs encountered in spacecraft atmospheres (as low as 26% RH), electrolytes composed of mixtures of carbonate salts were studied. The premise for the study was that two dissimilar salts can produce concentrated solutions of greater ionic solubility than the concentrated solution of either single salt. This increased ionic solubility could maintain an increased ionic water binding force resulting in decreasing the water vapor pressure (pH_2O) of the solution. For EDC electrolytes it is necessary to consider the dew point depression characteristics of both the carbonate ($CO_3^=$) and bicarbonate (HCO_3^-) forms of the electrolyte mixture since both species are present in an operating EDC cell.

Mixture Selection Techniques

To match the low spacecraft atmosphere RH's (26% RH) requires electrolytes which exhibit a high dew point depression. The electrolytes must still be carbonates to satisfy the basic EDC requirements. In this study the salts of the alkali metal family were considered.

Both analytical and experimental evaluation of potential mixtures of the salts were used in order to predict potentially promising ratios. Initially,

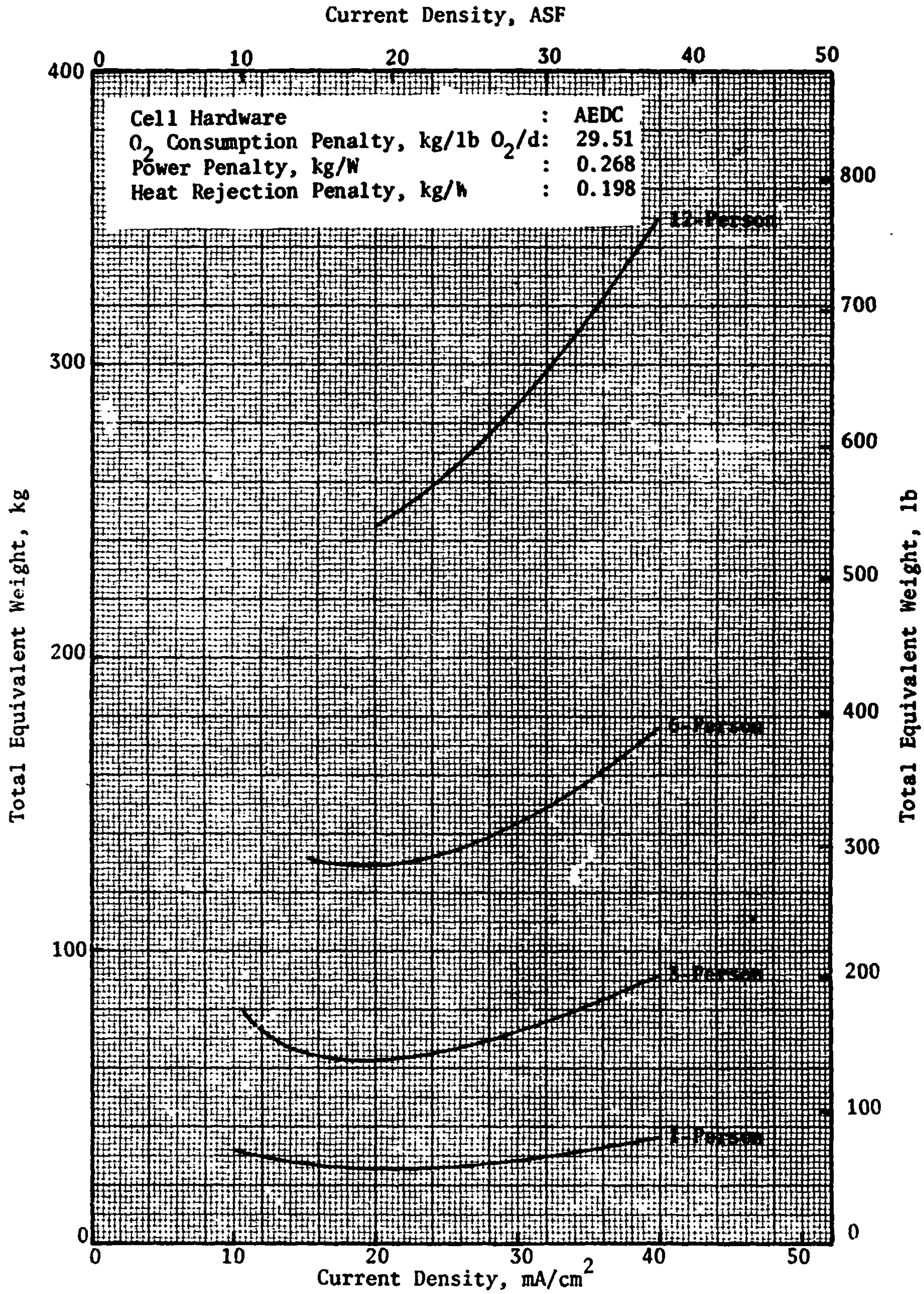

FIGURE 56 TOTAL EQUIVALENT WEIGHT AS A FUNCTION OF CURRENT DENSITY

potential mixtures were evaluated for optimum solubility based on the activity coefficients of the independent salt concentrations in the solution. The dew point depression characteristics of several of these mixtures were then experimentally determined. Correlation between analytical prediction and experimental results were difficult to establish and were inconclusive. Analyses indicated that an equilibrium with 25% RH air was possible. However, practical EDC cell operation would be substantially more limited due to operational gradients and mass transport limits. Full-sized cell testing was therefore selected for final determinations.

Single Cell Testing

A test program was performed in an attempt to predict electrolyte mixture effects on EDC operation. The objectives of the test were to quantify possible effects of the electrolyte mixtures on the CO_2 removal and electrical efficiencies of an EDC cell as a function of inlet air pCO_2 level, current density and inlet RH. The electrolyte mixture with the potentially highest dew point depression was selected. A single cell EDC was assembled utilizing the CS-6 type hardware and charged with the electrolyte. The charge concentration was adjusted to an ionic concentration equivalent to the baseline FDC Cs_2CO_3 charge solution.

The test results illustrated only baseline performance, indicating that the overall effects of mixed electrolytes on performance and RH capabilities are negligible within the baseline operating ranges of an EDC.

Hydrated Salt Electrolytes

A study was conducted to determine if hydrated salt electrolytes could be used to improve EDC voltage performance since hydrated salts allow generally for increased operating temperatures. Higher operating temperatures have been shown to result in higher cell voltage performance of the EDC cell.

A search of potential hydrated salts was made. Metal carbonates (e.g., Li_2CO_3, K_2CO_3) have too high of a melting temperature to be applicable. The desired melting temperature is below 366 K (200 F). A group of organic carbonates had properties that met this requirement. For example, tetramethylammonium carbonate with various hydration states has melting points at 342 K (156 F) and near 368 K (203 F). From this consideration alone, certain organic carbonates are potential EDC electrolytes. Further investigation, however, indicated that their vapor pressure characteristics may not be compatible with process air moisture content. In addition, electrode poisoning due to electrolyte decomposition in a basic solution was a potential problem.

On a subsystem level the high temperature EDC operation would require heating the inlet process air. Even using a regenerative heat exchanger (i.e., recovering the heat in the process air outlet) would place excessive weight, size and power penalties on the concept. The increased penalties more than offset the advantage obtained from higher cell voltage operation on an equivalent launch weight basis. For this and the above reasons, further studies of hydrated salt electrolytes were not recommended.

B-Level Performance Technology Study

This study activity was directed toward the testing and analysis of LSI-generated hardware concepts which indicated improvement in performance. Performance levels were selected as goals to judge and compare EDC cell operation. These performance levels were termed B-level performance goals. Previous EDC performance goals, termed A-level, had been established prior to the development of the one-person[5] and the six-person EDCs.[6] These goals were demonstrated and exceeded during these developments. Therefore, the establishment of B-level performance goals was required to further direct EDC technology advancement.

Comparisons of A- and B-level performance as a function of inlet air pCO_2, operating current density and inlet air RH are presented in Figures 57, 58 and 59, respectively. The operating conditions for these comparisons are shown in Table 13.

Study Approach

The testing to demonstrate B-level technology consisted of evaluating four EDC hardware configurations or concepts (selected from eight potential candidate configurations). Three levels of testing, consisting of checkout/acceptance, parametric and endurance testing were conducted. The checkout/acceptance test screened the performance of each of the four concepts. Two were selected for further parametric testing to determine the effects of the inlet air pCO_2, current density and inlet air RH.

Concept Selection Approach

The four cell hardware concepts tested during the B-level technology study were chosen from a list of eight LSI-generated hardware configurations using short-term screening tests (less than six hours) as required. The approach for the selection of hardware concepts was based on three factors. The first factor was the ability of the EDC hardware concept to demonstrate the complete range of B-level performance goals. The second factor was the ability of the concept to improve operational reliability through increased cell voltage and increased tolerance to wide ranges in air RH. The last factor was the potential of the concept to perform better in any single one of the performance characterization areas (e.g., cell voltage, CO_2 removal efficiency) of the B-level performance goals established.

Table 14 is a list of the four concepts selected for the B-level technology study. This table also defines the basic cell hardware stackup, the type of electrochemical cell hardware utilized and the primary reason for the selection of the concept.

Test Results and Analysis

The four concepts selected and listed in Table 14 were evaluated according to the approach defined above.

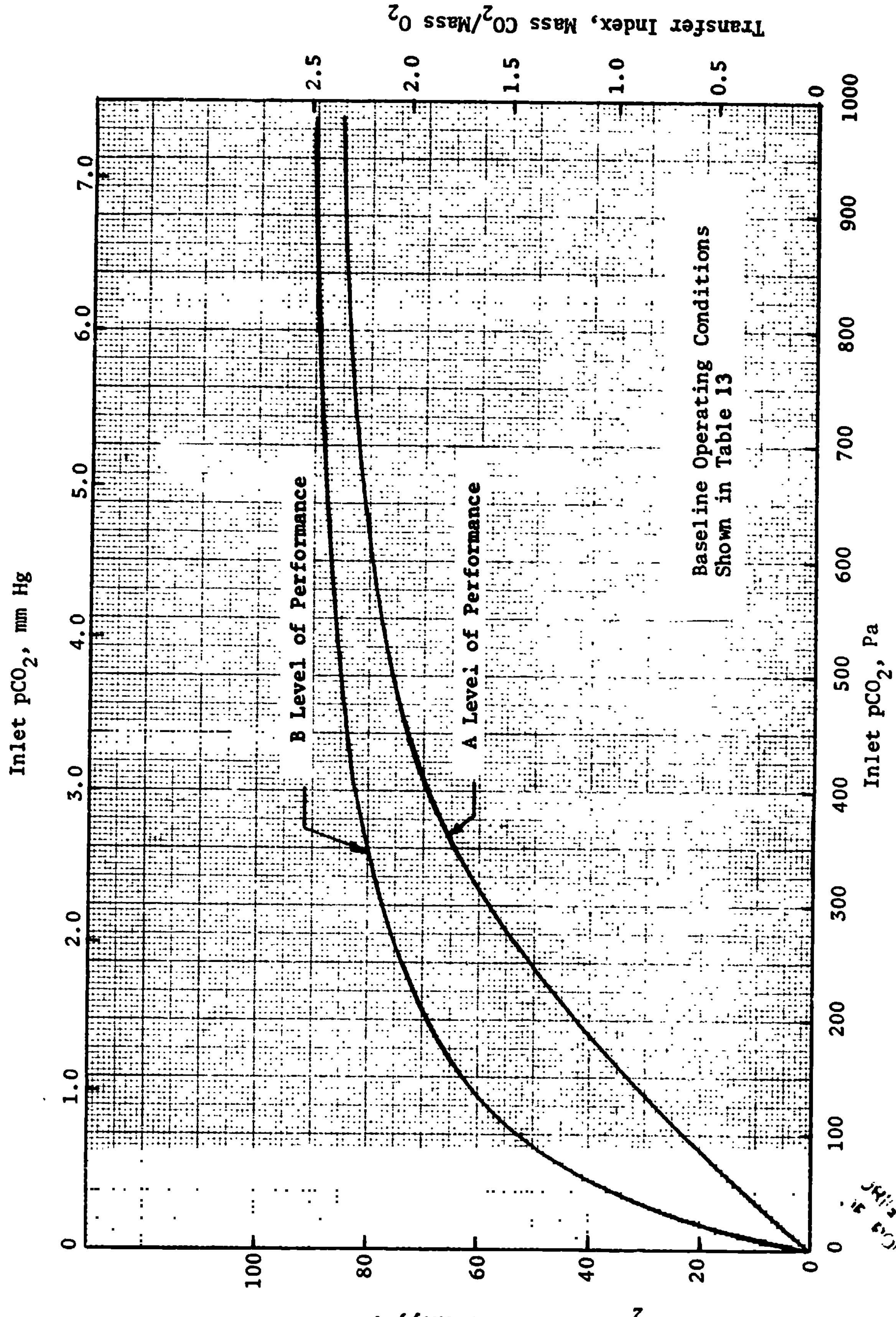

FIGURE 57 COMPARISON OF A AND B LEVEL OF EDC PERFORMANCE (INLET pCO_2)

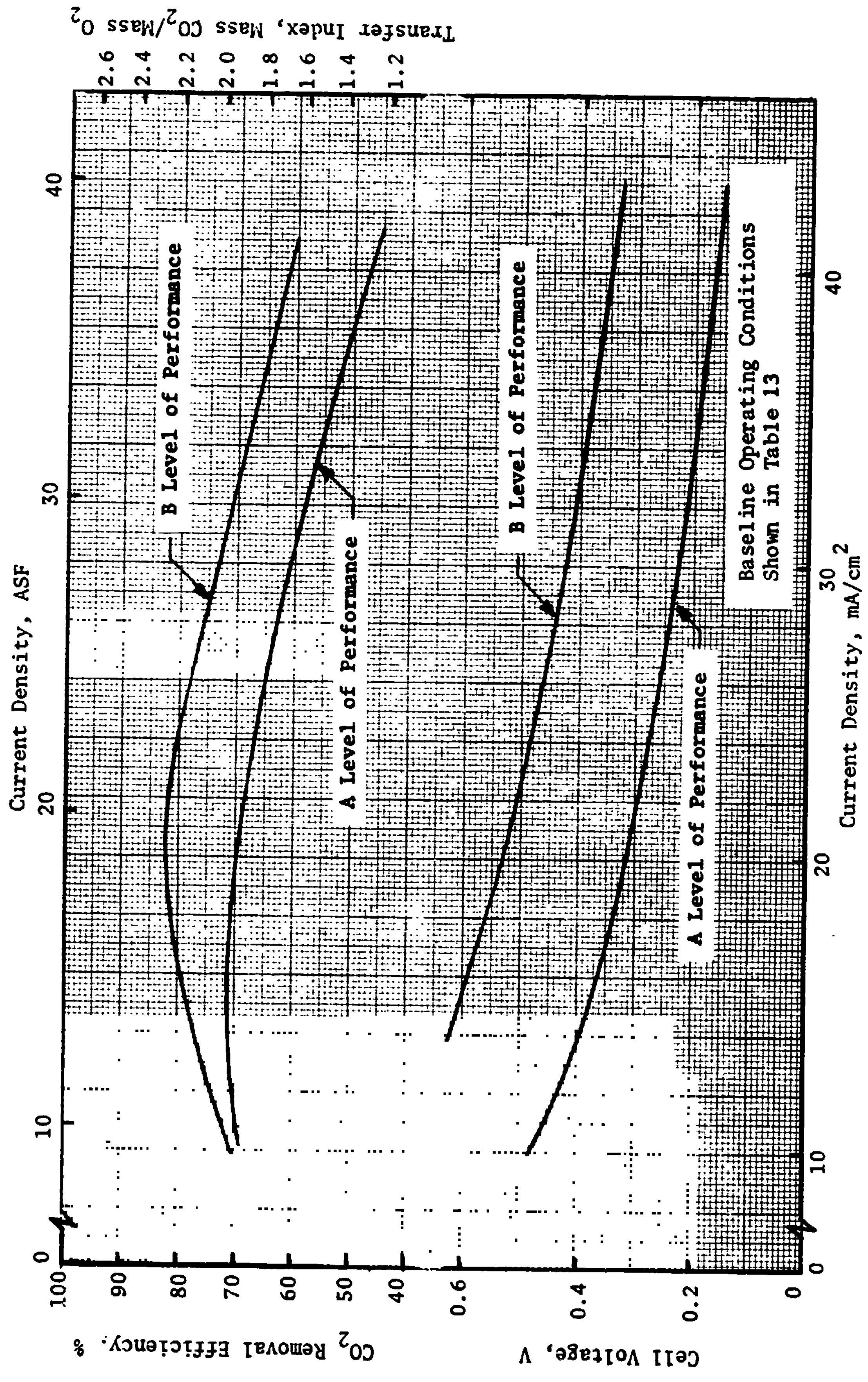

FIGURE 58 COMPARISON OF A AND B LEVEL OF EDC PERFORMANCE (CURRENT DENSITY)

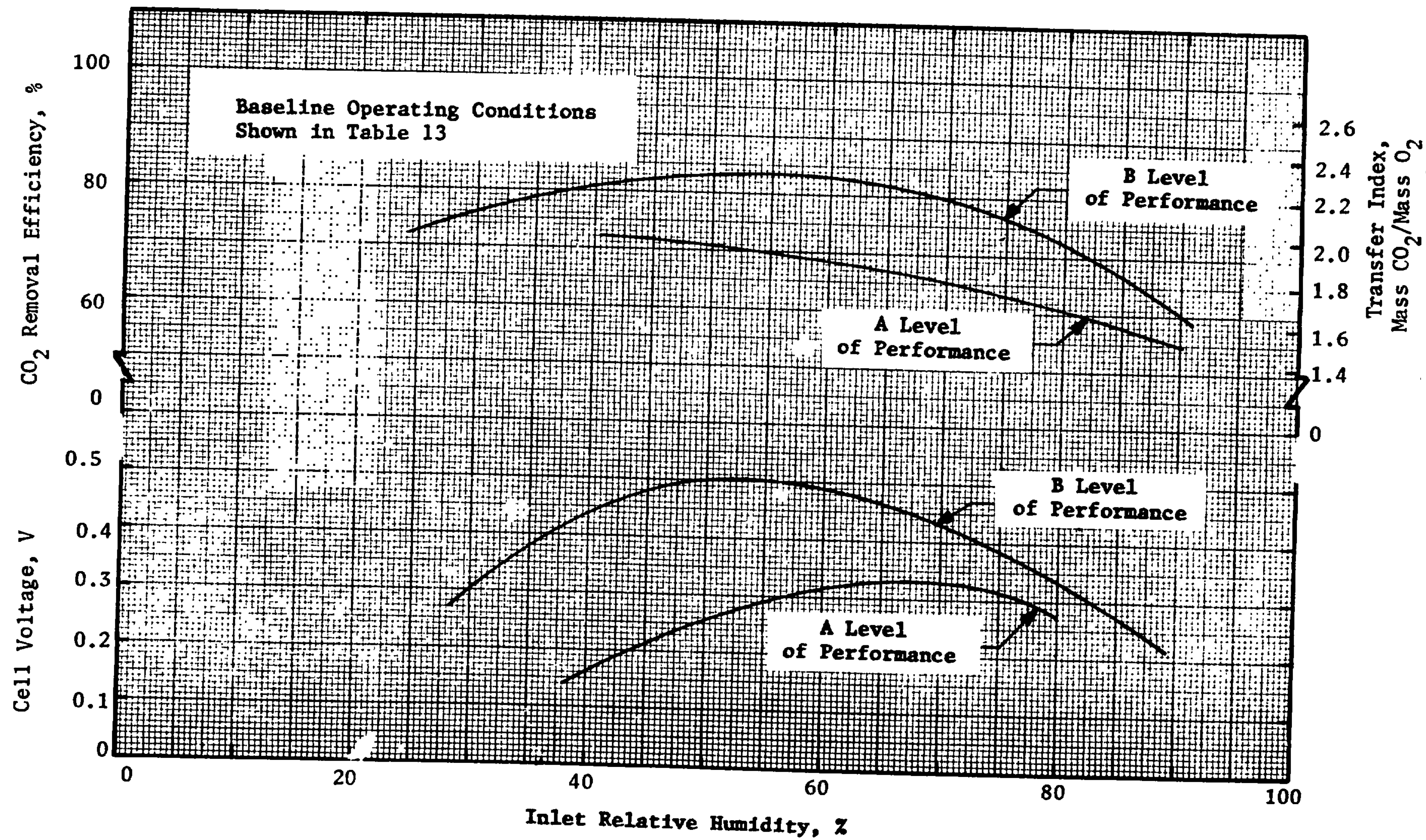

FIGURE 59 COMPARISON OF A AND B LEVEL OF EDC PERFORMANCE GOALS (RELATIVE HUMIDITY)

TABLE 13 BASELINE OPERATING CONDITIONS FOR A AND B LEVEL PERFORMANCE COMPARISONS

pCO_2, Pa (mm Hg)	400 (3.0)[a]
Current Density, mA/cm^2 (ASF)	21.5 (20)[b]
Air Flow/Cell,[c] dm^3/min (scfm)	4.5 (1.6)
Inlet Process Air Temperature, K (F)	294 ±3 (70 ±5)
Inlet RH, %	
A Level	70 to 80
B Level	50 to 60
H_2 + CO_2 Backpressure, Pa (psig)	Ambient

(a) Variable for Figure 57
(b) Variable for Figure 58
(c) For a 4.6 dm^2 (0.5 ft^2) active cell area

TABLE 14 CELL CONCEPTS FOR B-LEVEL TECHNOLOGY TESTS

Cell Design Concept No.	Concept Description	Stack-up Designation (Cathode/ Matrix/Anode)	Cell Hardware	Primary Reason for Selection
1	High Moisture Tolerance Design	10/20/30	AEDC[a]	Demonstrate all B-level performance goals
2	E-10 EDC Design	10/20/30	CS-6[b]	Demonstrate all B-level performance with special emphasis on exceeding voltage goal
3	Internal Electrolyte Reservoir Design	10/20/10	AEDC[a]	Demonstrate B-level performance over widest range possible in inlet air relative humidity
4	Secondary Electrode Design	10/30/10	CS-6[c]	Demonstrate concept for altering the water concentration of an operating EDC with less dependency on inlet parameters

(a) 4.6 dm^2 (0.5 ft^2) advanced, lightweight cell hardware, internally air-cooled.
(b) 2.3 dm^2 (0.25 ft^2) cell hardware as used for CS-6, internally air-cooled.
(c) 2.3 dm^2 (0.25 ft^2) cell hardware as used for CS-6, externally air-cooled fins.

High Moisture Tolerance Cell Design. The initial checkout testing of the high moisture tolerance cell demonstrated sufficiently high performance levels to be accepted for parametric testing. The baseline operating conditions selected for all tests of this concept are defined in Table 15. The parametric test results of this cell design are shown in Figures 60 through 63. The dashed lines in each figure represent the B-level technology goals established for EDC performance.

The performance of the high moisture tolerance cell design as a function of inlet pCO_2 matched, within experimental error, the design goal, as indicated in Figure 60. A shift in the peak of the performance curve as a function of current density for the high moisture tolerance design is indicated in Figure 61. The maximum removal efficiency of 85% occurred at a current density of 26.9 mA/cm^2 (25 ASF) compared to the B-level goal of 82% at a current of 20.4 mA/cm^2 (19 ASF). Electrical performance of the cell was approximately 0.1 V below the goal.

The high moisture tolerance cell was operated over a wide range of inlet RH conditions as illustrated in Figure 62. The cell performance as a function of inlet air RH is shown in Figure 63. The cell showed excellent operating tolerance over a range of inlet air RH (33 to 72%). The characteristically curved shape of EDC performance versus RH was observed, with decreases in performance both at high and low RH ranges. For the cell tested over the indicated range in RH, the CO_2 removal performance varied from 60 to 85%. The peak CO_2 removal efficiency occurred at an inlet RH level of 52%.

Based on the results of the parametric testing, the high moisture tolerance cell was selected for endurance testing. The cell was successfully operated for 75 days.

E-10 EDC Cell Design. The E-10 EDC is similar to the Contractor's high moisture tolerance cell design except the baseline cathode is exchanged for an E-10 type electrode. This electrode has a modified catalyst composition which was previously demonstrated as an efficient O_2 evolution electrode. The potential for increasing EDC operating voltages was projected using this electrode as the cathode of an EDC. However, during the initial checkout testing the E-10 EDC showed very high voltages (greater than 0.5 V) but failed to maintain positive voltage operation after 24 hours and the testing was discontinued.

Internal Electrolyte Reservoir Cell Design. The initial checkout testing of the internal electrolyte reservoir cell design was performed at the baseline conditions defined in Table 16. The results of the checkout testing demonstrated promising performance and, hence, acceptance for parametric testing. The results of the parametric characterizations are shown in Figures 64 through 67.

Carbon dioxide removal efficiency of the internal electrolyte reservoir cell as a function of inlet pCO_2 is shown in Figure 64. As shown, B-level technology performance above an inlet pCO_2 level of 400 Pa (3 mm Hg) was obtained. At lower pCO_2 levels, the cell performance was slightly below the established

TABLE 15 HIGH MOISTURE TOLERANCE CELL BASELINE OPERATING CONDITIONS

Number of Cells	1
Current, A	9.76
Active Surface Area, dm^2 (ft^2)	4.6 (0.5)
Electrolyte	LSI-D
Temperature, K (F)	299 ±1.6 (78 ±3)
Air Inlet Dew Point, K (F)	285 ±2.2 (54 ±4)
Air Pressure	Ambient
Air Inlet pCO_2, Pa (mm Hg)	400 (3.0)
Air Flow Rate, dm^3/min (scfm)	56 (2.0)
H_2 Flow Rate, dm^3/min (ft^3/h)	0.20 (0.42)

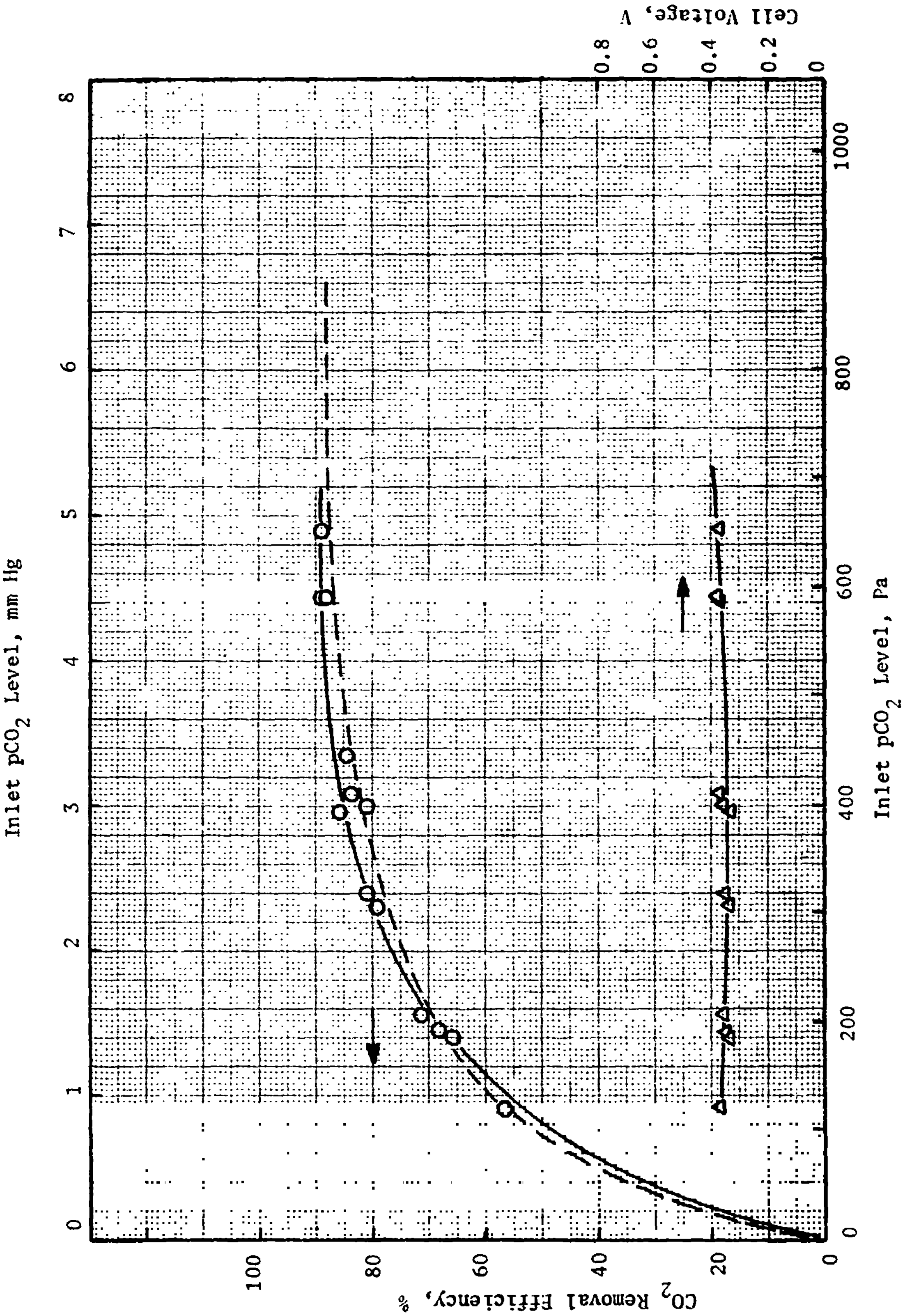

FIGURE 60 HIGH MOISTURE TOLERANCE CELL, INLET pCO_2 PERFORMANCE

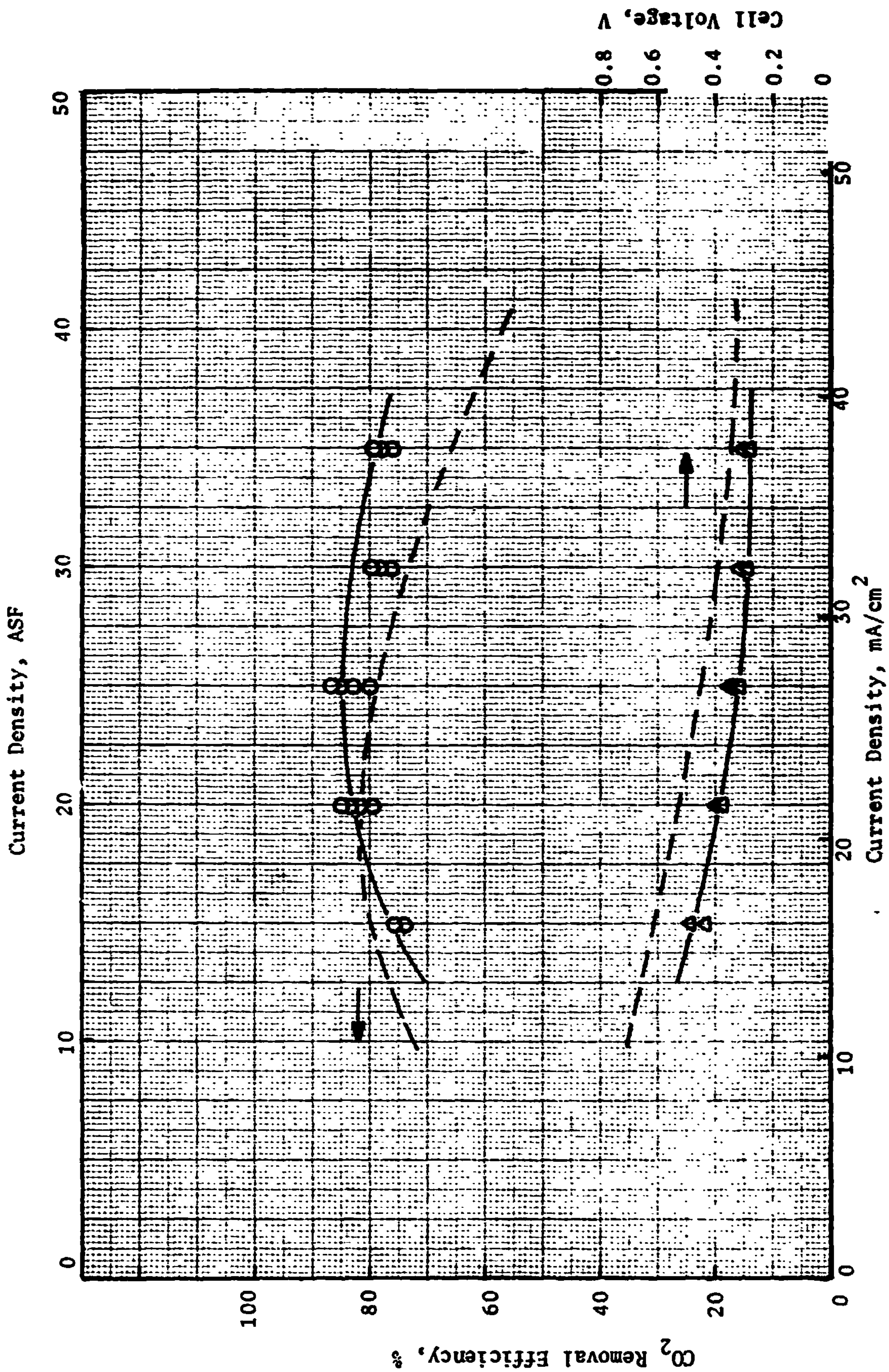

FIGURE 61 HIGH MOISTURE TOLERANCE CELL, CURRENT DENSITY PERFORMANCE

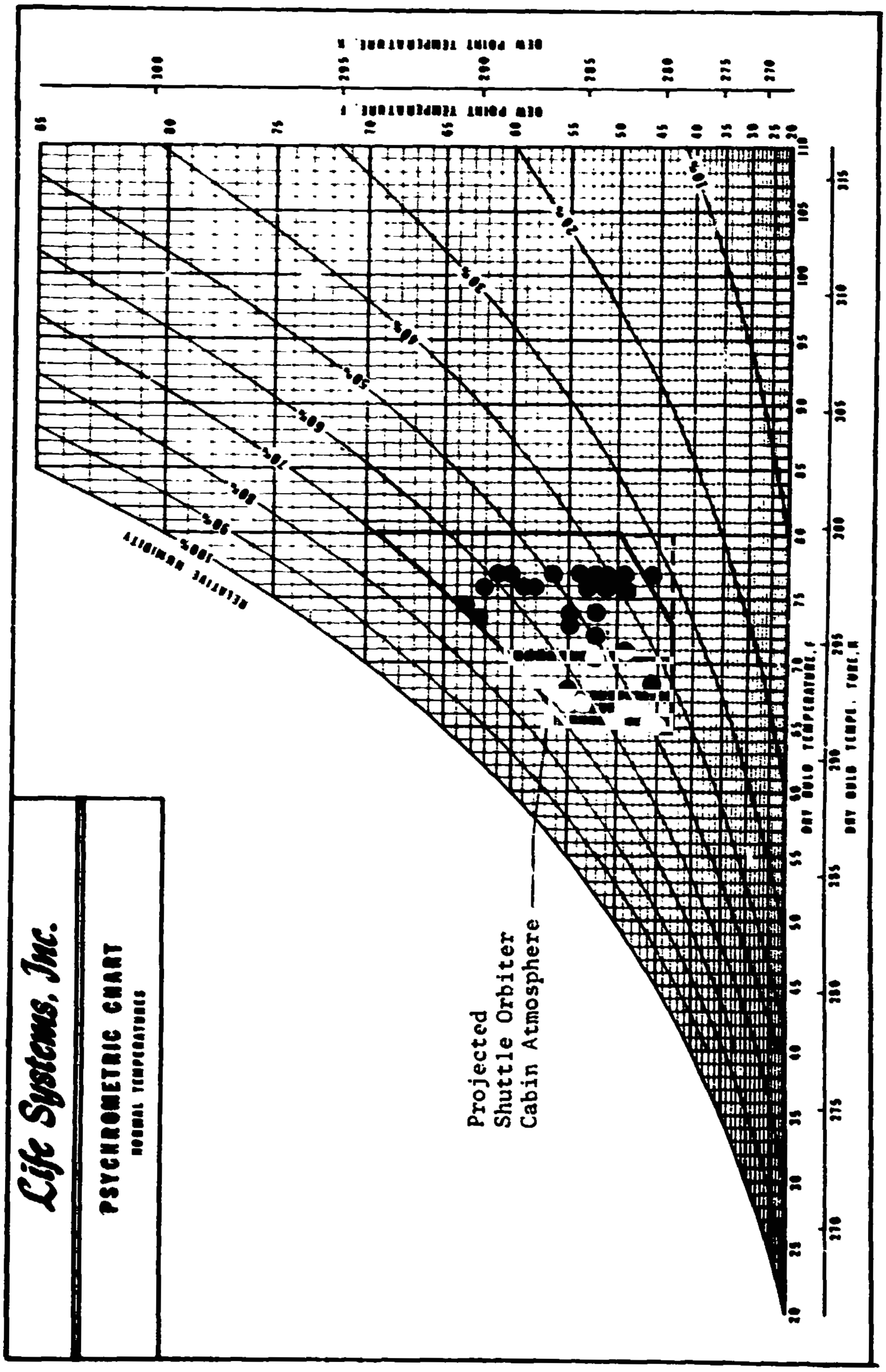

FIGURE 62 HIGH MOISTURE TOLERANCE CELL, AIR HUMIDITY PERFORMANCE

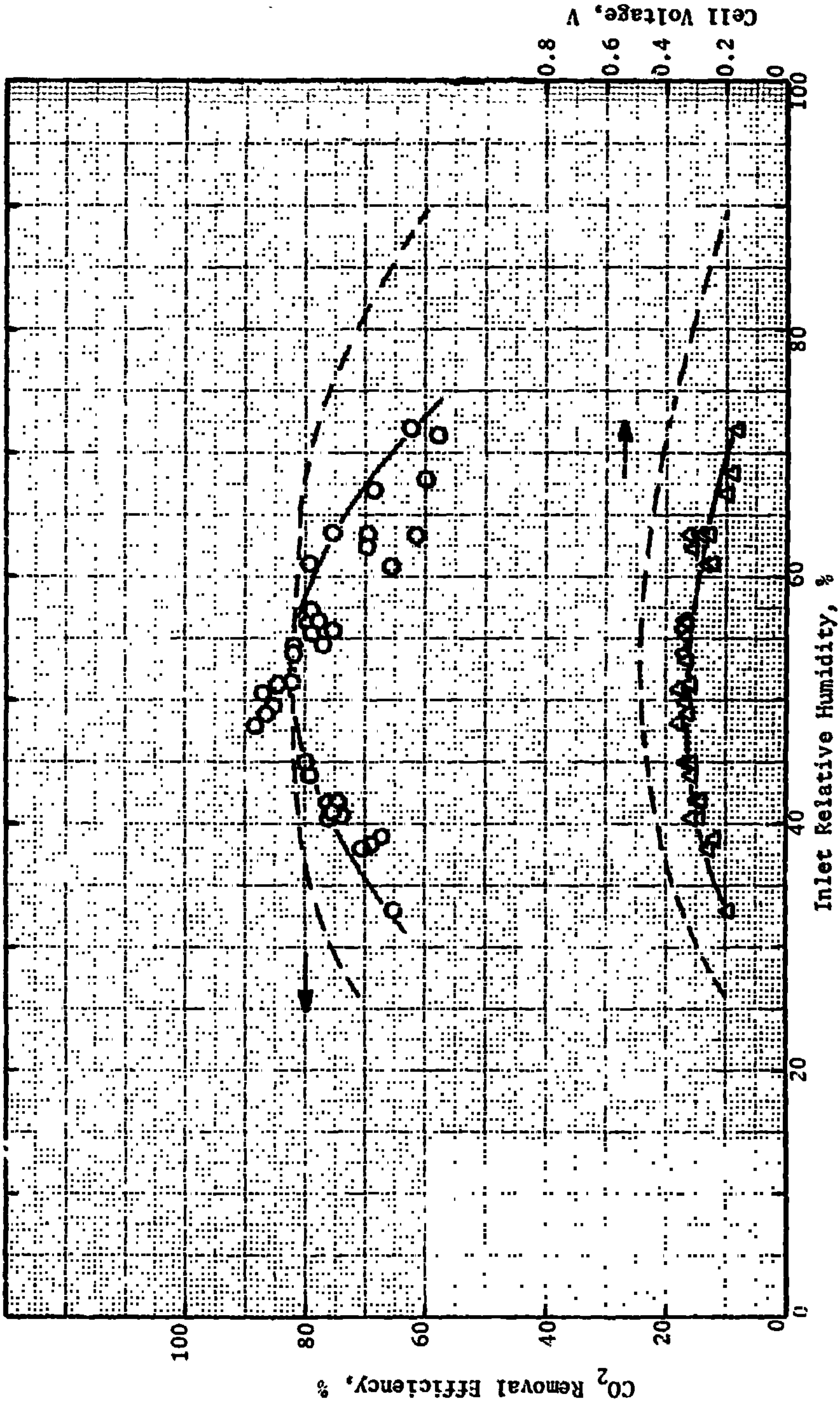

FIGURE 63 HIGH MOISTURE TOLERANCE CELL, INLET RELATIVE HUMIDITY PERFORMANCE

TABLE 16 INTERNAL ELECTROLYTE RESERVOIR CELL
BASELINE OPERATING CONDITIONS

Number of Cells	1
Current, A	9.4
Active Surface Area, cm^2 (ft^2)	438 (0.47)
Electrolyte	LSI-D
Temperature, K (F)	299 ±1.5 (79 ±3)
Air Inlet Dew Point, K (F)	285 ±0.5 (54 ±1)
Air Pressure	Ambient
Air Inlet pCO_2, Pa (mm Hg)	400 (3.0)
Air Flow Rate, dm^3/min (scfm)	59 (2.1)
H_2 Flow Rate, dm^3/min (ft^3/h)	0.22 (0.46)

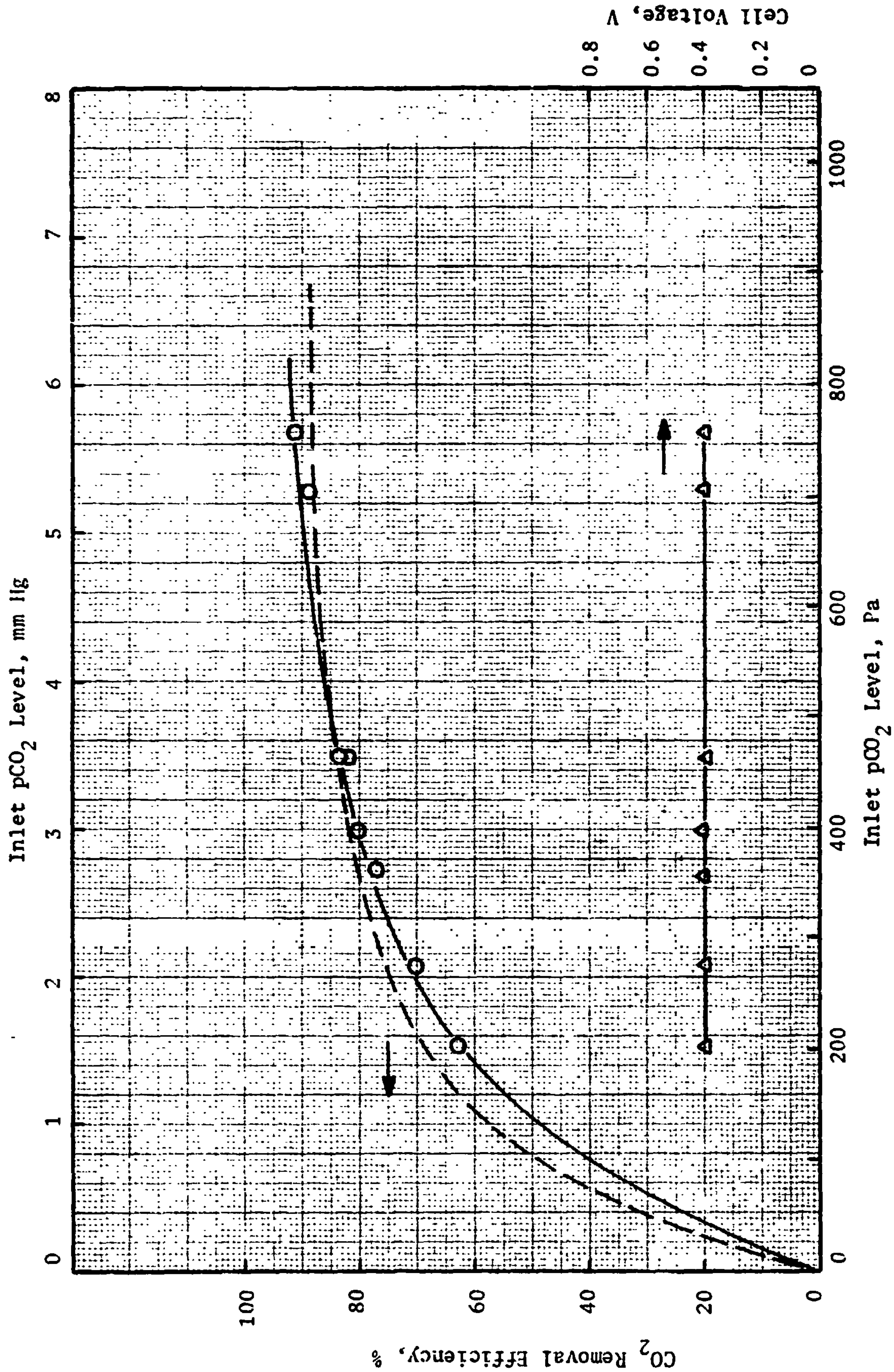

FIGURE 64 INTERNAL ELECTROLYTE RESERVOIR CELL, INLET pCO$_2$ PERFORMANCE

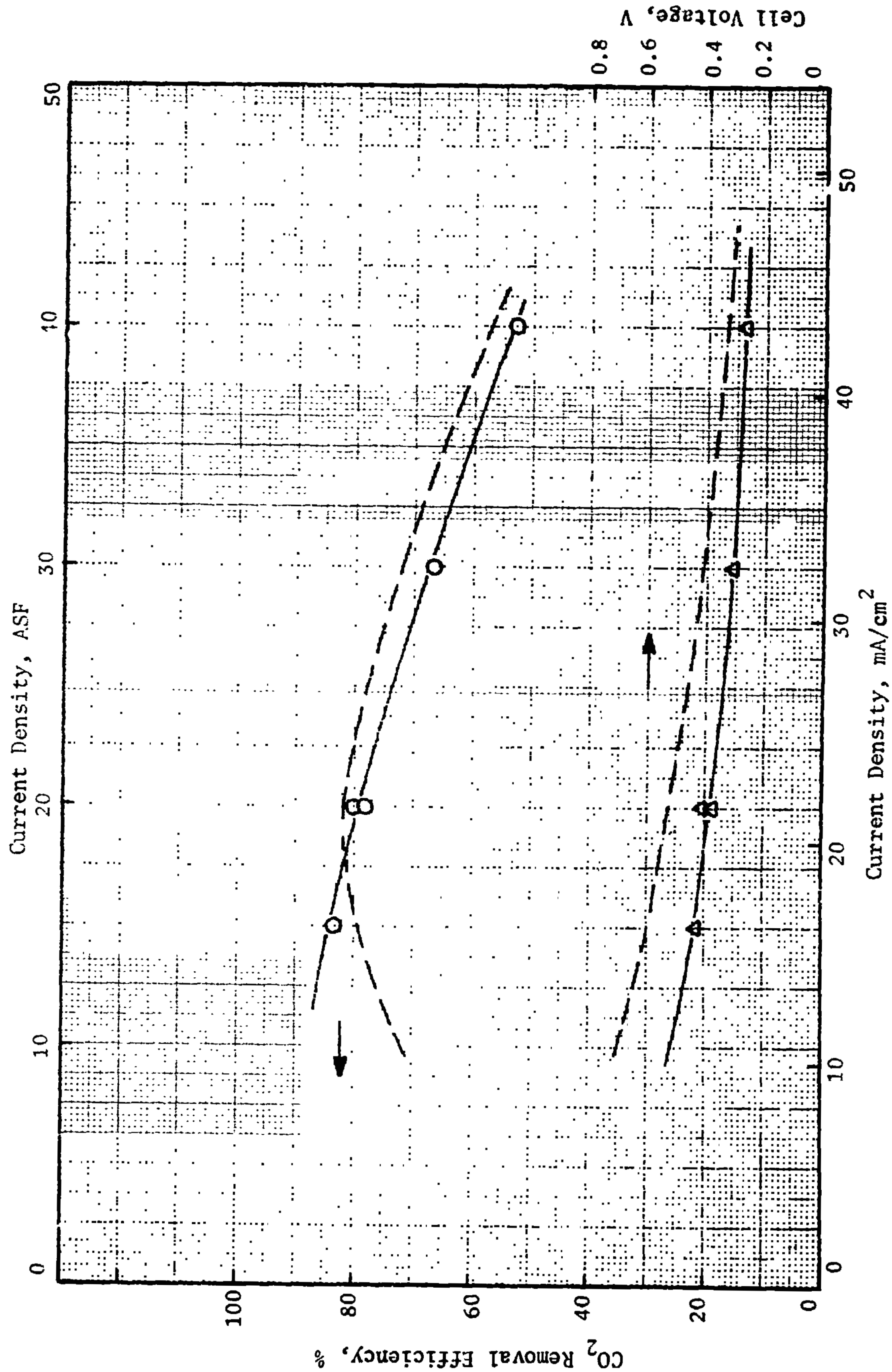

FIGURE 65 INTERNAL ELECTROLYTE RESERVOIR CELL, CURRENT DENSITY PERFORMANCE

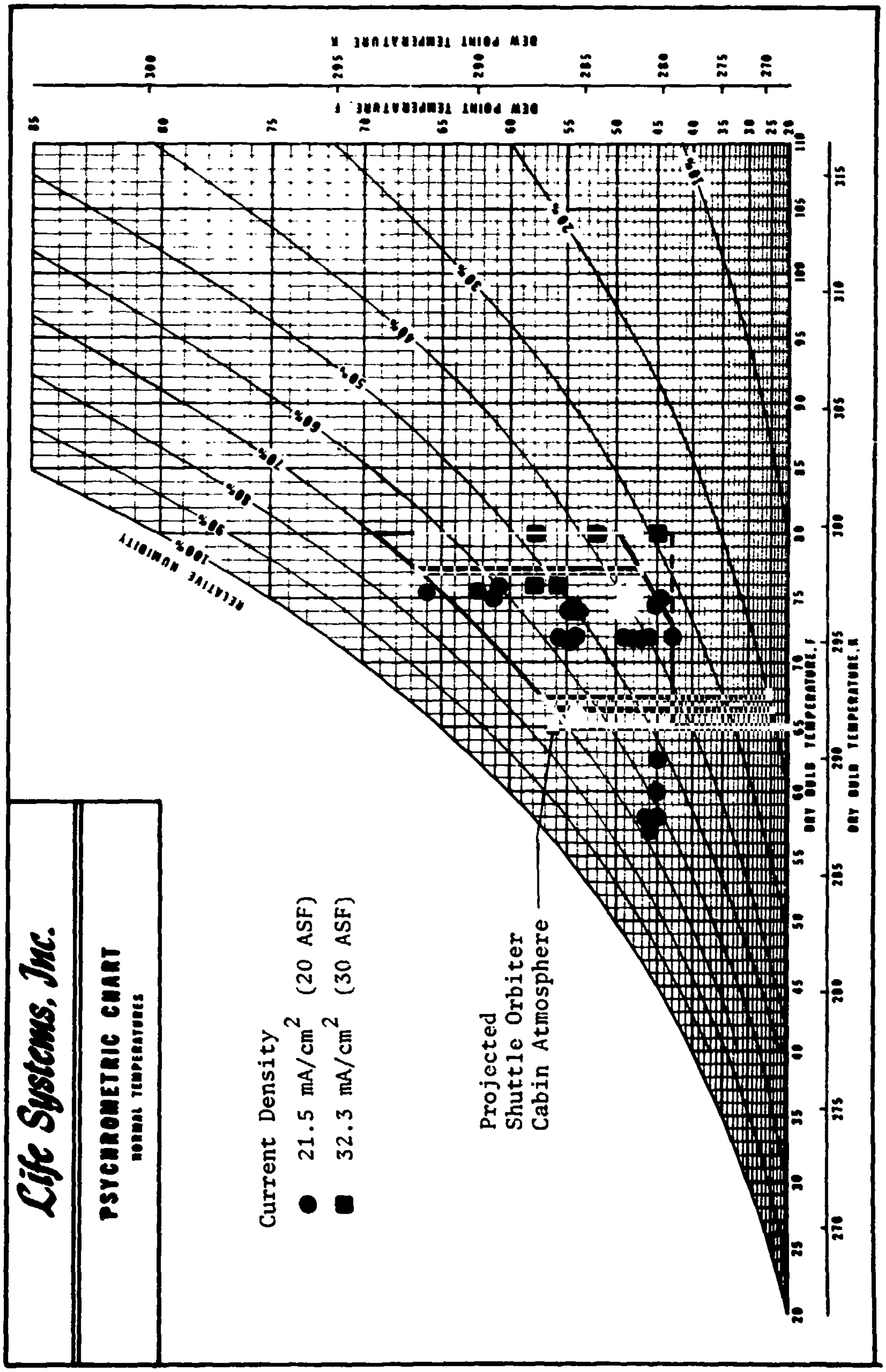

FIGURE 66 INTERNAL ELECTROLYTE RESERVOIR CELL, AIR HUMIDITY PERFORMANCE

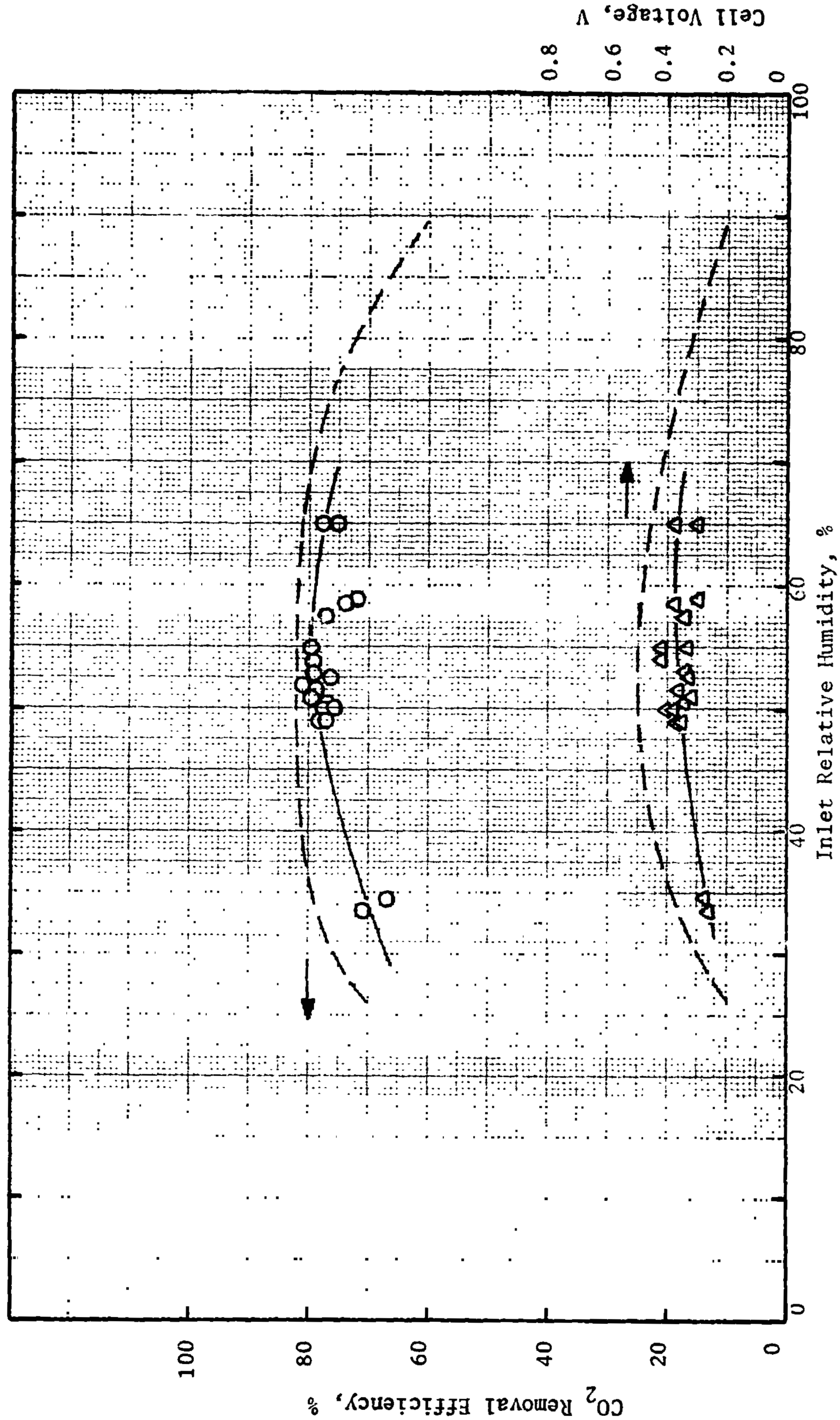

FIGURE 67 INTERNAL ELECTROLYTE RESERVOIR CELL, INLET RELATIVE HUMIDITY PERFORMANCE

technology goal. As shown in Figure 65, no peak in CO_2 removal efficiency was observed as a function of current density over the range tested. As indicated, performance was steadily increasing with decreasing current density level and exceeded the goal above 19.4 mA/cm^2 (18 ASF). Above that current density the performance was slightly less than the performance goals established. The range of inlet RH over which the electrolyte reservoir cell was tested is defined in Figure 66 and the performance results are shown in Figure 67. The cell was successfully operated over a range of 33 to 65% RH. A performance peak was observed at an inlet RH level of 56% resulting in a CO_2 removal efficiency of 80%. Voltage levels were generally less than the goals established.

While the internal electrolyte reservoir cell did not expand the operational tolerance to RH, it demonstrated better performance levels, both CO_2 removal and cell voltage, as a function of air RH. Also, operation at lower absolute dew points and dry bulb temperatures still yielded good performance. Also, with an increased current density of 32.3 mA/cm^2 (30 ASF), versus a baseline of 21.5 mA/cm^2 (20 ASF), the cell successfully tolerated 28% RH.

The cell was selected for endurance testing based on the B-level of performance demonstrated by the electrolyte reservoir cell during the parametric testing and was successfully tested for 67 days.

Membrane Electrode Cell Design. The fourth cell design projected to demonstrate B-level performance was the membrane electrode design. This concept was projected as a method for altering the moisture content of an operational EDC without changing the inlet air RH condition.

During the initial screening tests the membrane electrode concept demonstrated two major effects on EDC cell performance. First, the projected change in moisture content, hence potentially wide RH tolerance, was demonstrated. Second, an increase in CO_2 removal performance was observed. For example, a 20% increase in CO_2 removal efficiency from 75 to 90% was demonstrated. The cell, however, demonstrated voltage stability problems and further analysis and testing is required to fully characterize the potential of this concept.

CONCLUSIONS

The following conclusions are a direct result of the program studies.

1. The state of technology development for the EDC concept has reached a level where a functionally self-contained ARS design centered around the advanced, liquid-cooled EDC has been demonstrated. The ARS design incorporates a S-CRS, OGS, CHCS and NSS and water handling and coolant flow hardware. This entire system is controlled and monitored by a single, multipurpose C/M I.

2. The electrochemical CO_2 removal concept can be readily integrated with an OGS and either a S-CRS or a B-CRS with only a minimum number of interface components and using state-of-the-art hardware. No problems have been identified with using OGS-generated H_2 in the EDC, nor either of the CRSs using the EDC exhaust gases.

3. A five-cell, liquid-cooled EDC operating at 30 mA/cm^2 (28 ASF) with the 4.6 dm^2 (0.50 ft^2) advanced cells can remove the CO_2 metabolically generated by one person. High cell voltages (0.4 V) and CO_2 transfer efficiencies (76%) have been demonstrated over a 30-day endurance test.

4. The capability for operating an EDC directly with a varying spacecraft environment in terms of CO_2 and humidity loading conditions now exists. This capability is provided by the development of several humidity control subsystem components including diverter valves, heat exchangers and two types of liquid/gas separators.

5. A closed-loop spacecraft cabin environment simulator or ASU capability exists which will permit long-duration testing of future EDC subsystems. This ASU can cover a wide range of environmental conditions including changing temperature, humidity, CO_2 and O_2 levels.

6. An alternate anode current collector design, integral to the cell frame, is feasible and can be implemented with the advanced EDC cell hardware. The design uses a metal foil, metallurgically bonded to the current collector tabs. The new current collector design has shown significant reduction in internal resistance losses and fabrication cost of the cell.

7. The optimum EDC current density required to minimize total equivalent weight of a spacecraft CO_2 removal subsystem is that current density that optimizes CO_2 removal efficiency. This is true (within less than 2%) when considering use of the electrical power generated by an EDC.

8. Electrolyte (Cs_2CO_3) precipitation, caused by out-of-tolerance interface or operating conditions, causes apparent current density maldistributions in EDC cells. These maldistributions result in subnormal CO_2 removal and electrical efficiencies. Development of advanced C/M^2I to monitor and control within preset limits prevents subnormal performance. An LSI-developed electrolyte, LSI-D, greatly increases operating ranges.

9. Electrode Teflon loading studies have indicated that the optimum Teflon loading for maximum CO_2 removal is at the baseline loading presently being used. Relatively minor changes in cell performance would be obtained by either increasing or decreasing the Teflon loading, i.e., cell voltage can be increased by up to 0.1 V with decreased Teflon loading of 5 to 10% from baseline.

10. A series of supporting technology studies have verified that higher, termed B-level, performance goals for EDC technology advancement are achievable especially with respect to CO_2 removal efficiency. New EDC cell concepts and designs, including a high moisture tolerance cell design and internal electrolyte reservoir cell design, have shown that cell voltages above 0.4 V can be achieved over fairly wide ranges of pCO_2, current density and RH. This level, however, is still approximately 0.1 V less than the goal established for the B-level.

RECOMMENDATIONS

The following recommendations are a direct result of the program's conclusions.

1. Integration technology of an EDC with an OGS and a Bosch and/or Sabatier-based CO_2 reduction process has been demonstrated. A one-person capacity, experimental, laboratory breadboard ARS integrating the EDC with a CHCS, S-CRS, OGS and NSS and water handling and distribution hardware has been designed, fabricated and assembled and tested. A centralized C/M I approach for all ARS functions has been implemented. The next steps recommended for advancing EDC technology as part of an ARS are to (1) initiate the development of a preprototype, one-person ARS leading to a flight experiment to be flown aboard Shuttle/Spacelab, with emphasis being placed on designing for Spacelab interfaces, developing optimum packaging, minimizing crew involvement and developing required ancillary components, (2) continue testing of the existing ARX-1 to broaden the technology base for the flight experiment ARS and (3) verify the compatibility of the regenerated atmosphere with living organisms such as mammals and/or any negative effects of the mammal-generated contaminants on the equipment.

2. The development of an independent EDC subsystem for integration with other RLSE components at the three-person level has been achieved. For extended duration Shuttle missions, the regenerable CO_2 removal concept based on the EDC offers significant advantages over any nonregenerable approach. It is recommended that a seven-person capacity EDC subsystem be developed for the extended Shuttle missions. A Sabatier reactor should be packaged with the EDC to provide O_2 recovery in the form of product water.

3. Integration of the EDC with other EC/LSS subsystems demonstrated the simplification of the overall ARS function by the elimination of redundant components. Further simplification at the subsystem level is possible and recommended by combining actuator and sensor functions into single hardware assemblies. For example, the fluid control function now performed in an EDC by four solenoid valves, one orifice, three pressure transducers, two flow sensors and one pressure regulator, should be packaged into one assembly.

4. High performance levels have been demonstrated by individual, advanced cells or a low number (less than 16) of advanced cells packaged into modules. Fabrication techniques and cell configurations should be developed to ensure reproducibility at a larger scale of the EDC cell characteristics responsible for the high performance levels.

5. Performance improvement experiments should be continued to more fully establish the new advanced B-level of EDC technology. This effort should focus on (1) increasing cell voltage to greater than or equal to 0.5 V and (2) achieving constant performance over wide ranges in RH. Previous testing established that the new goal for CO_2 removal efficiency could be met. Following establishment of a

new baseline EDC cell electrode/matrix/electrolyte combination through the B-level test activities, it should be incorporated and tested at a scaled-up level using the EDC hardware of the ARX-1 as a test bed.

REFERENCES

1. Samonski, F. H. and Neel, J. M , "Atmosphere Pevitalization for Manned Spacecraft - An Assessment of Technology Readiness," presented at the 24th Congress, Baku USSR; October, 1973.

2. Quattrone, P. D., "Spacecraft Oxygen Recovery System," Astronautica Acta 18, No. 4, pp. 261-272; October, 1973.

3. Quattrone, P. D.; Babinski, A. D. and Wynveen, R. A., "Carbon Dioxide Control and Oxygen Generation," presented at the ASME Conference, Paper No. 70-AV/SpT-8, Los Angeles, CA; June, 1970.

4. Wynveen, R. A. and Quattrone, P. D., "Electrochemical Carbon Dioxide Concentrating System" presented at the SAE/ASME/AIAA Conference, Paper No. 71-Av-21, San Francisco, CA; July, 1971.

5. Wynveen, R. A.; Schubert, F. H. and Powell, J. D., "One-Man, Self-Contained CO_2 Concentrator System," Final Report, Contract NAS2-6118, NASA CR-114426, Life Systems, Inc., Cleveland, OH; March, 1972.

6. Powell, J. D.; Schubert, F. H.; Marshall, R. D. and Shumar, J. W., "Six-Man, Self-Contained Carbon Dioxide Concentrator Subsystem," Final Report, Contract NAS2-6478, NASA CR-114743, Life Systems, Inc., Cleveland, OH; June, 1974.

7. Kostell, G. D.; Schubert, F. H.; Shumar, J. W., Hallick, T. M. and Jensen, F. C., "Six-Man, Self-Contained Carbon Dioxide Concentrator Subsystem for Space Station Prototype (SSP) Application," Final Report, Contract NAS2-6478, NASA CR-114742, Life Systems, Inc., Cleveland, OH; May, 1974.

8. Schubert, F. H. and Quattrone, P. D., "Development of a Six-Man, Self-Contained Carbon Dioxide Collection Subsystem for Spacecraft Application," Paper No. 74-ENAs-16, Intersociety Conference on Environmental Systems, Seattle, WA; July, 1974.

9. Winnick, J.; Marshall, R. D. and Schubert, F. H., "An Electrochemical Device for Carbon Dioxide Concentration, I. System Design and Performance," I&EC Process Design and Development, Volume 13, pp. 59-63; January, 1974.

10. Schneider, J. J.; Schubert, F. H.; Hallick, T. M. and Woods, R. R., "Electrochemical Carbon Dioxide Concentrator Advanced Technology Tasks," Final Report, Contract NAS2-6478, CR-137732, Life Systems, Inc., Cleveland, OH; October, 1975.

11. Schubert, F. H.; Woods, R. R.; Hallick, T. M. and Heppner, D. B., "Technology Advancement of the Electrochemical CO_2 Concentrating Process," Annual Report, Contract NAS2-8666, NASA CR-151995, Life Systems, Inc., Cleveland, OH; April, 1977.

12. Schubert, F. H.; Woods, R. R.; Hallick, T. M. and Heppner, D. B., "Technology Advancement of the Electrochemical CO_2 Concentrating Process," Annual Report, Contract NAS2-8666, CR-152098, Life Systems, Inc., Cleveland, OH; March, 1978.

13. Yang, P. Y.; Gyorki, J. R. and Wynveen, R. A., "Instrumentation for Controlling and Monitoring Environmental Control and Life Support Systems," Paper No. 78-ENAs-40, Intersociety Conference on Environmental Systems, San Diego, CA; July, 1978.

14. Heppner, D. B.; Sharma, M. P. and Schubert, F. H. "Preprototype Electrochemical CO_2 Concentrator Subsystem," Computer Math Model User's Manual, Contract NAS2-8666, Life Systems, Inc., Cleveland, OH; September, 1978.

15. Schubert, F. H.; Quattrone, P. D. and Clark, D. C., "Integrated Testing of an Electrochemical Depolarized CO_2 Concentrator (EDC) and a Bosch CO_2 Reduction Subsystem (BRS)," Paper No. 76-ENAs-35, Intersociety Conference on Environmental Systems, San Diego, CA; July, 1976.

16. Heppner, D. B.; Hallick, T. M. and Schubert, F. H., "Integrated Operation of a Bosch-Based Oxygen Recovery System," Final Report, Contract NAS8-30891, Life Systems, Inc., Cleveland, OH; September, 1977.

17. Schubert, F. H. and Wynveen, R. A., "Technology Advancement of the Static Feed Water Electrolysis Process," Final Report, Contract NAS2-8682, NASA CR-152073, Life Systems, Inc., Cleveland, OH; November, 1977.

18. Marshall, R. D. and Knebel, W. J., "Evaluation of a Spacecraft Nitrogen Generator," Annual Report, Contract NAS2-8782, NASA CR-151983, Life Systems, Inc., Cleveland, OH; January, 1977.